Research Technical Completion Report
684K823

A Transfer Function Model for Prediction of Solute Transport in Surface Irrigated Fields

Behzad Izadi, Bradley King and Ian McCann

Department of Agricultural Engineering
University of Idaho
USA

Submitted to

U.S. Geological Survey
United States Department of the Interior
Washington, D.C. 20242

Idaho Water Resources Institute
University of Idaho
Moscow, ID 83843
May 1992

TABLE OF CONTENTS

ACKNOWLEDGEMENTS

The authors wish to acknowledge the support of the Office of Water Policy, U.S. Department of the Interior who funded this research project through the Water Resources Institute Program under Project No. 684K823.

The authors would like to recognize the USDA-ARS at Kimberly, Idaho for their cooperation and technical assistance. Special thanks go to Dr. D. T. Westermann, Dr. Jim Wrigth, Dr. Tom Trout, Robert Moulson, and Mike Humpherys for their assistance in field preparation and data collection.

LIST OF FIGURES

LIST OF TABLES

ABSTRACT

An experiment was conducted during summer of 1991 to validate the simple Transfer Function Model (TFM) under variable conditions observed in a 0.9 ha furrow irrigated fallow field. Twenty one spatially distributed sampling stations were established to monitor movement of bromide (Br). Each station consisted of soil solution samplers at 0.3 m and 0.9 m depth, and a neutron probe access tube to a depth of 2.1 m. A narrow pulse of Br tracer was applied by injection through a sprinkle irrigation system. The tracer was subsequently transported downwards by 3 furrow irrigation events, approximately 3 weeks apart. Soil samples were taken to a depth of 2.4 m prior to each irrigation and at the end of 63 day study period. The Br concentration data were normalized at each station, and the field-average Br profiles were determined for each soil sampling date. Methods based on Darcy velocity and piston flow under-predicted the final Br position. The simple TFM calibration functions were successfully developed based on both soil sample and solution sampler data. The simple TFM calibrated based on soil samples predicted the Br position and general Br profile with reasonable accuracy. The simple TFM predicted a slower movement of the solute front when the calibration function based on 0.3 m solution sampler data was used. The delayed response was attributed to lack of direct contact to soil macropores. Considering the variability and sources of error in a study such as this, use of the TFM based on soil sampling is a promising approach for field-scale prediction of solute movement.

INTRODUCTION

Basis for development and fundamental concepts of the Transfer Function Model

Prior to the development of the Transfer Function Model (TFM), models were divided into deterministic mechanistic, deterministic-functional, and stochastic mechanistic categories (Addiscott and Wagenet, 1985). Inherent in the conceptualization of all these models is a complex or simple method of describing the mass balance, Darcy's law, and pertinent chemical processes.

The TFM is developed based on the premise that the conceptual validity of existing models are questionable under variable field conditions (Jury, 1982). Furthermore, the processes involved in chemical movement through soil is probabilistic, which may or may not follow the fundamental mechanisms of water and solute transport processes (Ammozegar-Fard et al., 1982; Rubin, 1983; Dagan, 1986; Jury et al., 1986; Sposito et al., 1986). A probabilistic view is taken because the parameters involved in field-scale chemical transport are temporally and spatially varied, and the chemical processes are poorly known under conditions of physical or chemical non-equilibrium (Dyson et al., 1990).

The TFM was recently developed by soil scientists at the University of California, Riverside (Jury et al., 1986), and Oxford University, England (White et al., 1986). It is a linear model that treats the soil (system) as a "black box". The input to this system is the amount of solutes added to the soil surface while the output is solute concentration at various depths. The TFM requires a calibration function which can be estimated by applying a narrow pulse of solute and determining the average breakthrough curve at a given depth in the field. variability. Furthermore, the TFM has the flexibility of including different processes in more or less detail; thus it can be used as a research or management/screening tool.

Need for future research

The TFM is still in the preliminary stages of development, therefore there are several possible areas for future research. Dyson et al. (1990), indicated the following research priorities:

1) To develop an extensive database to test and extend the range of application of the TFM;
2) To include chemical processes such as sorption, decay and plant uptake in the TFM;
3) To explore the relation between chemical movement in time and in space;
4) To investigate whether the calibration function is different under ponded vs unponded condition;
5) To investigate the effect of intermittent water inputs, particularly when evaporation and/or macropore flow is present;
6) To modify the TFM and apply it to multi-layered media; and
7) To investigate the usefulness of various types of probability density functions for fitting the calibration curve.

OBJECTIVES

The overall objective of this study was to validate the simple TFM under highly variable conditions observed in a furrow irrigated fallow field. In the process of achieving this objective, three of the research priority areas mentioned above (1, 3, and 5) were addressed. The specific objectives were:

1. To conduct a comprehensive field experiment to monitor movement of nitrate and bromide in a furrow irrigated fallow field;
2. To develop the field-average calibration functions; and
3. To validate the simple TFM using both solution sampler and soil sample calibration functions.

THEORY

Simple Transfer Function Model

The simple TFM is based on the assumption that solute movement from the soil surface to any depth depends on the amount of water applied. Furthermore, dispersion is implicitly represented by the travel time variations. The soil is modeled as a linear system, where a narrow pulse of solute at the entrance surface (i.e. soil surface) is the input and the average concentration at the exit surface (i.e depth L) is the output. The linear response to a narrow solute pulse is the average concentration of the solute, C(L,I), at a given depth as a function of the net amount of water (I) infiltrated at the surface (Figure 1):

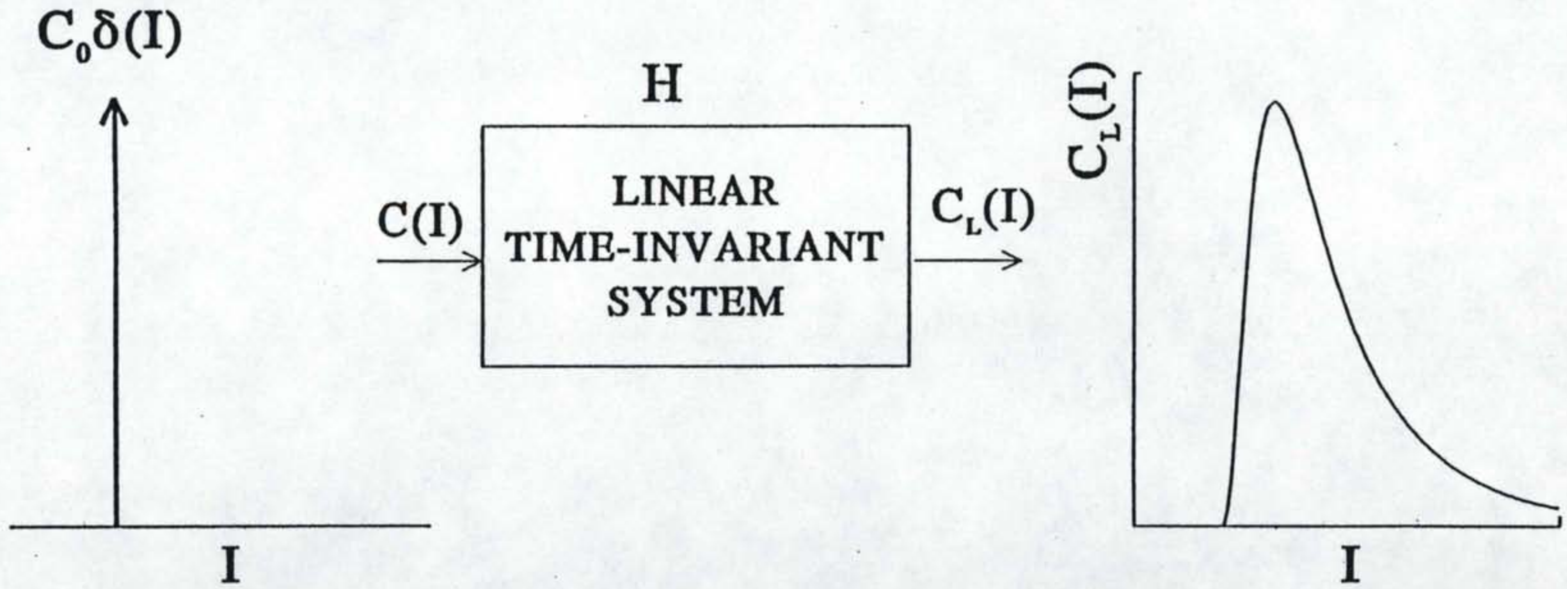

Figure 1. Impulse response to a linear system.

where:

C_0 = Concentration of the narrow pulse [M L^{-3}],

$\delta(I)$ = Dirac delta function, and

H = Linear operator.

The unit impulse response can be determined by dividing both sides of equation 1 by C_0:

$$H*\delta\,(I) = \frac{C\,(\,L,\,I\,)}{C_0} \qquad [2]$$

Referring to Figure 1, C_0 can be considered as the total mass of solute applied per unit area, which is equal to the area under the C(L,I) curve:

$$H*\delta(I) = \frac{C\,(L,\,I)}{\int C\,(L,\,I)\,dI} = f_L\,(I) \qquad [3]$$

The function $f_L(I)$ is the probability that the tracer will arrive at depth L when I amount of water is infiltrated at the surface.

If the input is not a narrow pulse, any arbitrary input can be resolved into a continuum of unit impulses using the superposition integral:

$$C(I) = \int_0^\infty C\,(I')\;\delta\;(I - I')\;dI' \qquad [4]$$

where I′ is a dummy variable.

The response to a linear system with an arbitrary input C(I) is:

$$C\,(L,\,I) = H*C\,(I) = H*\int_0^\infty\,C\,(I')\;\delta(I\text{-}I')\;dI' \qquad [5]$$

Invoking the principle of superposition the operator H can be moved inside the integral:

$$C\ (L, I) = \int_0^\infty H*[\ C\ (I')\ \delta(I-I')\ ]\ dI' \qquad [6]$$

Using the principle of proportionality H can be an operator for the delta function:

$$C(L, I) = \int_0^\infty C\ (I')\ H*\delta(I-I')\ dI' \qquad [7]$$

Considering the time invariancy of the system the variables I′ and I-I′ can be exchanged:

$$C\ (\ L, I\ ) = \int_0^\infty C(I-I')\ H*\delta\ (I')\ dI' \qquad [8]$$

The function H $\delta(I')$ is the unit impulse response $f_L(I')$:

$$C(L, I) = \int_0^\infty C(I-I')\, f_L\ (I')\ dI' \qquad [9]$$

Equation 9 is the response of the linear system to any arbitrary input.

Due to the linearity and time invariancy of the system the unit impulse response at any depth Z, $f_Z(I)$, can be determined from the known unit impulse response $f_L(I)$ (Jury, 1982):

$$f_Z\ (I) = \frac{L}{Z}\ f_L\ (\frac{IL}{Z}) \qquad [10]$$

Equations 9 and 10 can be combined to determine the concentration at any given depth:

$$C(Z, I) = \int_0^\infty C(I-I') \frac{L}{Z} f_L \left(\frac{I'L}{Z}\right) dI' \qquad [11]$$

For a square pulse input and a lognormally distributed f_L the analytical solution for equation 11 is:

$$C(Z, I) = \frac{C_0}{2}\left\{ erf\left[\frac{\ln\left(\frac{IL}{Z}\right) - \mu}{2^{1/2}\,\sigma}\right] - erf\left[\frac{\ln\,(I - \Delta I)\,\frac{L}{Z} - \mu}{2^{1/2}\,\sigma}\right]\right\} \qquad [12]$$

where:

μ = Mean of the lognormal distribution, and

σ = Standard deviation of the lognormal distribution.

LITERATURE REVIEW

The available literature on the TFM is relatively small and mostly limited to those institutions where the idea originated. However, due to the importance of the TFM approach, more and more scientists are investigating its potential for various applications. It is anticipated that upon the completion of the on-going studies, the TFM will be recognized as an important stochastic non mechanistic model for field-scale solute transport modeling. An attempt is made here to summarize all the pertinent literature available on the TFM.

Generalized form of the TFM

Jury et al. (1986) developed a generalized form of the TFM to describe the movement of a solute that undergoes physical, chemical, or biological transformations in a soil unit. They introduced a lifetime probability density function, $g(t-t' \mid t')$, the probability that solutes entering the transport volume at time t' will exit the transport volume at time t, and developed the following transfer function equation under steady state water flow conditions :

$$C_{out}(t) = \int_0^t g(t - t' | t')\, C_{in}(t')\, dt' \qquad [13]$$

where:

$C_{out}(t)$ = the rate of solute mass output from the transport volume at time t, [M L^{-3}], and

$C_{in}(t')$ = The rate of solute mass input into the transport volume at time t', [M L^{-3}].

Equation 13 is a generalized form of the TFM because any solute mass added to the system is considered input (i.e. solute production in the transport volume), and any solute mass lost from the system is considered output (i.e. solute transformation in the transport volume). The simple TFM is a special form of equation 13, where it is assumed that the only significant inputs and outputs are through an exterior entrance and exit surface, respectively. Furthermore, it is assumed that the solute lifetime $(t-t')$ is independent of solute input time t':

$$C(L, t) = \int_0^t g(t - t')\, C(t')dt' \qquad [14]$$

Time as an independent variable can be changed to the cumulative water input I, where I is the product of a constant flux and elapsed time (Jury et al., 1986):

$$C(L, I) = \int_0^I f_L(I - I')\, C(I')\, dI' \qquad [15]$$

Upon exchanging the variables I′ and I-I′, equation 15 transforms into the simple TFM (Eqn. 9) used in this study. Note that the upper limit of the integral can be extended to infinity, since f_L(I-I′) =0 when I′>I.

The TFM under transient conditions

It is assumed that the probability density function f_L(I) is reproducible under any flow conditions. However, if a calibration experiment is repeated under a different initial water content, the probability density function should be shifted to account for this change in water-storage volume. For example, if f_L(I) was measured when water content between 0 and L was θ_o, and the measurement was repeated when water content was θ_1, the measured probability density function would have been f_L(I-L(θ_1-θ_o)).

Jury et al. (1990) transformed equation 15 into a travel-time probability density function to determine the outflow flux concentrations under unsteady state flow conditions:

$$C(L, t) = \int_0^t C[(I_0(t) - I_0\,(t')]\, f_l\{I_L(t') - \Delta W[I_0(t) - I_0(t')]\}\, J_W(L, t')\, dt'$$

where:

$I_0(t)$ = Net cumulative input past the surface at time t [L],

$I_L(t)$ = Cumulative drainage past depth L [L],

$\Delta W(t)$ = Difference in storage volume between the state at time t and the steady state [L], and

$J_w(L,t')$ = The water flux at depth L and time t [L T^{-1}].

The difficulty in applying the above equation is the determination of $J_w(L,t)$. Jury et al. (1990), used the water balance model and a simulated drainage experiment based on 56 air-entry permeameter measurements of unsaturated hydraulic conductivity to predict the field-scale drainage rate. Inherent in their procedure for simulating a drainage experiment was the assumption that the soil consisted of 56 parallel soil columns, each having a drainage rate measured by the air-entry permeameter method. Furthermore, they assumed that the difference in storage between the steady state and the transient experiment is negligible.

Equation 9 is directly applicable to the transient conditions if the cumulative drainage past depth L rather than cumulative input at the surface is used as I. This can be achieved by using mass balance, in which the net input at the soil surface is measured, and the change in storage within the 0 to L profile is monitored periodically, using a device such as neutron probe. Whenever possible, this method is preferable over Jurys' et al. (1990) method, since it does not require a simulation study to predict the drainage rate. Furthermore, any differences in volumetric water content is implicitly included in the estimated drainage past depth L.

The validation of the simple TFM in the field

The first field experiment for calibration and validation of the simple TFM was conducted by Jury et al. (1982). A narrow pulse of Br was applied through a sprinkle irrigation system to a 0.64 ha field. Fifteen spatially distributed stations were established. Within each station 6 solution samplers at depths of 0.3, 0.6, 0.9, 1.2, 1.8, and 3.05 m were installed. Solution samplers were used to monitor the movement of Br during a winter of 0.93 m rainfall over 100 days. The simple TFM approach was used to calibrate the model at 0.3 m depth and successfully validate it at the subsequent depths.

Jury et al. (1990), adopted the simple TFM theory to a transient water flow condition as it was discussed under "the TFM under transient conditions". They successfully validated their model using the experiment of Jury et al. (1982) discussed above.

The only comprehensive ponded study was conducted by Rice et al. (1986) in 56 subplots, 12.2 m by 9.1 m, spatially distributed in a 0.62 ha field. At the beginning of the experiment, KBr was uniformly sprayed on each subplot at the rate of 135 Kg Br ha^{-1}. The Br application was immediately followed by 100 mm of flood irrigation. Seven additional 50 mm irrigations were applied throughout the 159 day experiment. After each irrigation, 2 soil cores were taken from each subplot at 0.3 m increments to a depth of 2.7 m. The field-average concentration measured by the first core sample was used to calibrate the simple TFM. The analytical solution to the simple TFM with a square pulse input (Eqn. 12) was used to predict Br movement in soil. The model successfully predicted the position of maximum concentration only when the infiltration rate based on the tracer flux was used. The model failed to predict the magnitude of Br concentration. The poor performance of the simple TFM may be attributed to approximating a transient flow with a steady state flow condition, hence, not correcting for the storage. Furthermore, the assumption of uniform infiltration rate over the irrigated areas may not be warranted.

The only furrow irrigation study so far reported was conducted by the authors at the Kimberly Research and Extension Center in the state of Idaho, USA (Izadi et al., 1990). In this preliminary study a 20 hour continuous flow furrow irrigation event was conducted on a Portneuf silt-loam soil. Nitrate and Br were injected into flowing furrows during the first half hour of the irrigation using marionette syphons. Nitrate and Br solution samples from 21 pairs of solution samplers were collected during and after the irrigation event at depths of .3 m and .8 m within a 150 m by 13 m field plot. Soil samples were collected before and after irrigation to a depth of 0.9 m to determine gravimetric water content and resident nitrate and Br concentrations. The validation attempt failed, since the amount of water infiltrated was not sufficient to develop the average breakthrough curve at .8 m. Furthermore, despite the effort to apply a uniform pulse of nitrate, the estimated coefficient of variation in input pulse concentration was over 18%.

MATERIALS AND METHODS

Experimental design

Field research was conducted at the Kimberly Research and Extension Center, during the summer of 1991. Seven sets of furrows spatially distributed in a 145 m by 60 m field were selected for this study (Figure 2). The field was planted to oats in early spring to extract residual nitrogen from the soil. The oats were green chopped in early June and sprayed with herbicides to stop growth and eliminate plant uptake of water and nutrients. Each set of furrows consisted of one monitored furrow with two buffer furrows on each side. Three sampling stations were established along each of the monitored furrows at 20 m , 80 m and 140 m from the inlet. Overall, 21 sampling stations were established each consisting of a solution sampler at 0.3 m and 0.9 m and a neutron probe access tube installed to a depth of 2.4 m to measure soil moisture. The solution samplers and neutron access tubes were installed near the edge of the furrow, on the furrow bed. Flumes connected to a data logger were used to measure the outflow from each monitored furrow during irrigation events. The cross-sections of the monitored furrows at each station were determined using a profilometer before each irrigation.

Initially, a solid set sprinkle system was installed to apply a uniform and narrow pulse of nitrate and Br over the field. Overall, 45 kg N ha^{-1} as KNO_3 and 45 kg Br ha^{-1} as KBr was applied to the field. The initial irrigation was immediately followed by a sprinkler application of approximately 66 mm of water to leach the

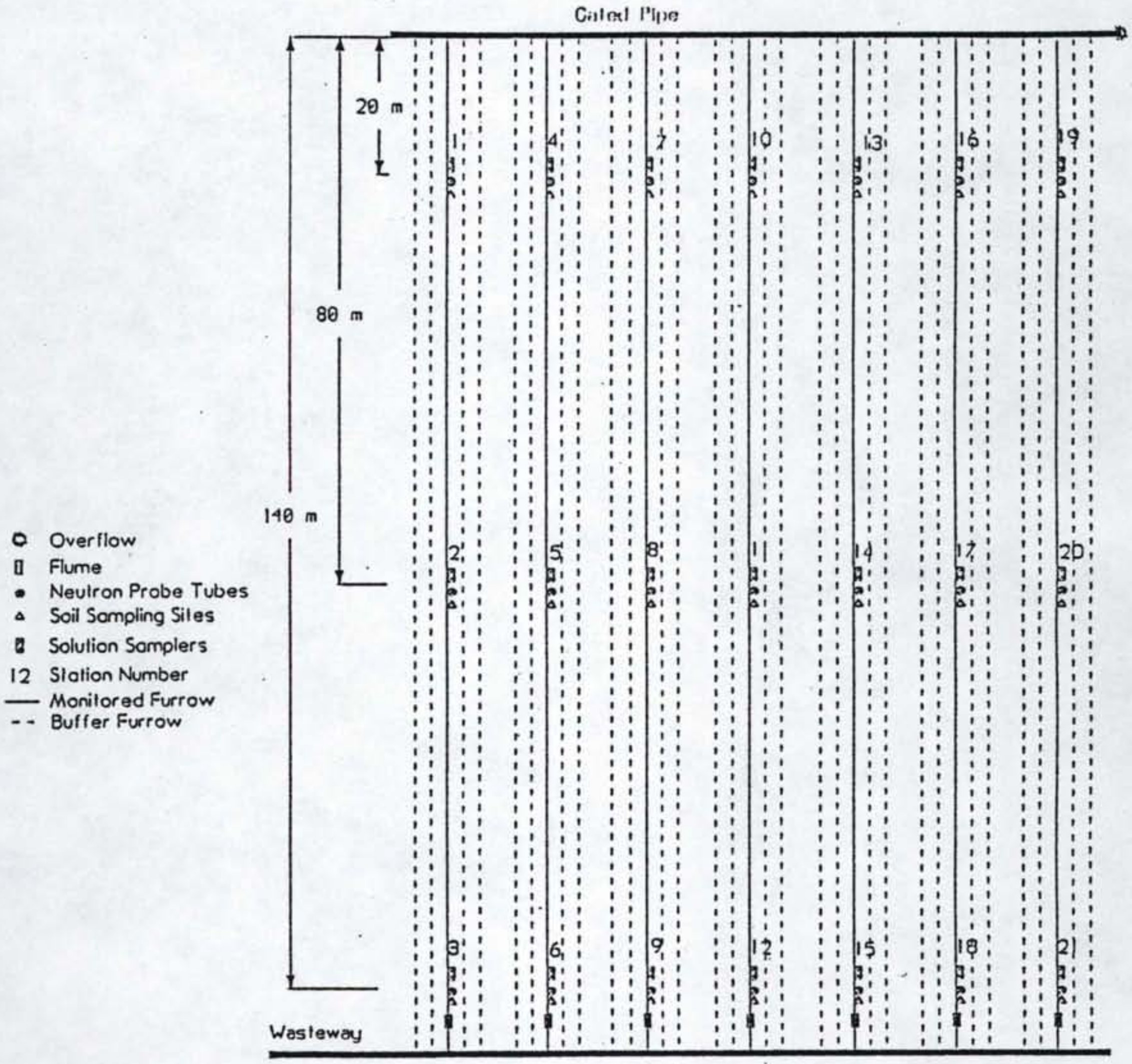

Figure 2. Plan view of the field experiment

solutes into the soil. The sprinkle irrigation setup was then removed and an 8-hour continuous flow furrow irrigation event was conducted on the following day. The first irrigation (June 21) was followed by another 8-hour irrigation on July 17 and a 36-hour final irrigation on August 6. Advance and recession data were collected at 20 m distances during each irrigation. To determine the resident concentration of solutes, soil samples were taken to a depth of 2.4 m in the field before each irrigation and after the last irrigation. Solution samplers were used to collect soil solution samples during as well as between irrigations. The soil moisture profile at each station was monitored frequently using a neutron probe. The schedule of events is shown in Table 1. Note that solution samples were collected frequently during and for 2 days after each irrigation, and with less frequency between irrigations. Care was taken to apply suction to the solution samplers for a short duration of time (≈ 30 min), so that the concentrations were more likely to resemble soil resident concentrations.

Method for estimating bare soil evaporation

Bare soil evaporation was estimated using the reference Evapotranspiration (ET) - crop coefficient approach (Wright, 1992). The alfalfa reference ET was computed using meteorological data from the National Weather Service Station located near the study field using procedures resulting from several years of research (Wright, 1981; Wright, 1982). A crop coefficient of 0.15 was selected for the bare, dry soil, and was allowed to increase to 1.0 when the soil surface was wet following

Table 1. Schedule of irrigation, precipitation, soil sample, and neutron probe measurement dates

Day	Irrigation mm	Irrigation CV	Precipitation mm	Soil♦ Sample	Neutron Probe
1	86♣	18			
3					x
5					x
8					x
11			6		
12					x
14					x
19					x
22					x
26				x	
28	75	10			
30					x
31					x
33					x
35					x
37					x
40					x
43					x
47				x	
48	227	31			x
49					x
51					x
52					x
54					x
57					x
61					
63				x	

♦ Soil samples were also collected prior to the beginning of the study.
♣ Irrigation amount includes both sprinkler and surface applications.

an irrigation. An observed drying time of 3 days was selected for the soil surface.

Method for estimating cumulative water input

Estimation of the volume of water infiltrated at a given station during furrow irrigation is dependent on local infiltration rates, and hence is difficult to measure. Comparison of volumetric water content values before and just after the first and second irrigations did not show a significant change in water content below the 1.8 m depth. This was no longer true during the last irrigation which lasted for 36 hours, as shown in appendix A and depicted in Figure 3 for station 10.

A water balance approach based on a 0 to 2.1 m control volume was used to determine cumulative water input during the first and second irrigations. Bare soil evaporation estimation was used as the sink term, and water content values measured by the neutron probe were used for estimating the change in storage. The near-surface (0 to 0.15 m) water content values were estimated using gravimetric data.

For the third irrigation, a volume balance approach was used to determine cumulative water inputs. The cumulative infiltration depth of each furrow was estimated by subtracting measured outflow and change in storage from measured inflow. For each of the 3 stations within a furrow, the cumulative water input was estimated by weighting the furrow infiltration estimations by their corresponding opportunity times. The opportunity time is the difference between observed recession and advance times, where water is available for infiltration at a given station. Table 1 shows the amount of field-average water input during each irrigation. Note the

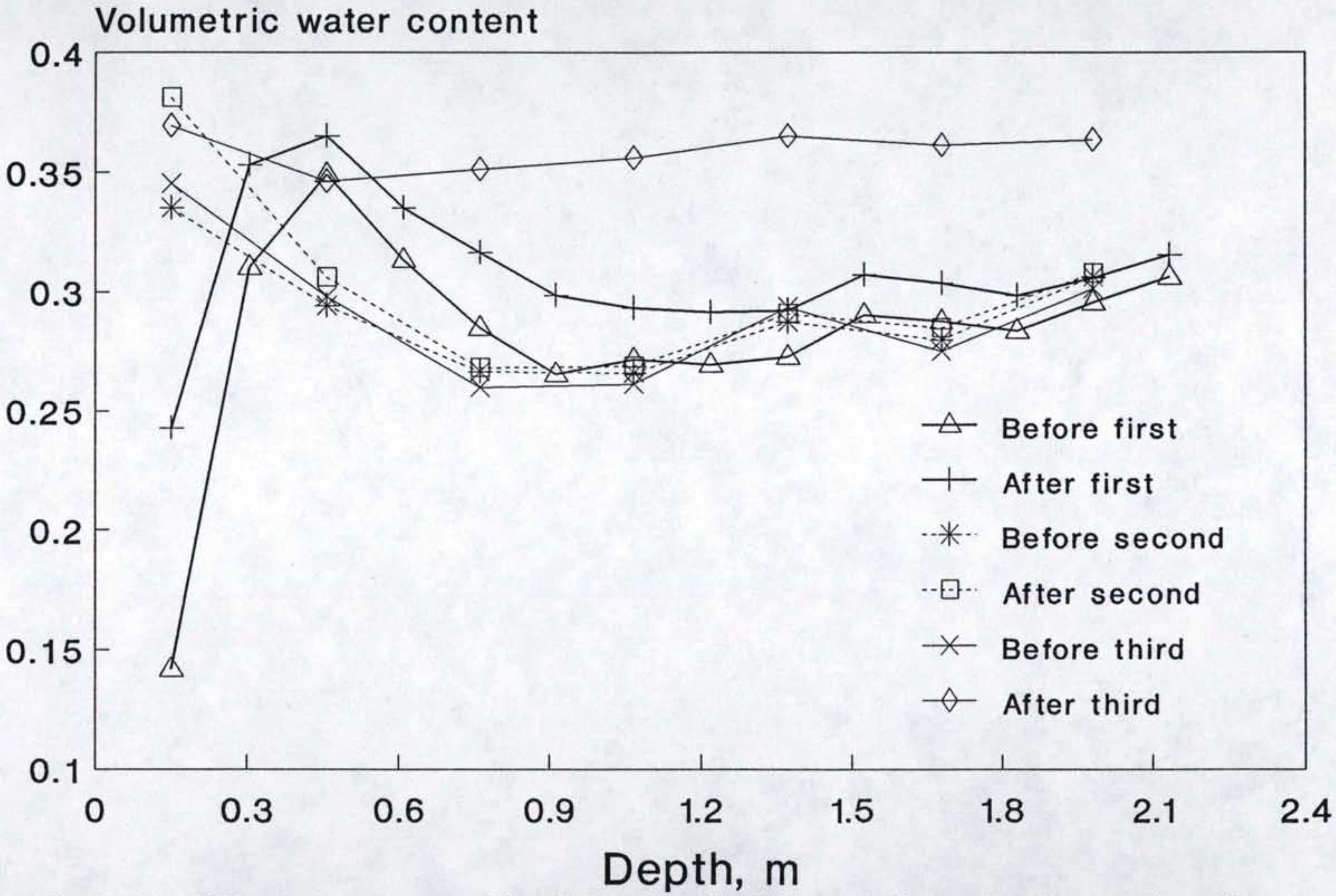

Figure 3. Water content profiles before and after each irrigation for station 10.

relatively high CV value for the third irrigation, which is an indication of temporal and spatial variability of infiltration rates observed during this 36-hour furrow irrigation event.

Method for estimating cumulative drainage

Cumulative drainage past 0.3 m, and 0.9 m depths was needed for the simple TFM validation. The water balance approach discussed above was used based on 0 to 0.3 m and 0 to 0.9 m control volumes for cumulative drainage estimations.

Method for Br analysis

All soil samples were air-dried at 30 C, crushed to pass a 0.002 m screen, and stored (<6 months) until analyzed. A predetermined amount of soil (12.5 g) was weighed into 25 ml of 0.01 M $CaCl_2$, shaken on a reciprocating shaker for 30 min, and filtered through a Whatman No. 42 filter paper. The filtrate was analyzed for Br by flow injection analysis (Lachat Instruments, Milwaukee, WI., Method No. 10-135-21-2-A). All water and soil-solution samples were stored at 7 C until analyzed for Br by the same flow injection procedure.

RESULTS AND DISCUSSIONS

Solute recovery

Initial nitrate concentration profiles showed that the oats failed to effectively remove the residual nitrate from the 0 to 0.9 m depth, where the solution samplers were installed. Therefore, only Br analysis will be discussed here. Table 2 shows solute recovery statistics for the soil sampling events and for the 0.3 m solution sampler. Br soil sample recovery of 64 to 83% with high coefficients of variation (CV) may be an indication of incorrect sample volume and/or nonuniform application of Br. We believe that neither of the two were the case for this study, since the soil cores were 50 mm in diameter, and catch can data showed relatively uniform Br application (CV=10%). The lower recovery values were probably due to the two-dimensional flow inherent in furrow irrigation. Despite our efforts to leach the Br below the bottom of furrow using an initial sprinkle irrigation, some Br did remain near the surface and was transported laterally to the middle of the furrow beds. The above argument is also applicable to the 0.3 m solution sampler, where a recovery of 85% with a high CV was observed (Table 2). To account for this apparent nonuniformity in solute amount, the concentration data for each station was normalized according to Dysons' et al. (1990) procedure prior to further analysis.

Field-scale movement of Bromide

Initial soil sampling showed negligible Br content. After each irrigation event, Br profiles measured using the soil samples (appendix B) were normalized on a station basis. The mass of Br recovery per unit volume of soil was determined by multiplying the measured concentration by the corresponding bulk density (Table 3), for each 0.15 m incremental depth. The incremental recovery values were divided by the total mass recovery of the corresponding station to determine the normalized

Table 2. Mass balance for soil samples and solution samplers at 0.3 m depth.

Soil Sample	Mean Recovery (%)	CV (%)
d26	71	42
d47	64	70
d63	83	88
Solution Sampler	85	75

Table 3. Average bulk density of soil profile.

Depth m	Bulk density Mg m^{-3}
0.15	1.53
0.30	1.40
0.45	1.41
0.60	1.45
0.75	1.42
0.90	1.39
1.00	1.36
1.20	1.33
1.50	1.35
1.80	1.35
2.10	1.35
2.40	1.37

concentration. Field-average normalized concentration of Br was determined for each incremental depth, at 3 different soil sampling periods using:

$$\left(\frac{C}{C_0}\right)_{i,\,d} = \sum_{j=1}^{21} \frac{A_j}{A} \left(\frac{C}{C_0}\right)_{i,\,j} \qquad [17]$$

where:

i = An integer ranging from 1 to 8 indicating the 0.15 m incremental depth.

d = The soil sampling day (d=26 or 47 or 63) [T],

A_j = The representative area covered by jth sampling station [L^2], and

A = Total field area [L^2].

The Br position was estimated as 0.23 m, 0.38 m, and 1.13 m, respectively, on the sampling dates corresponding to 26, 47, and 63 days since the study was begun (Figures 4 a-c). The relatively large amount of Br near the surface is an indication of lateral movement due to two-dimensional flow. This was observed on all 3 soil sample dates (d26, d47, and d63) as depicted in Figures 4 a-c. However, the near-surface Br concentration for d63 is more prominent, since the magnitude of the Br peak is reduced due to dispersion. Therefore, the true peak for the third sampling date is at 1.13 m with a secondary peak at 1.3 m.

Macroporosity considerations

Macropore flow is a possibility when observed Br movement is faster than that estimated by Darcy velocity or piston flow theory. Darcy velocity can be estimated for steady state periods by dividing depth of deep percolation for the period by the

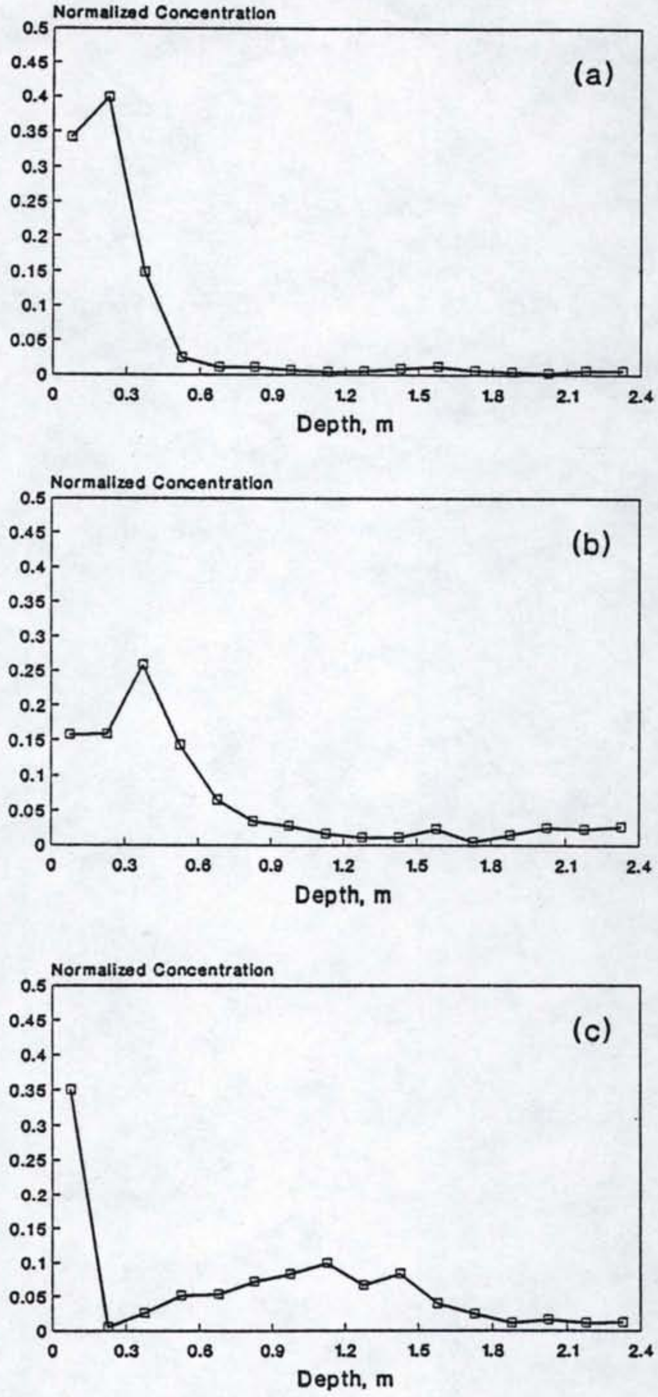

Figure 4. Field Average Br profiles from d26 (a), d47 (b), and d63 (c) Soil Sample data.

duration of the period. Furthermore, dividing the estimated Darcy velocity by the average volumetric water content will result in an estimate of the tracer velocity for any given observation period. Figure 5 shows cumulative drainage past 2.1 m depth as estimated by the water balance approach. The cumulative drainage curve was broken up into 4 straight line segments (periods). For each period tracer velocity, and the resulting depth of Br position was estimated. This method under-predicted solute position by 16 to 43 % as depicted in Figure 6, indicating the possibility of macropore flow.

A simple piston flow approach was also used to predict Br movement. It was assumed that Br will move with a uniform front depending on field capacity and effective depth of applied water:

$$d_{sf} = \frac{I_e}{fc} \qquad [18]$$

$$I_e = I_n - \Sigma E - I_{wd} \qquad [19]$$

$$I_{wd} = (fc - \overline{\Theta})\, d_{sf} \qquad [20]$$

where:

d_{sf} = Depth of solute front [L],

I_e = Effective depth of applied water [L],

fc = Volumetric water content at field capacity,

I_n = Net water input [L],

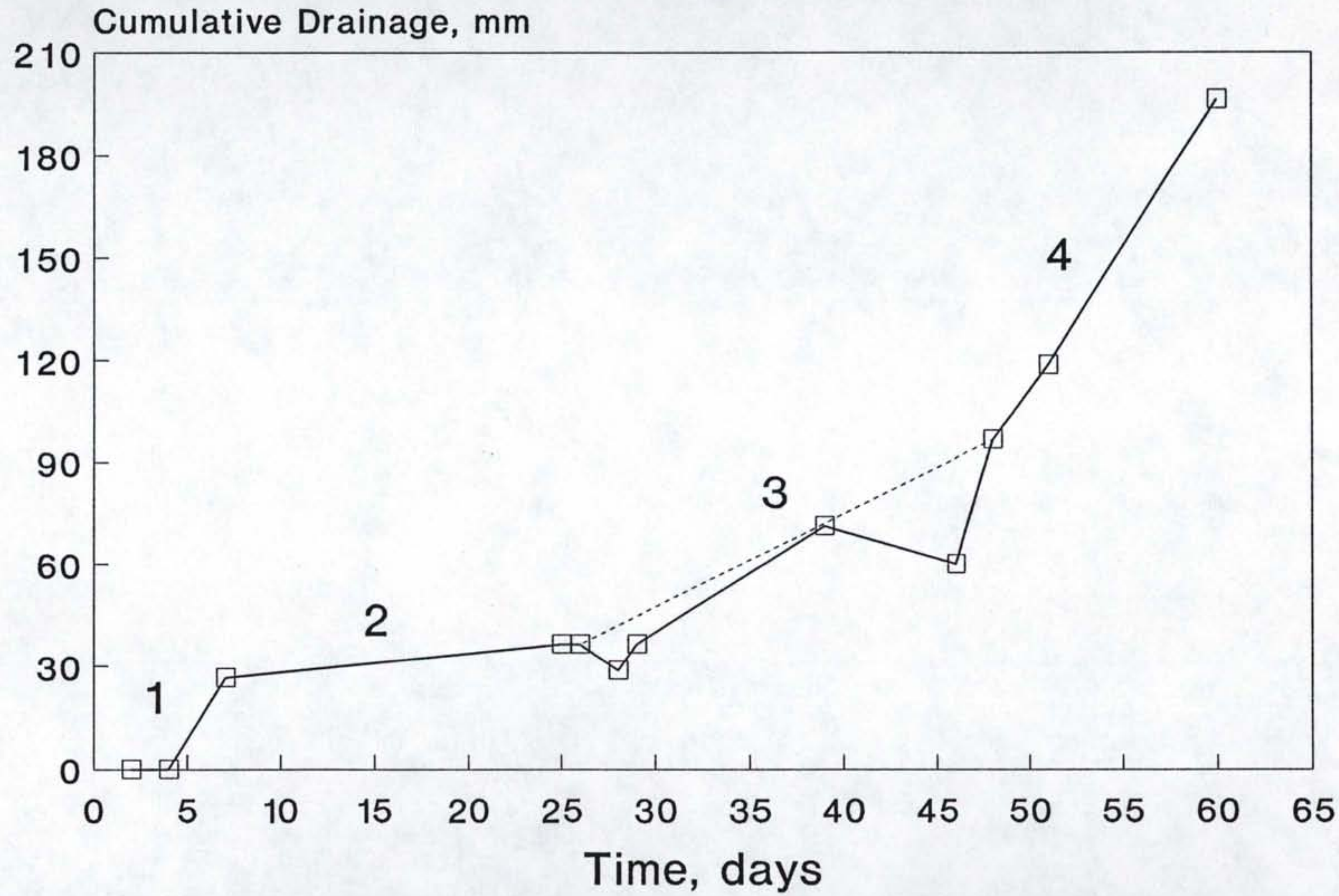

Figure 5. Cumulative drainage past 2.1 m depth as estimated from water balance approach.

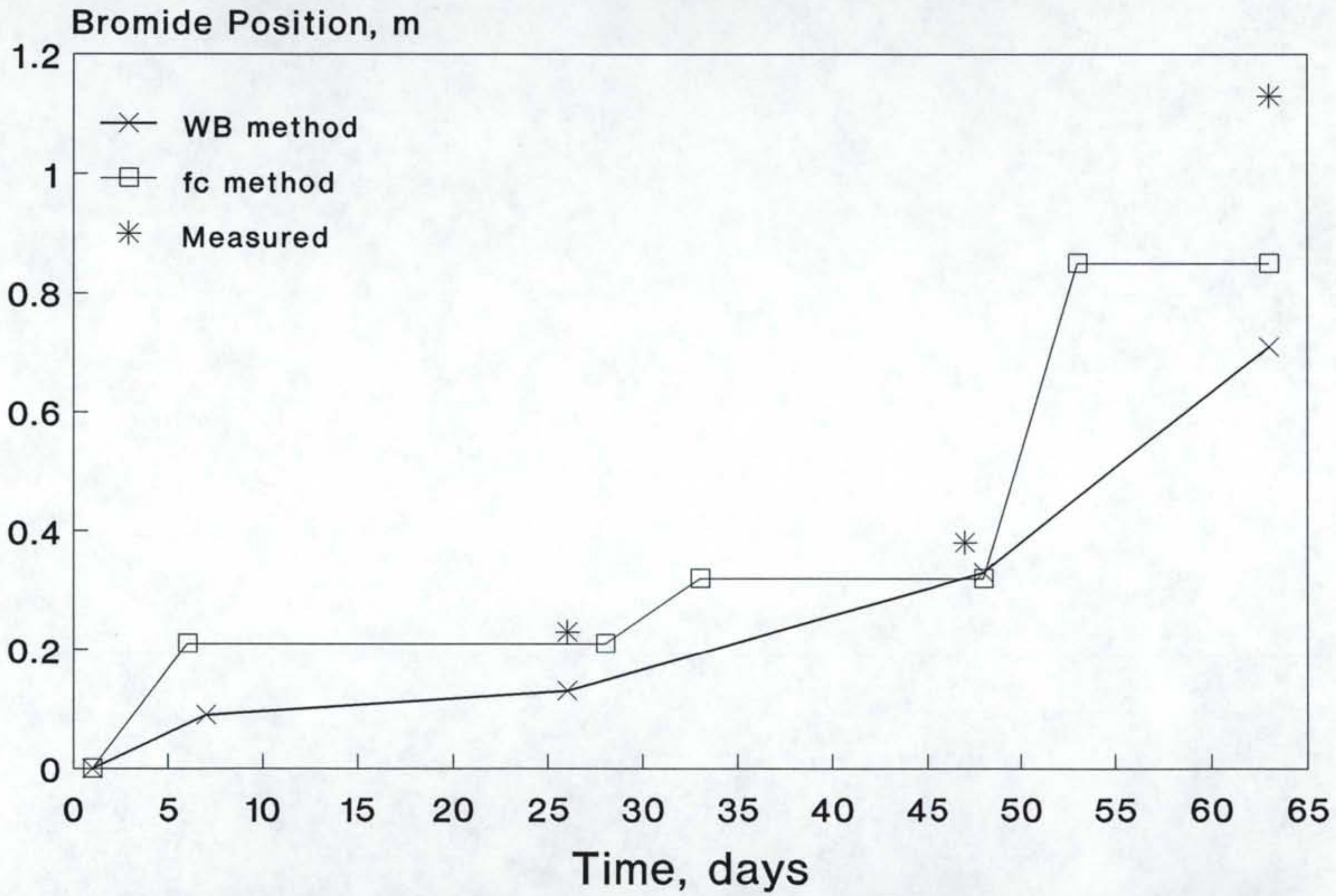

Figure 6. Measured field-average bromide position and predicted bromide movement by water balance (WB) and field capacity (fc) methods.

ΣE = Cumulative evaporation during the 5-day redistribution time after each irrigation [L],

I_{wd} = Depth of water deficit above the solute front [L], and

$\bar{\theta}$ = Average volumetric water content above the solute front prior to irrigation.

Field capacity was estimated as the average volumetric water content in the top soil (0 to 1.05 m) approximately 5 days after each irrigation. A fc of 0.307 was estimated, which agreed with previous observations on the same soil (Wright, 1992). The first irrigation moved the solute down to a depth of 0.21 m, resulting from 63 mm of effective applied water. Prior to the second and third irrigations, gravimetric soil samples were used to estimate the depth of water deficit above the predicted solute front. The second and third irrigations caused the solute to move to depths of 0.32 and 0.85 m, respectively. The simple piston flow approach under-estimated the final position of the solute front by 25%, indicating the possibility of macropore flow during the third irrigation (Figure 6).

Determination of calibration functions

The field-average calibration function was determined from both d26 and d47 soil sample and 0.3 m solution sampler data. For the case of the soil samples equation 10 was solved for f_L , where L was the 0.3 m depth, Z was a variable from 0.15 to 2.1 m, and f_z was the normalized concentration determined from the corresponding field-average Br profile (Figures 4 a-c). Parameter I was the average cumulative drainage depth past 0.3 m on the corresponding sampling date. Figure 7-a shows the calibration function from d26 soil samples. Note that only 3 prominent data points were available with all other data congregated near the origin. Since the general shape of the function was unknown, a straight line approximation was used over the interval where data were available, and the line was forced to pass through the origin. A similar approach was used to determine the calibration function at 0.3 m depth from d47 soil samples (Figure 7-b).

For the solution samplers at the 0.3 m depth, the concentration data were normalized on a station basis using equation 3 with I representing the cumulative drainage depth past 0.3 m depth. The calibration data (Figure 7-c) were lognormally distributed, as was also reported by Jury et al. (1982). The calibration function for the solution sampler is significantly different than those of the soil samples indicating differences in Br concentrations that they were sampling. We believe that the differences are due to the lack of hydraulic contact between the solution sampler and soil macropores, as will be discussed in the following section.

Validation of the TFM

Equation 10 was used to predict field-average Br profiles at different sampling dates for the d26 and d47 calibration functions. Note that predictions were only made for those ranges of drainage depths in which calibration functions were available. The shape of the profile and position of the peak on d47 were predicted by the d26 calibration function with reasonable accuracy (Figure 8). However, the d26 function

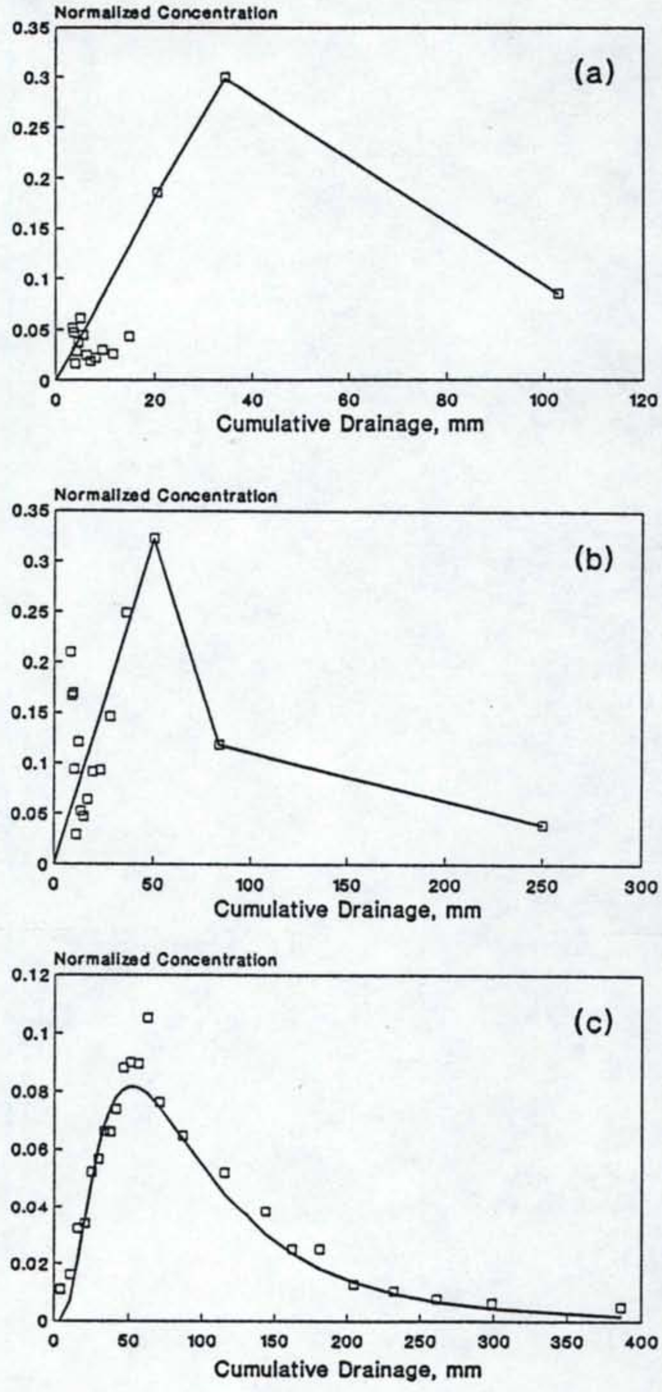

Figure 7. Calibration function at 0.3 m depth based on d26 (a) and d47 (b) soil sample and 0.3 m Solution Sampler (c) data.

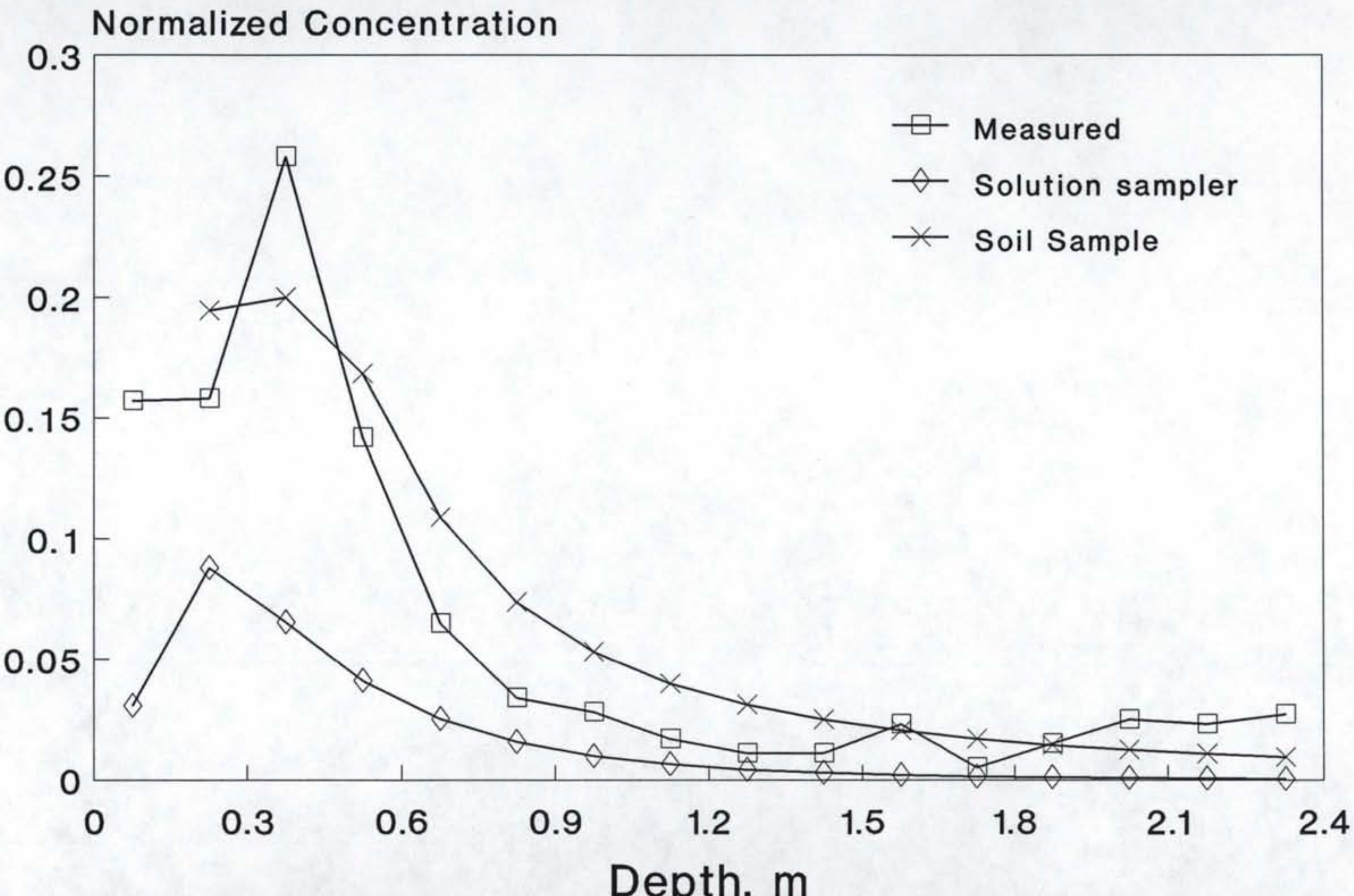

Figure 8. Field-average Br profile measured on d47 and predicted using d26 soil sample and 0.3 m Solution Sampler Calibration functions.

failed to predict the measured profile on d63 as depicted by Figure 9-a. The predictions for d63 measurements improved when d47 calibration function was used (Figure 9-b). This phenomena can be explained by the presence of a caliche layer, 50 to 150 mm in thickness, and spatially distributed in the field at 200 to 400 mm below the soil surface. On d26, the position of the solute front was approximately above this layer, while the solute front moved past this layer by d47. Therefore, solute movement in both the top soil and the caliche layer were included in the d47 calibration function which resulted in better predictions of the d63 measurements.

Validating simple TFM based on solution sampler data was not possible, since only 9 of the 0.9 m solution samplers collected solutions with significant Br content. Furthermore, it was not possible to normalize the concentration data from the 9 stations, since the complete breakthrough curves were not obtained. The lack of response for the rest of samplers were not due to inadequate net water input, since their mean net water input was only 9% lower than the other 9 samplers.

Macropores were observed within the soil profile and especially in the caliche layer. It was likely that some of the solution samplers were not in direct contact with the soil macropores (Litaor, 1988 ; Grossmann and Udluft, 1991), thus, resulting in a lack of response or a delayed response. The latter can be examined by using the calibration function based on 0.3 m solution samplers to validate d26 and d47 Br profiles. In both cases, the simple TFM predicted slower movement of Br and smaller magnitude of peak concentration as depicted in Figure 8 for d47 validation. The slower movement of Br might be an indication that the solution samplers failed to

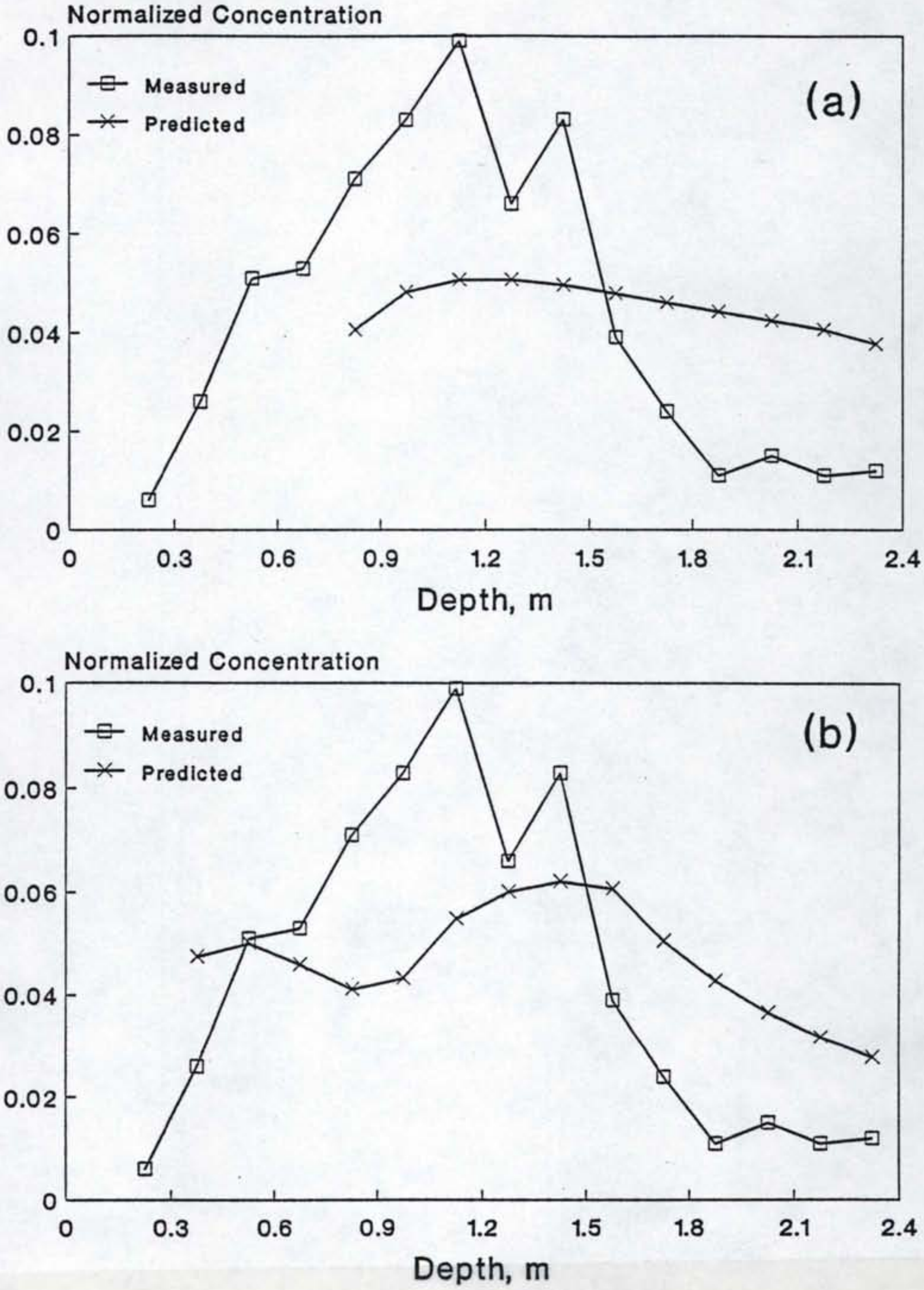

Figure 9. Field-Average Br profile measured on d63 and predicted using d26 (a) and d47 (b) calibration functions.

monitor the bypass flow that existed due to soil macropores. The latter might have also been the reason for significant differences in the magnitude of predicted peak concentrations. Another reason might be due to the inability of the solution samplers in sampling soil resident concentrations. This was less likely, since care were taken to apply short durations of suction (≈ 30 min) to the samplers .

SUMMARY AND CONCLUSIONS

The movement of bromide (Br) was monitored under variable conditions observed in a furrow irrigated field using solution samplers and soil samples. Simple models based on Darcy velocity and piston flow theory failed to predict the final Br position. The Br profiles were reasonably predicted by the simple TFM calibrated based on day 26 and day 47 soil samples. The simple TFM calibrated based on 0.3 m solution sampler data predicted a slower movement of the solute front. The delayed response was attributed to lack of direct contact to soil macropores. Use of soil samples is preferred over solution samplers for monitoring Br movement in soils with high macroporosity.

Considering the variable conditions observed in this study, such as nonuniformity in net water input, apparent nonuniformity in Br application, and transient water flow, use of the simple TFM based on soil sampling appears to be a promising approach for field-scale prediction of solute movement. Further research is needed to consider a generalized form of the TFM to account for lateral movement of solutes observed in furrow irrigation.

REFERENCES

Addiscott, T. M., and R. J. Wagenet. 1985. Concepts of solute leaching in soils: a review of modelling approaches. Journal of Soil Science, 36:411-424.

Amoozegar-Fard, A., D. R. Nielsen, and A. W. Warrick. 1982. Soil solute concentration distributions for spatially-varying pore water velocities and apparent diffusion coefficients. Soil Science Society of America Journal, 46:3-9.

Dagan, G. 1986. Statistical theory of groundwater flow and transport: pore to laboratory, laboratory to formation, and formation to the regional scale. Water Resources Research 22:1205-1345.

Dyson J. S., W. A. Jury, and G. L. Butters. 1990. The prediction and interpretation of chemical movement through porous media: the transfer function model approach. Final report to Electric Power Research Institute, Research Project 2485-6, EN-6853.

Izadi B., B. King, D. T. Westermann, and I. McCann. 1991. A transfer function model for prediction of solute transport in surface irrigated fields. ASAE paper No. PNW91-1002. Presented at the annual Pacific Northwest meeting of the ASAE at Sun Valley, Idaho.

Jury, W. A. 1982. Simulation of solute transport using a transfer model. Water Resources Research, 18:363-368.

Jury, W. A., L. H. Stolzy, and P. Shouse. 1982. A field test of the transfer function model for predicting solute transport. Water Resources Research, 18:369-375.

Jury, W. A., G. Sposito, and R. E. White. 1986. A transfer function model of solute transport through soil. 1. Fundamental concepts. Water Resources Research, 22:243-247.

Jury, W. A., J. S. Dyson, G. L. Butters. 1990. Transfer function model of field-scale solute transport under transient water flow. Soil Science Society of America Journal, 54:327-332.

Rice, R. C., R. S. Bowman, and D. B. Jaynes. 1986. Percolation of water below an irrigated field. Soil Science Society of America Journal, 50:855-859.

Rubin, J. 1983. Transport of reacting solutes in porous media: relation between mathematical nature of problem formulation and chemical nature of reactions. Water Resources Research, 19:1231-1252.

Sposito, G., W. A. Jury, and V. K. Gupta. 1986. Fundamental problems in the stochastic convection-dispersion model of solute transport in aquifers and field soils. Water Resources Research, 22:77-88.

White, R. E., J. S. Dyson, R. A. Haigh, W. A. Jury, and G. Sposito. 1986. The transfer function model of solute transport through soil. 2. Illustrative applications. Water Resources Research 22:248-254.

Wright, J. L. 1981. Crop coefficients for estimates of daily crop evapotranspiration. Proceedings of the Irrigation Scheduling Conference, ASAE, pp. 18-26.

Wright, J. L. 1982. New evapotranspiration crop coefficients. Journal of Irrigation and Drainage Division, ASCE, IR1, 108:57-74.

Wright, J. L. 1992. Personal communications.

APPENDIX A

Water Content Profiles before and
after each Irrigation

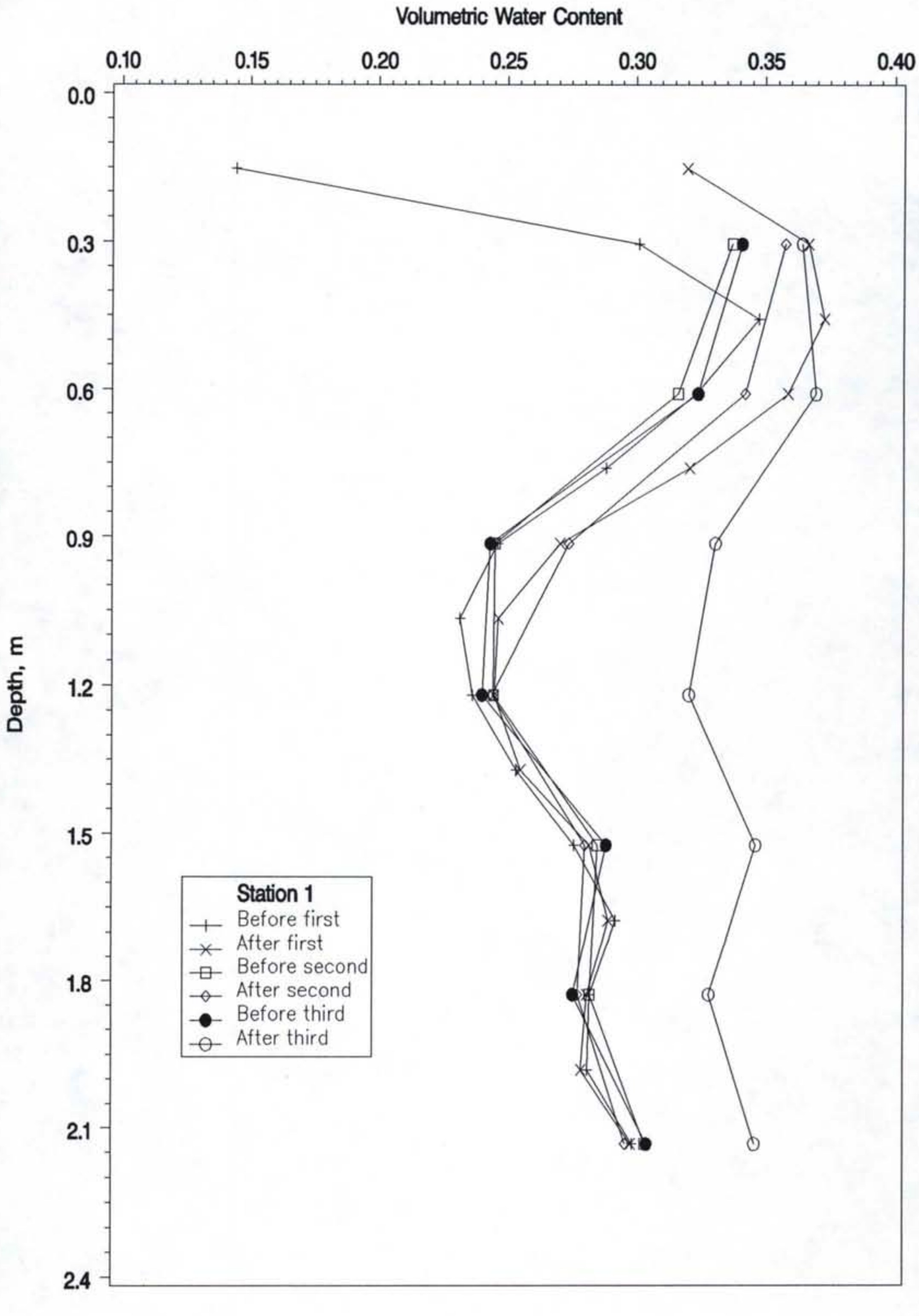

Volumetric Water Content
0.10
0.15
0.20
0.25
0.30
0.35
0.40
0.0
0.3
0.6
0.9
1.2
1.5
1.8
2.1
2.4
Depth, m
Station 1
Before first
After first
Before second
After second
Before third
After third

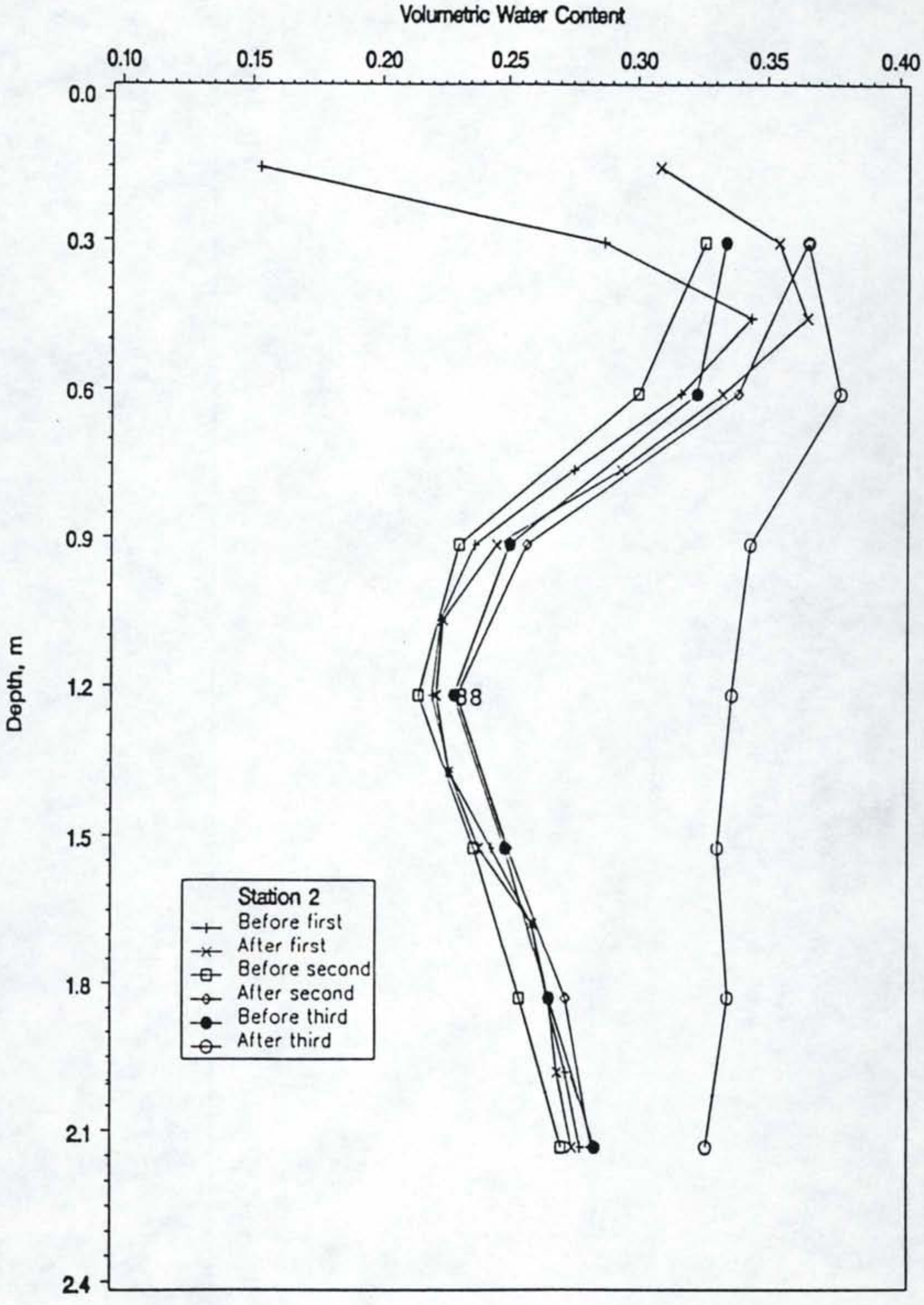

Volumetric Water Content
0.10
0.15
0.20
0.25
0.30
0.35
0.40
0.0
0.3
0.6
0.9
1.2
1.5
1.8
2.1
2.4
Depth, m
Station 2
Before first
After first
Before second
After second
Before third
After third

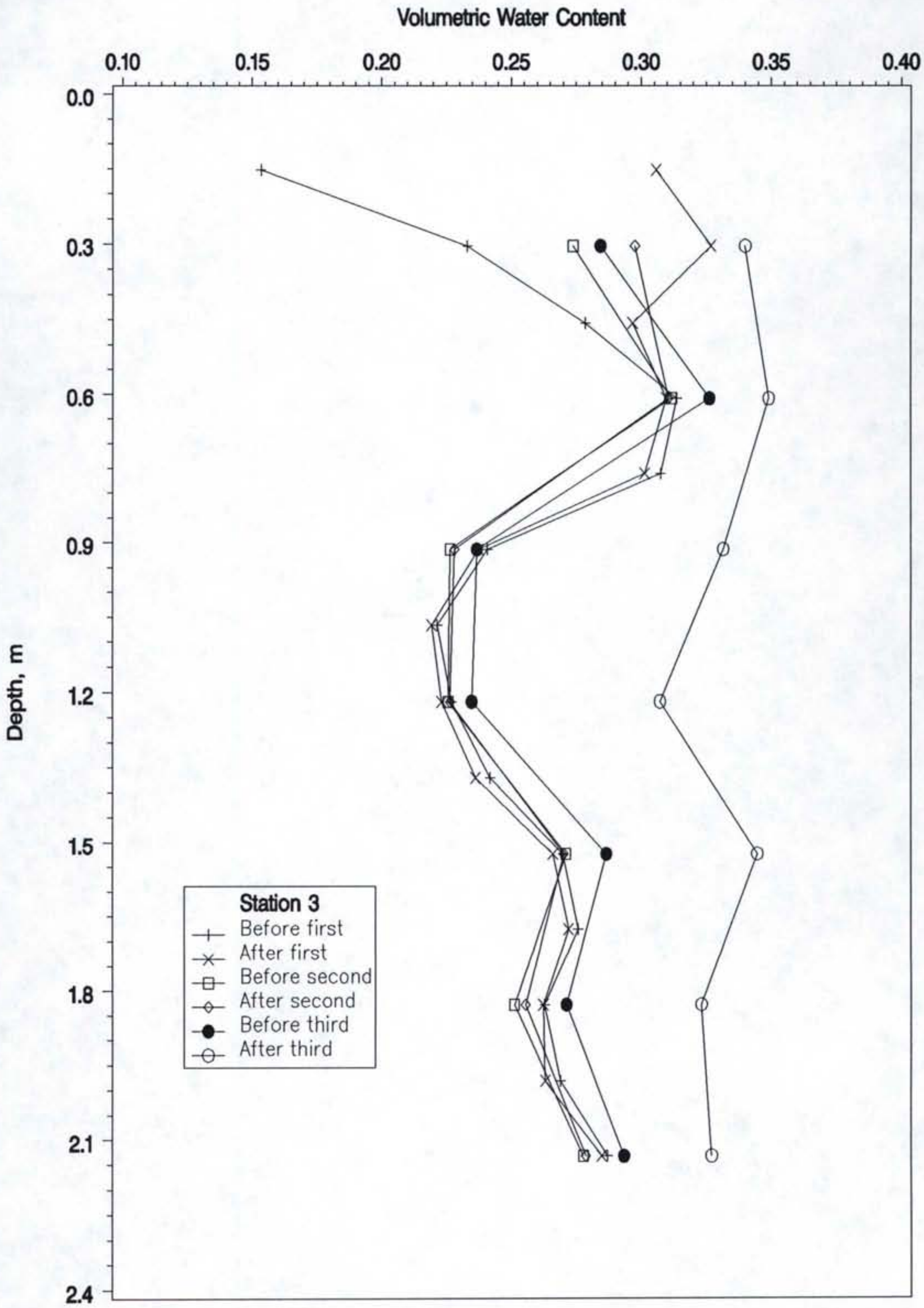

Volumetric Water Content
0.10
0.15
0.20
0.25
0.30
0.35
0.40
0.0
0.3
0.6
0.9
1.2
1.5
1.8
2.1
2.4
Depth, m
Station 3
Before first
After first
Before second
After second
Before third
After third

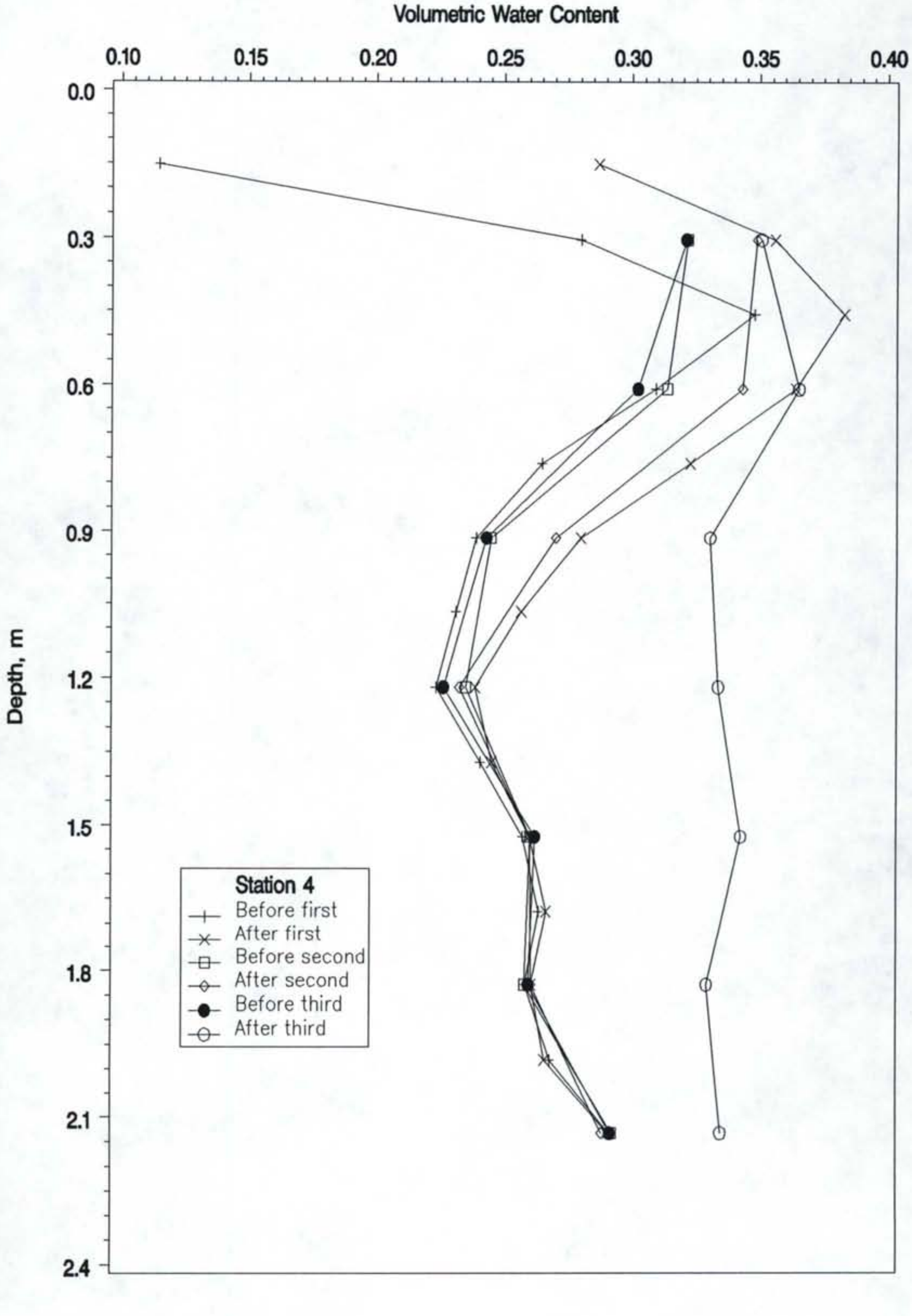

Volumetric Water Content
0.10
0.15
0.20
0.25
0.30
0.35
0.40
0.0
0.3
0.6
0.9
1.2
1.5
1.8
2.1
2.4
Depth, m
Station 4
Before first
After first
Before second
After second
Before third
After third

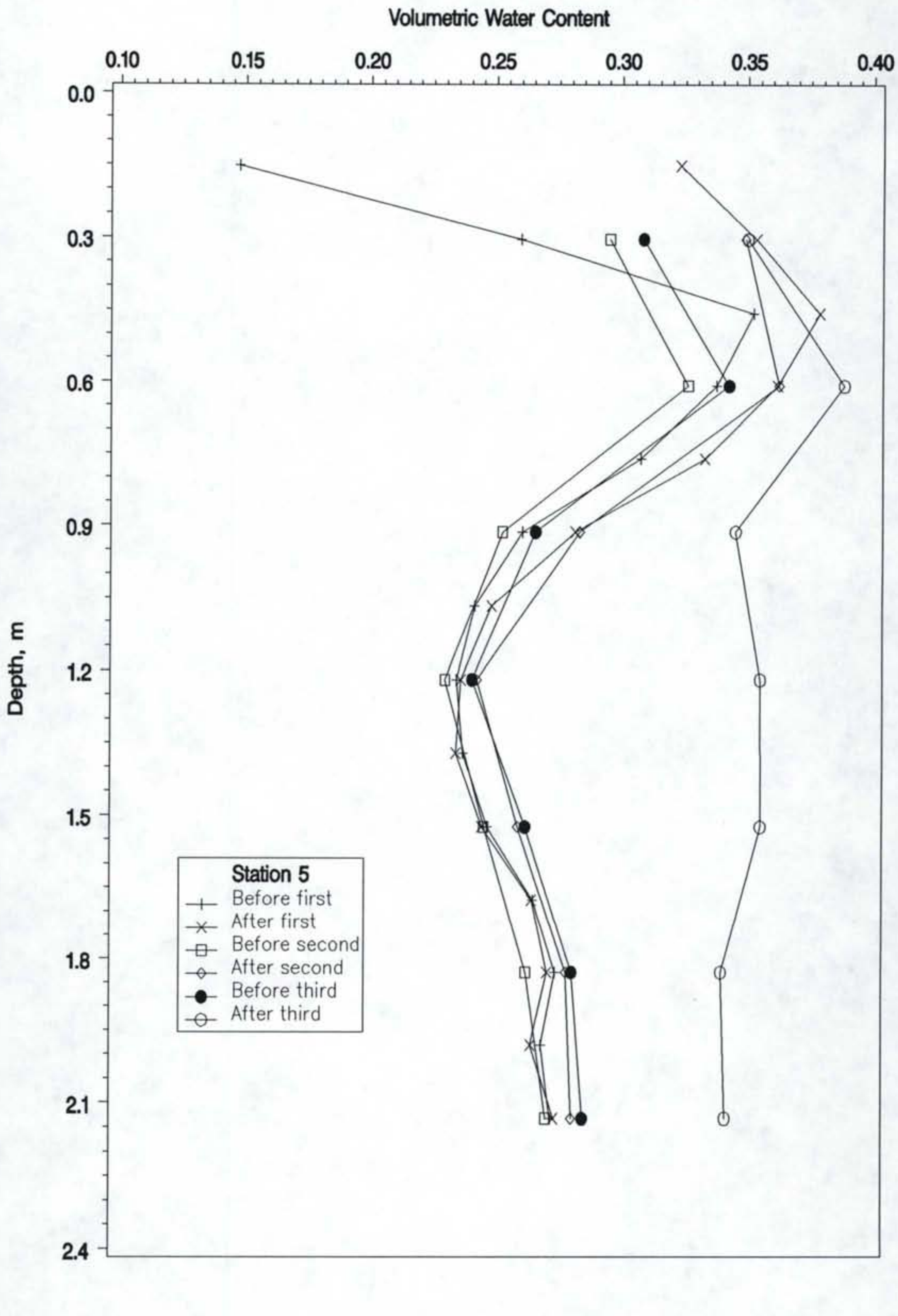
Volumetric Water Content
0.10
0.15
0.20
0.25
0.30
0.35
0.40
Depth, m
0.0
0.3
0.6
0.9
1.2
1.5
1.8
2.1
2.4
Station 5
Before first
After first
Before second
After second
Before third
After third

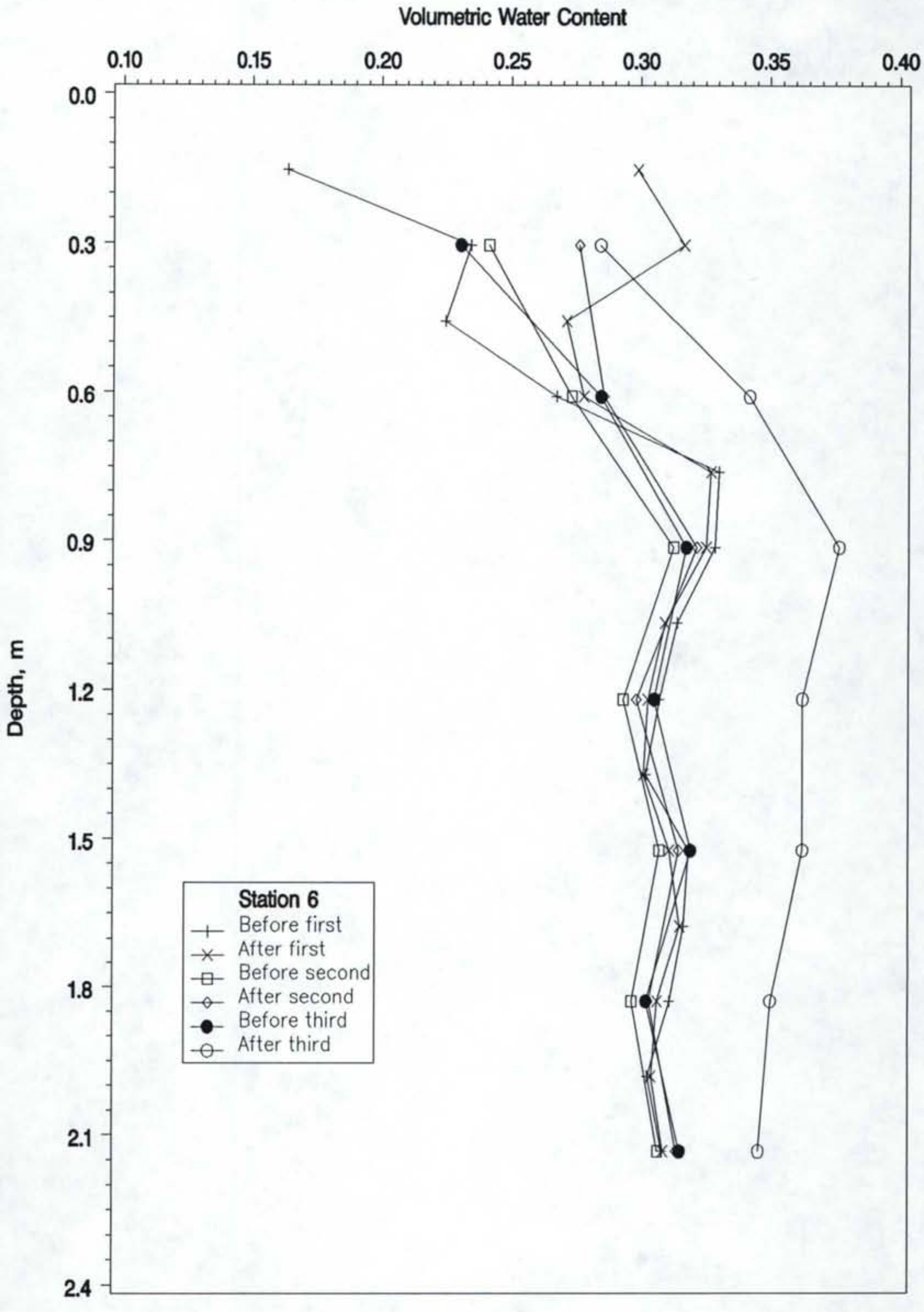

Volumetric Water Content
0.10
0.15
0.20
0.25
0.30
0.35
0.40
0.0
0.3
0.6
0.9
1.2
1.5
1.8
2.1
2.4
Depth, m
Station 6
Before first
After first
Before second
After second
Before third
After third

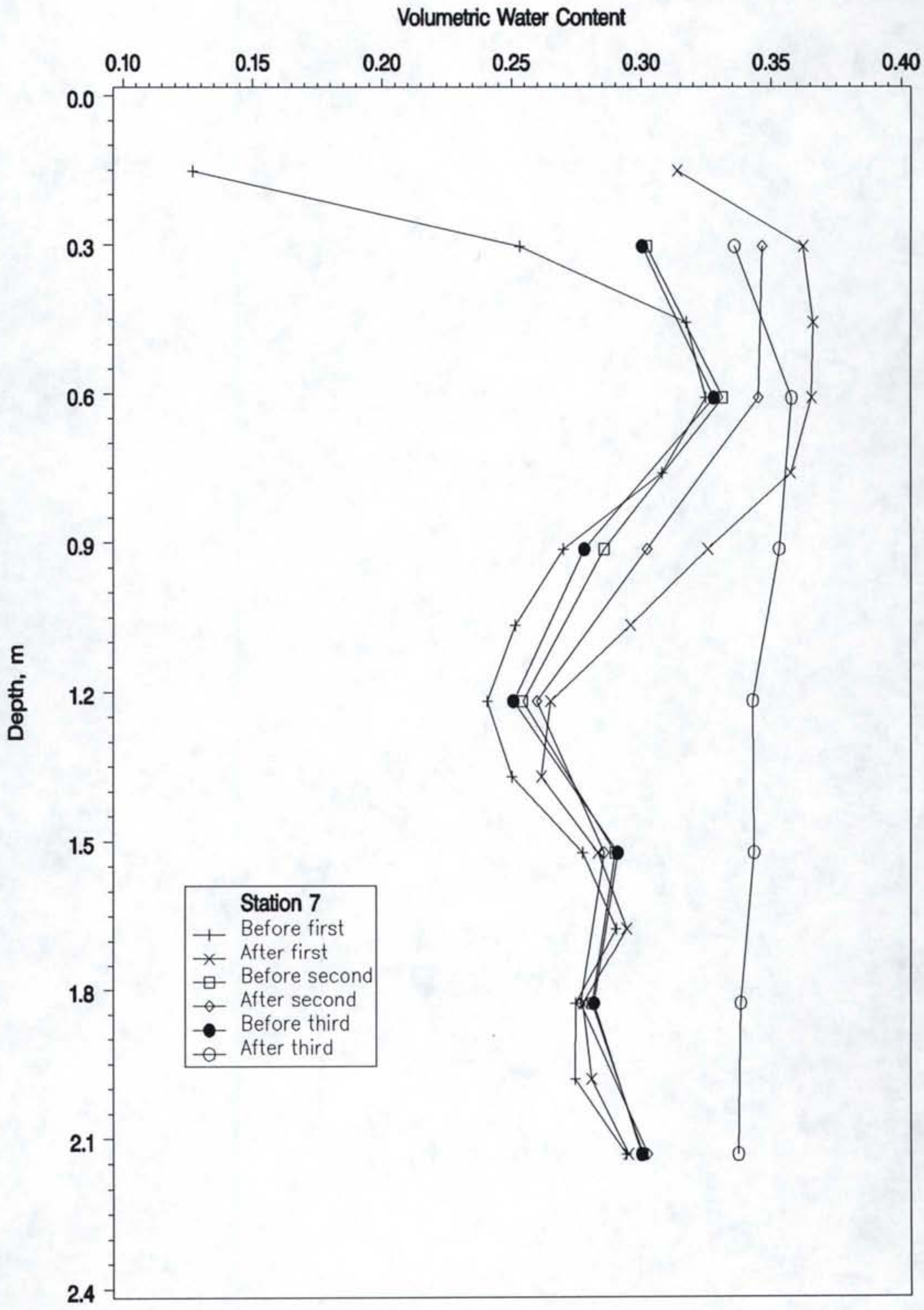
Volumetric Water Content
0.10
0.15
0.20
0.25
0.30
0.35
0.40
0.0
0.3
0.6
0.9
1.2
1.5
1.8
2.1
2.4
Depth, m
Station 7
Before first
After first
Before second
After second
Before third
After third

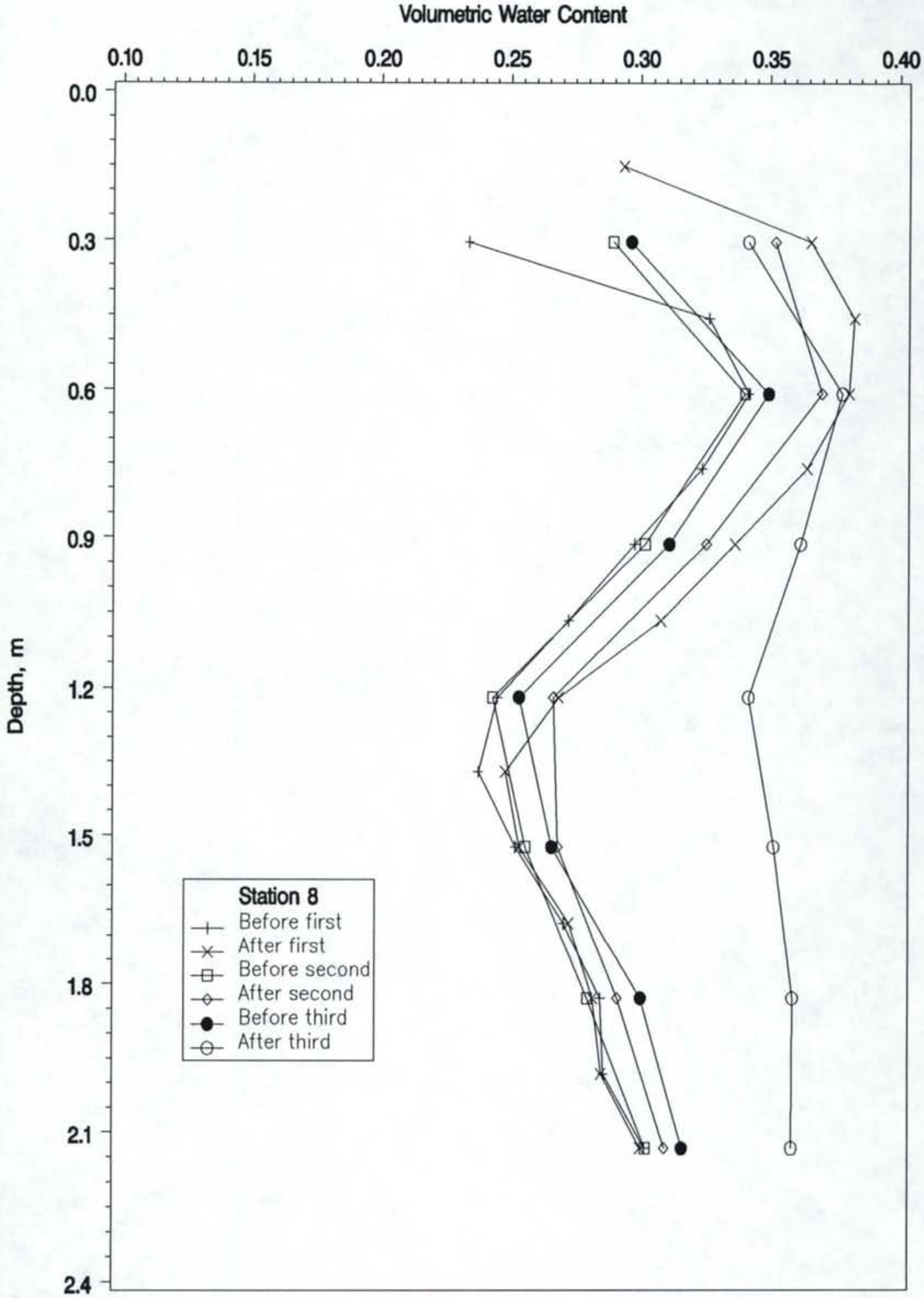
Volumetric Water Content
0.10
0.15
0.20
0.25
0.30
0.35
0.40
0.0
0.3
0.6
0.9
1.2
1.5
1.8
2.1
2.4
Depth, m
Station 8
Before first
After first
Before second
After second
Before third
After third

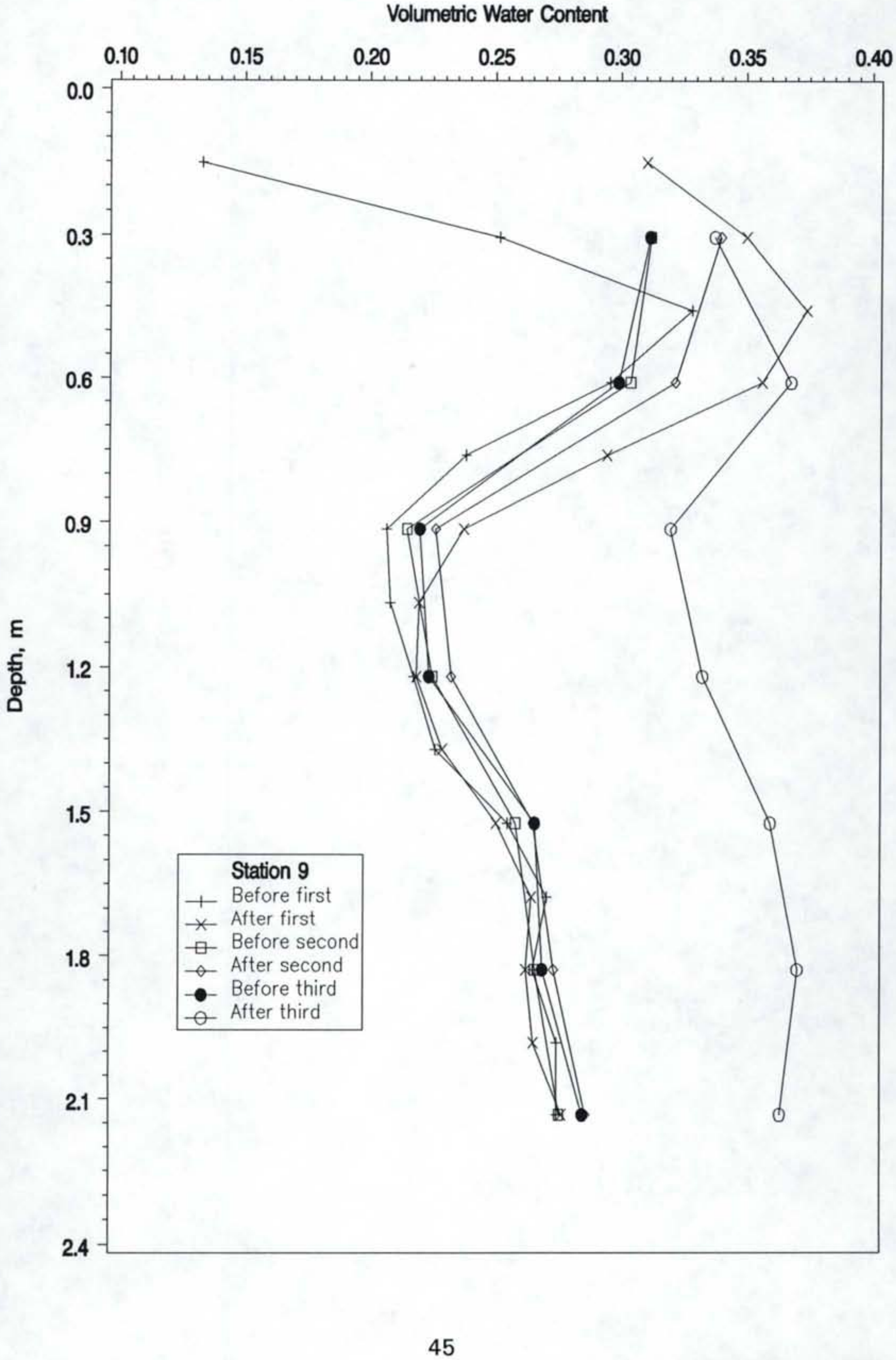

Volumetric Water Content
0.10
0.15
0.20
0.25
0.30
0.35
0.40
0.0
0.3
0.6
0.9
1.2
1.5
1.8
2.1
2.4
Depth, m
Station 9
Before first
After first
Before second
After second
Before third
After third

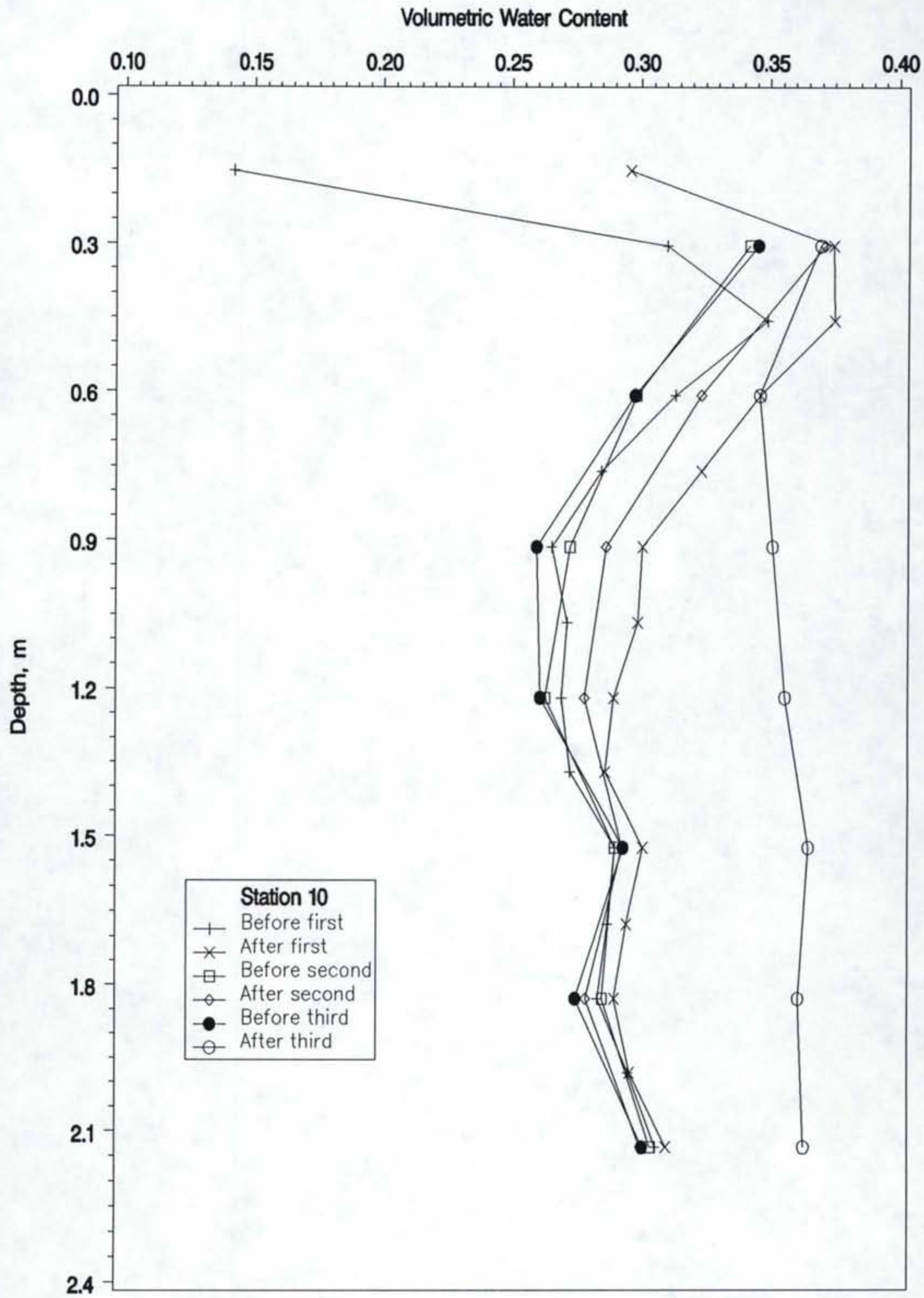
Volumetric Water Content
0.10
0.15
0.20
0.25
0.30
0.35
0.40
0.0
0.3
0.6
0.9
1.2
1.5
1.8
2.1
2.4
Depth, m
Station 10
Before first
After first
Before second
After second
Before third
After third

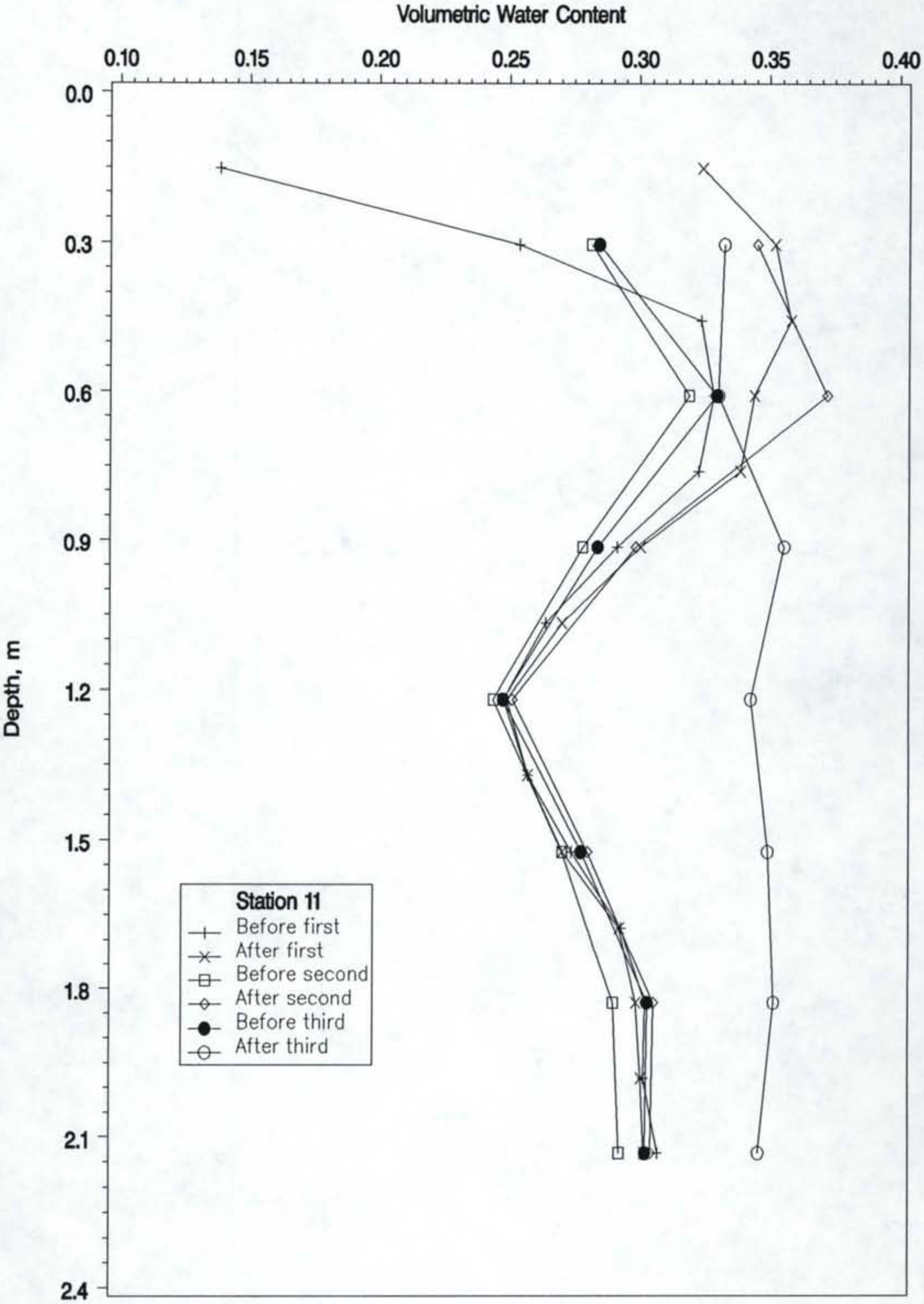
Volumetric Water Content
0.10
0.15
0.20
0.25
0.30
0.35
0.40
0.0
0.3
0.6
0.9
1.2
1.5
1.8
2.1
2.4
Depth, m
Station 11
Before first
After first
Before second
After second
Before third
After third

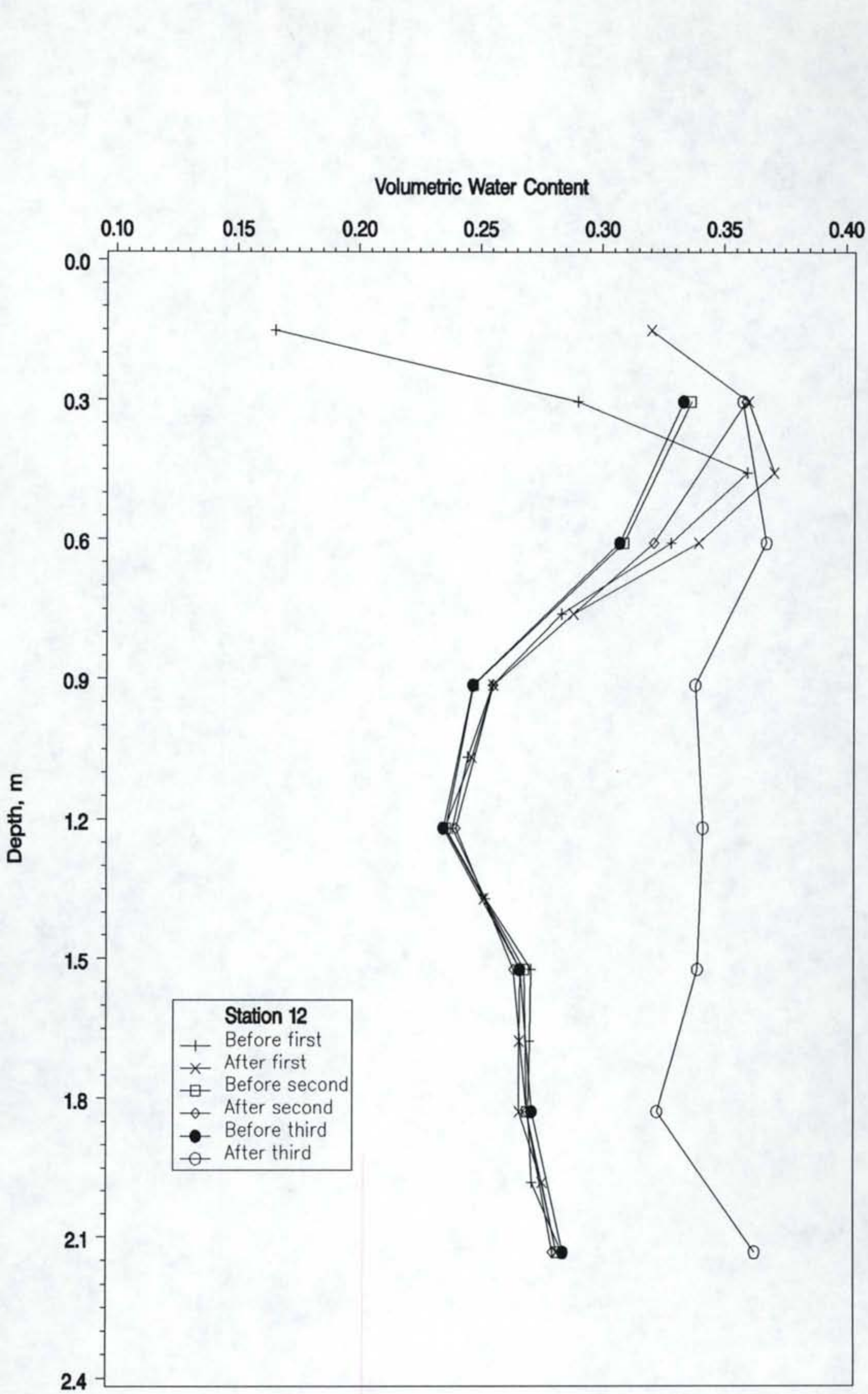
Volumetric Water Content
0.10
0.15
0.20
0.25
0.30
0.35
0.40
0.0
0.3
0.6
0.9
1.2
1.5
1.8
2.1
2.4
Depth, m
Station 12
Before first
After first
Before second
After second
Before third
After third

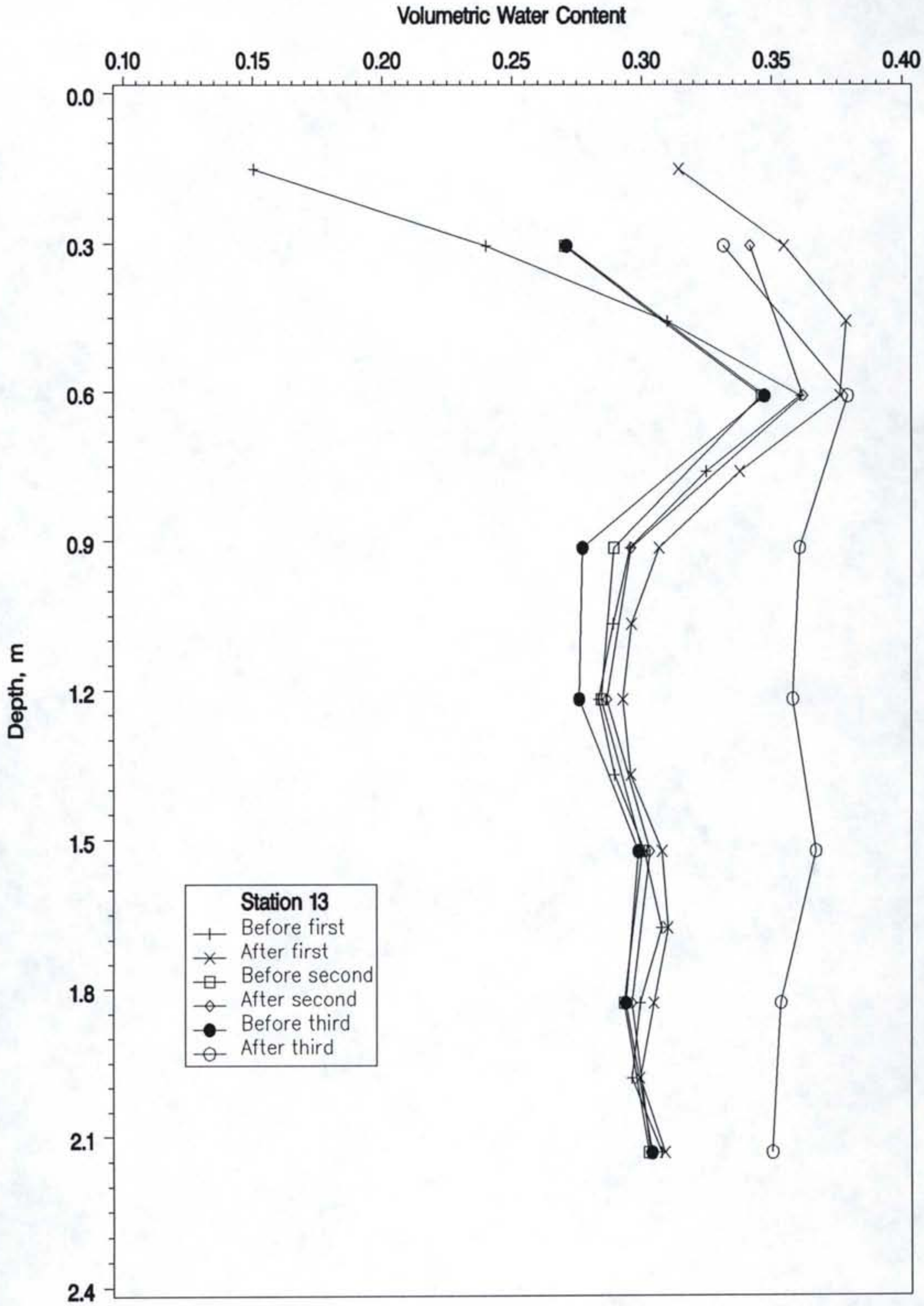

Volumetric Water Content
0.10
0.15
0.20
0.25
0.30
0.35
0.40
0.0
0.3
0.6
0.9
1.2
1.5
1.8
2.1
2.4
Depth, m
Station 13
Before first
After first
Before second
After second
Before third
After third

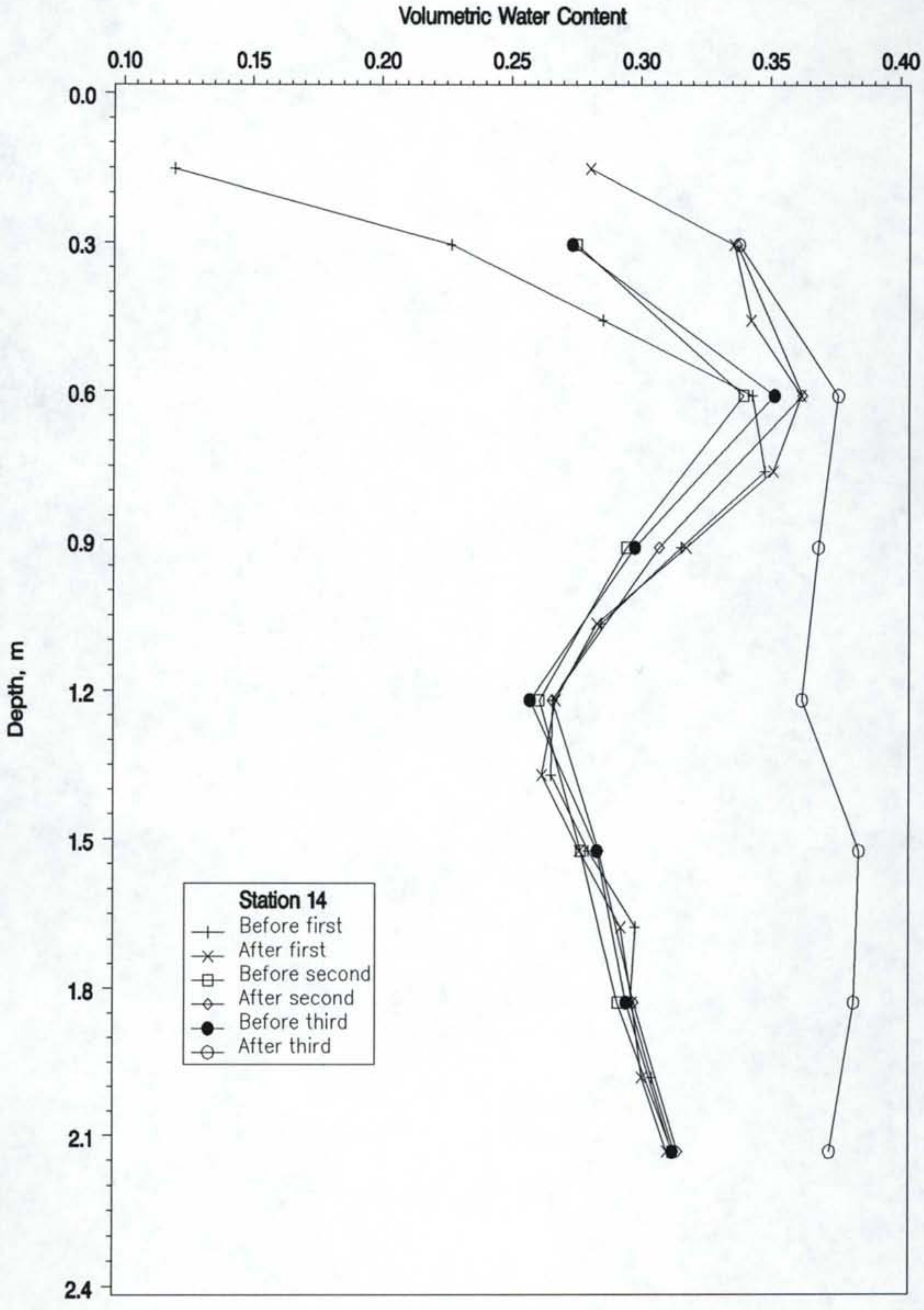

Volumetric Water Content
0.10
0.15
0.20
0.25
0.30
0.35
0.40
0.0
0.3
0.6
0.9
1.2
1.5
1.8
2.1
2.4
Depth, m
Station 14
Before first
After first
Before second
After second
Before third
After third

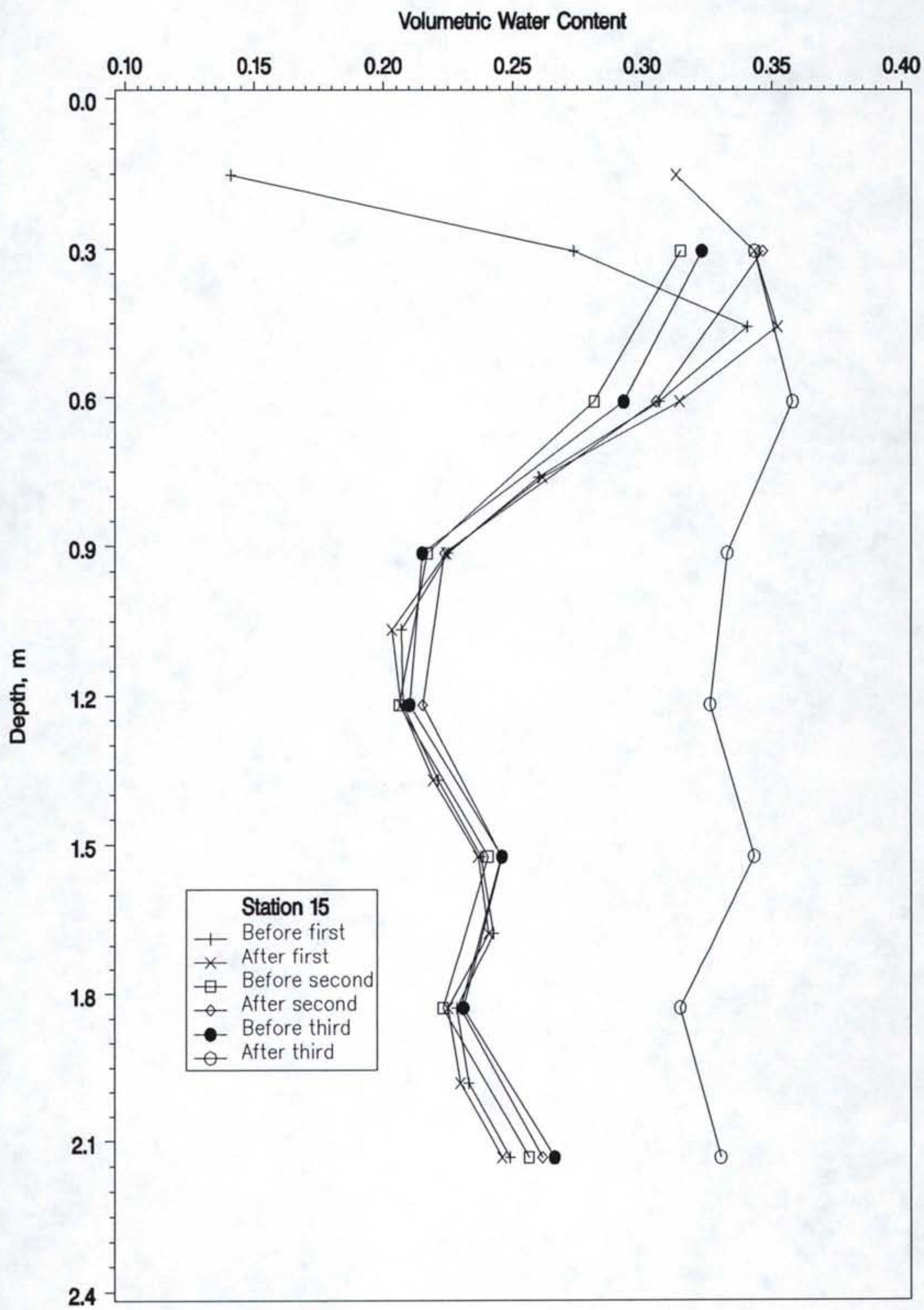
Volumetric Water Content
0.10
0.15
0.20
0.25
0.30
0.35
0.40
Depth, m
0.0
0.3
0.6
0.9
1.2
1.5
1.8
2.1
2.4
Station 15
Before first
After first
Before second
After second
Before third
After third

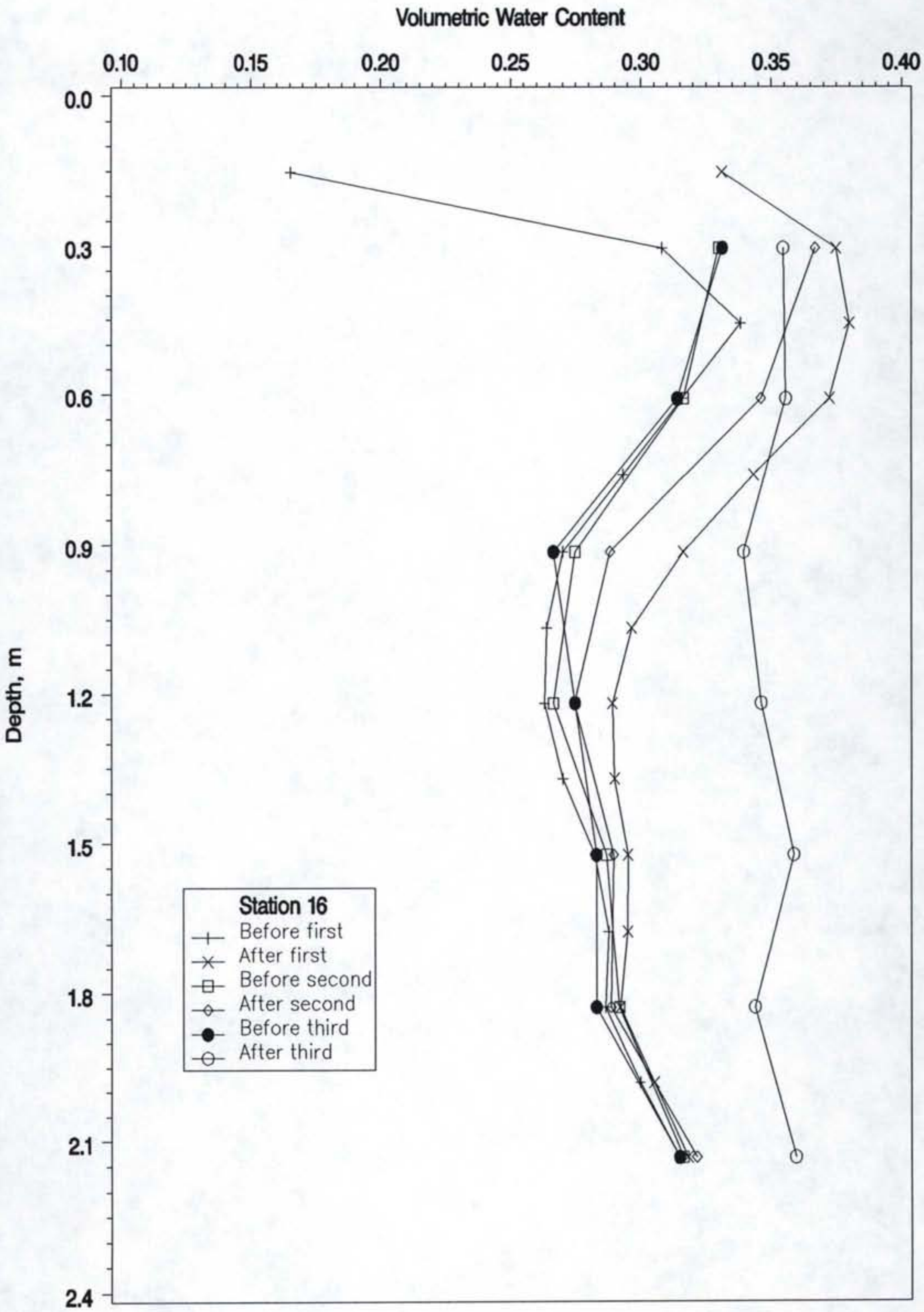
Volumetric Water Content
0.10
0.15
0.20
0.25
0.30
0.35
0.40
Depth, m
0.0
0.3
0.6
0.9
1.2
1.5
1.8
2.1
2.4
Station 16
Before first
After first
Before second
After second
Before third
After third

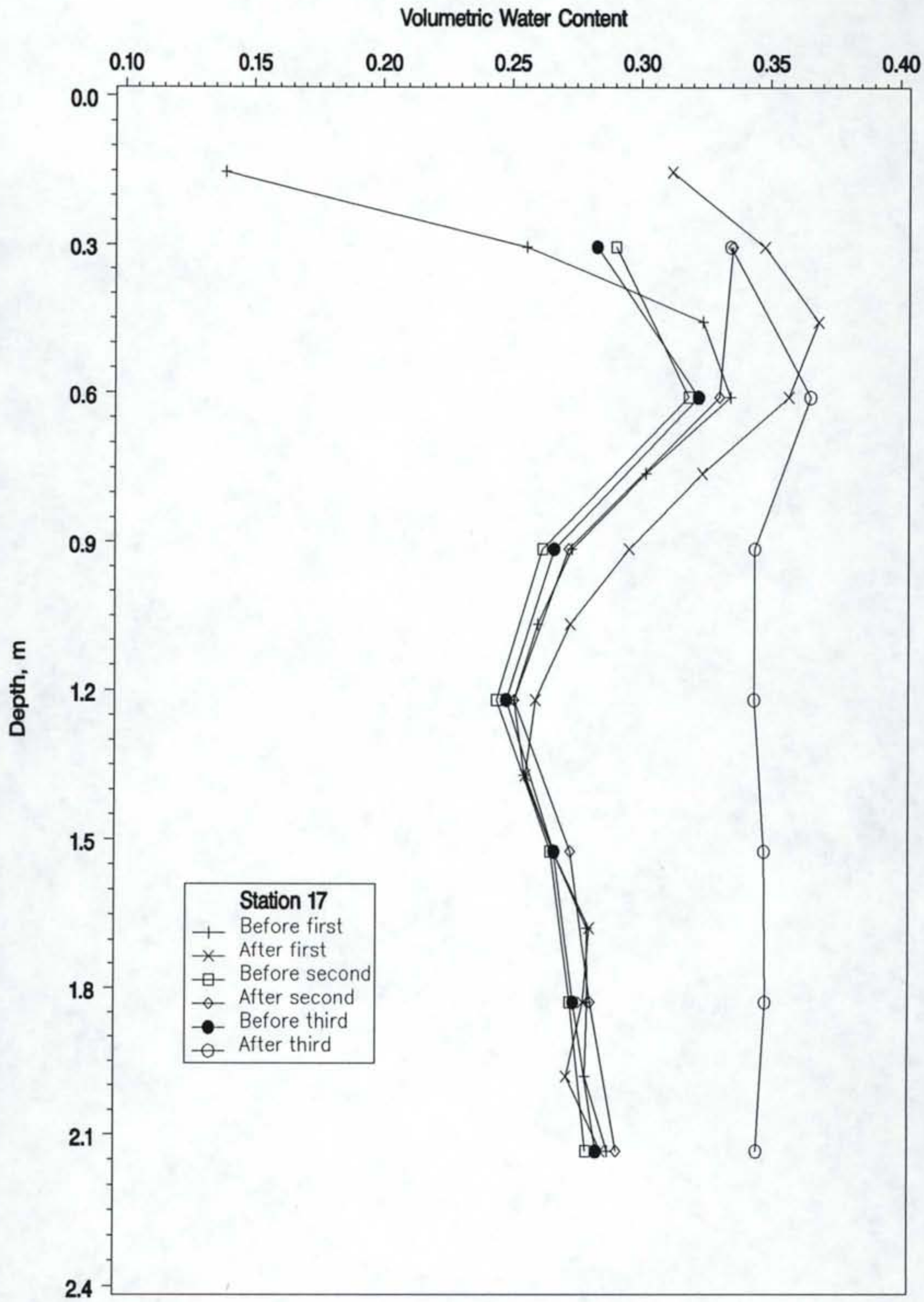

Volumetric Water Content
0.10
0.15
0.20
0.25
0.30
0.35
0.40
0.0
0.3
0.6
0.9
1.2
1.5
1.8
2.1
2.4
Depth, m
Station 17
Before first
After first
Before second
After second
Before third
After third

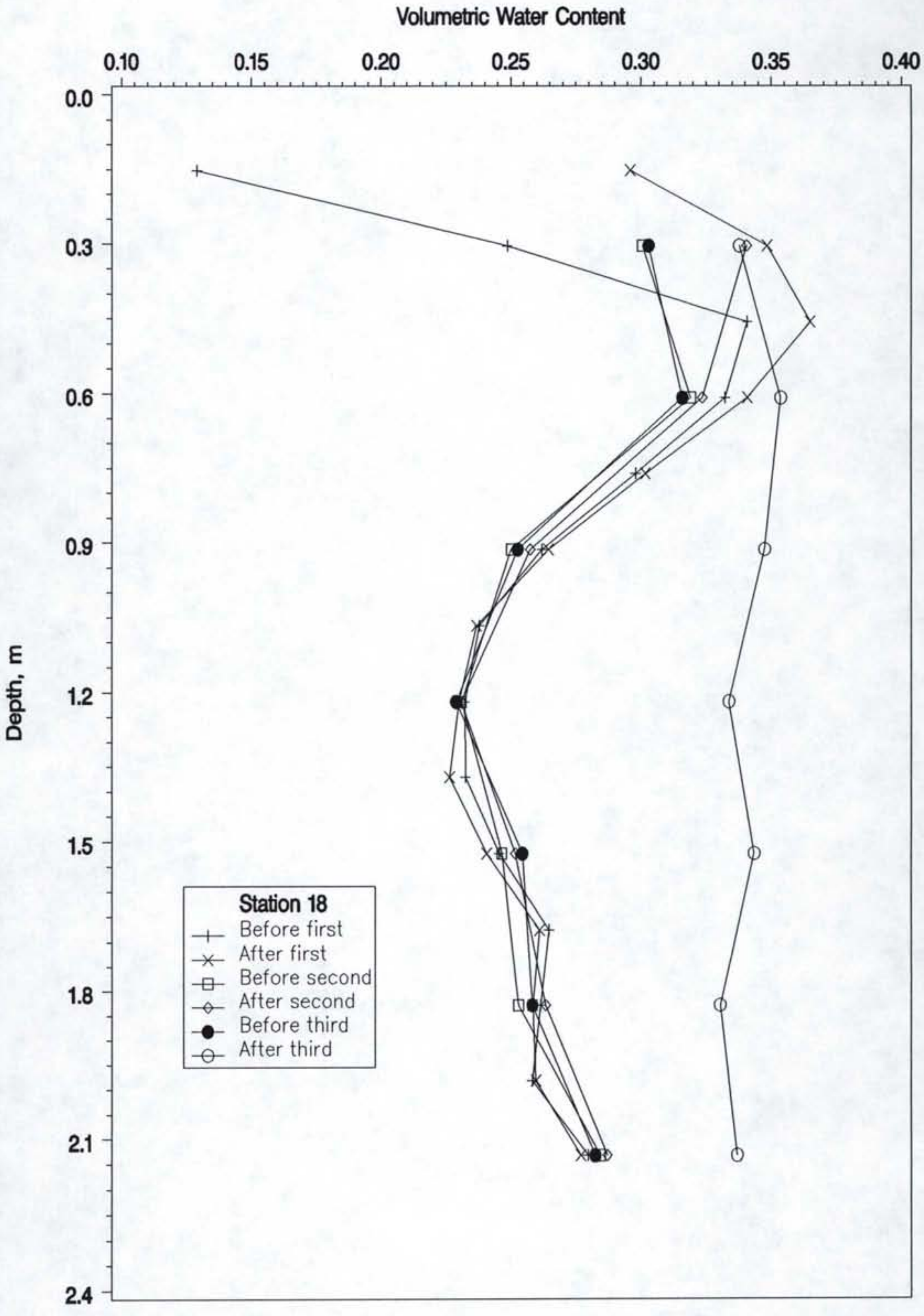

Volumetric Water Content
0.10
0.15
0.20
0.25
0.30
0.35
0.40
0.0
0.3
0.6
0.9
1.2
1.5
1.8
2.1
2.4
Depth, m
Station 18
Before first
After first
Before second
After second
Before third
After third

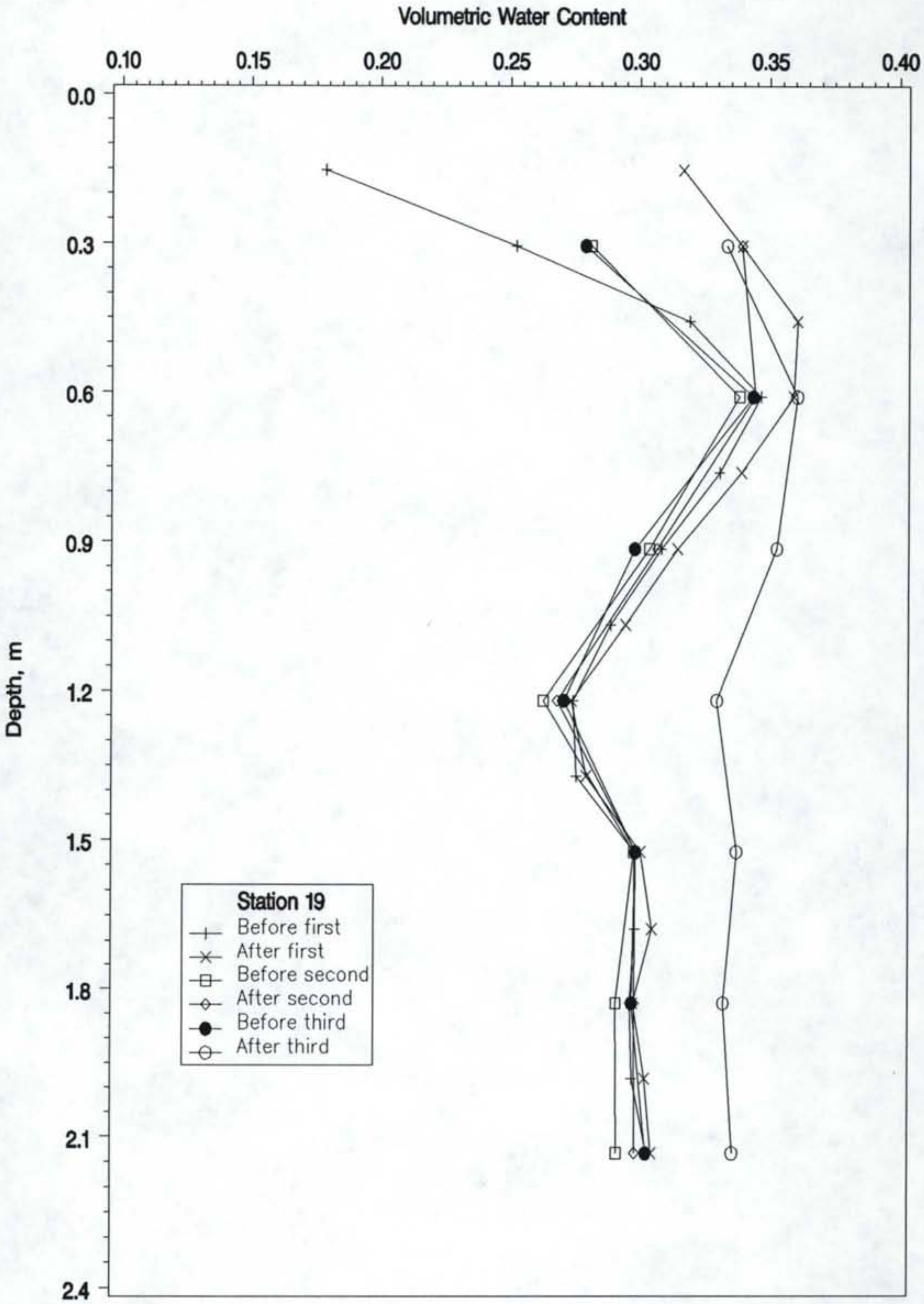
Volumetric Water Content
0.10
0.15
0.20
0.25
0.30
0.35
0.40
0.0
0.3
0.6
0.9
1.2
1.5
1.8
2.1
2.4
Depth, m
Station 19
Before first
After first
Before second
After second
Before third
After third

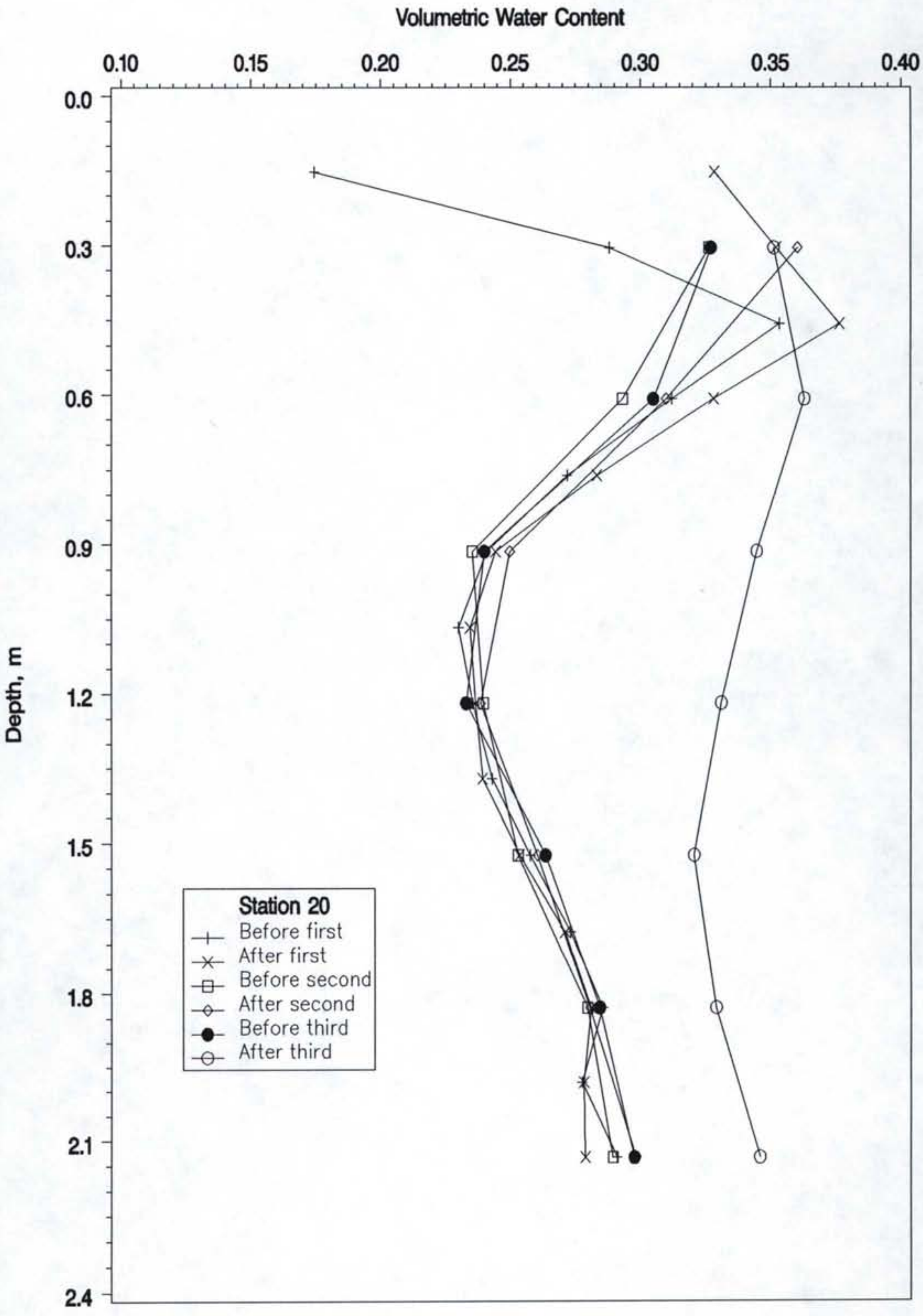

Volumetric Water Content
0.10
0.15
0.20
0.25
0.30
0.35
0.40
0.0
0.3
0.6
0.9
1.2
1.5
1.8
2.1
2.4
Depth, m
Station 20
Before first
After first
Before second
After second
Before third
After third

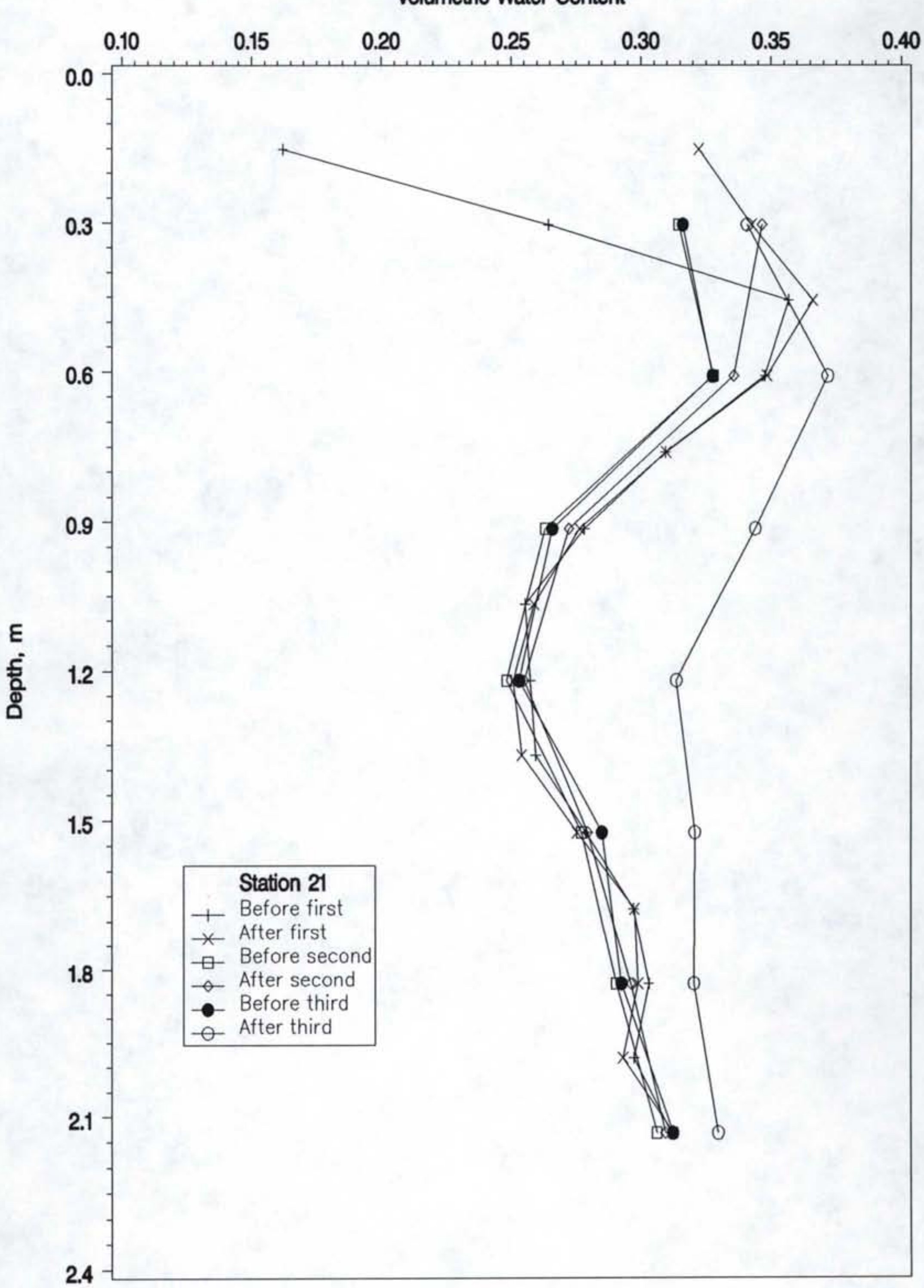
Volumetric Water Content
0.10
0.15
0.20
0.25
0.30
0.35
0.40
Depth, m
0.0
0.3
0.6
0.9
1.2
1.5
1.8
2.1
2.4
Station 21
Before first
After first
Before second
After second
Before third
After third

APPENDIX B

Bromide Profiles Measured Using the Soil Samples
after each Irrigation Event

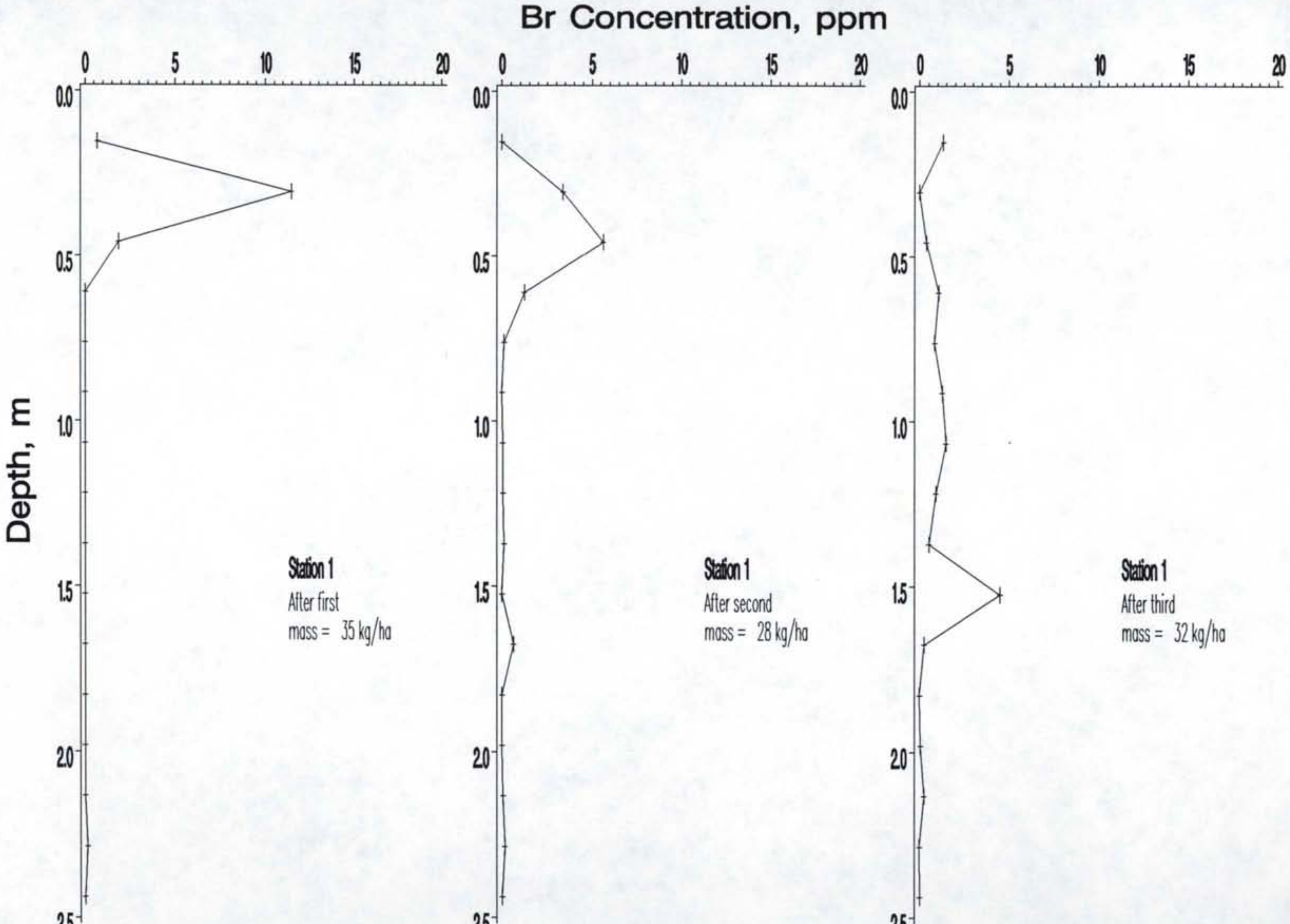
Br Concentration, ppm
Depth, m
Station 1
After first
mass = 35 kg/ha
Station 1
After second
mass = 28 kg/ha
Station 1
After third
mass = 32 kg/ha

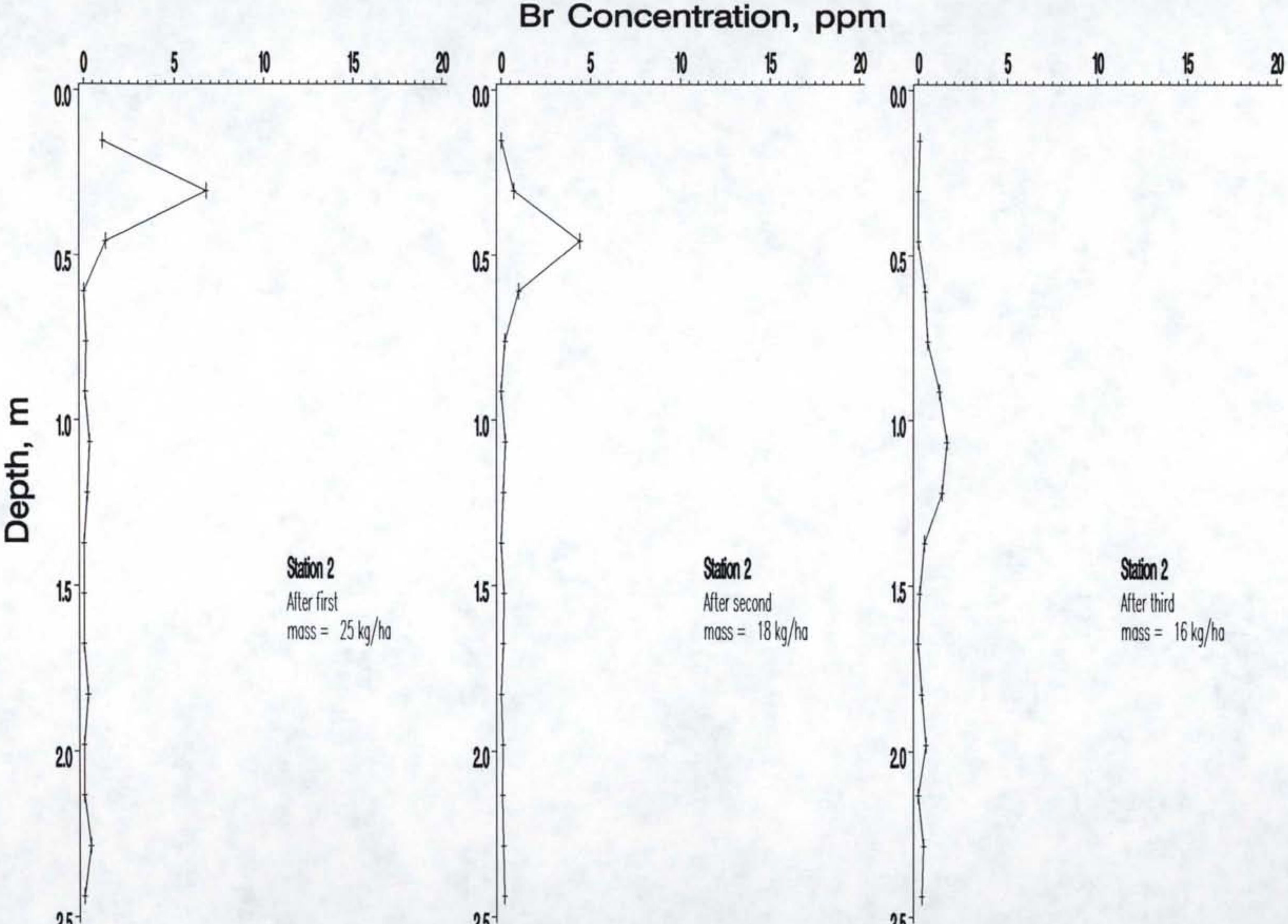
Br Concentration, ppm
Depth, m
Station 2
After first
mass = 25 kg/ha
Station 2
After second
mass = 18 kg/ha
Station 2
After third
mass = 16 kg/ha

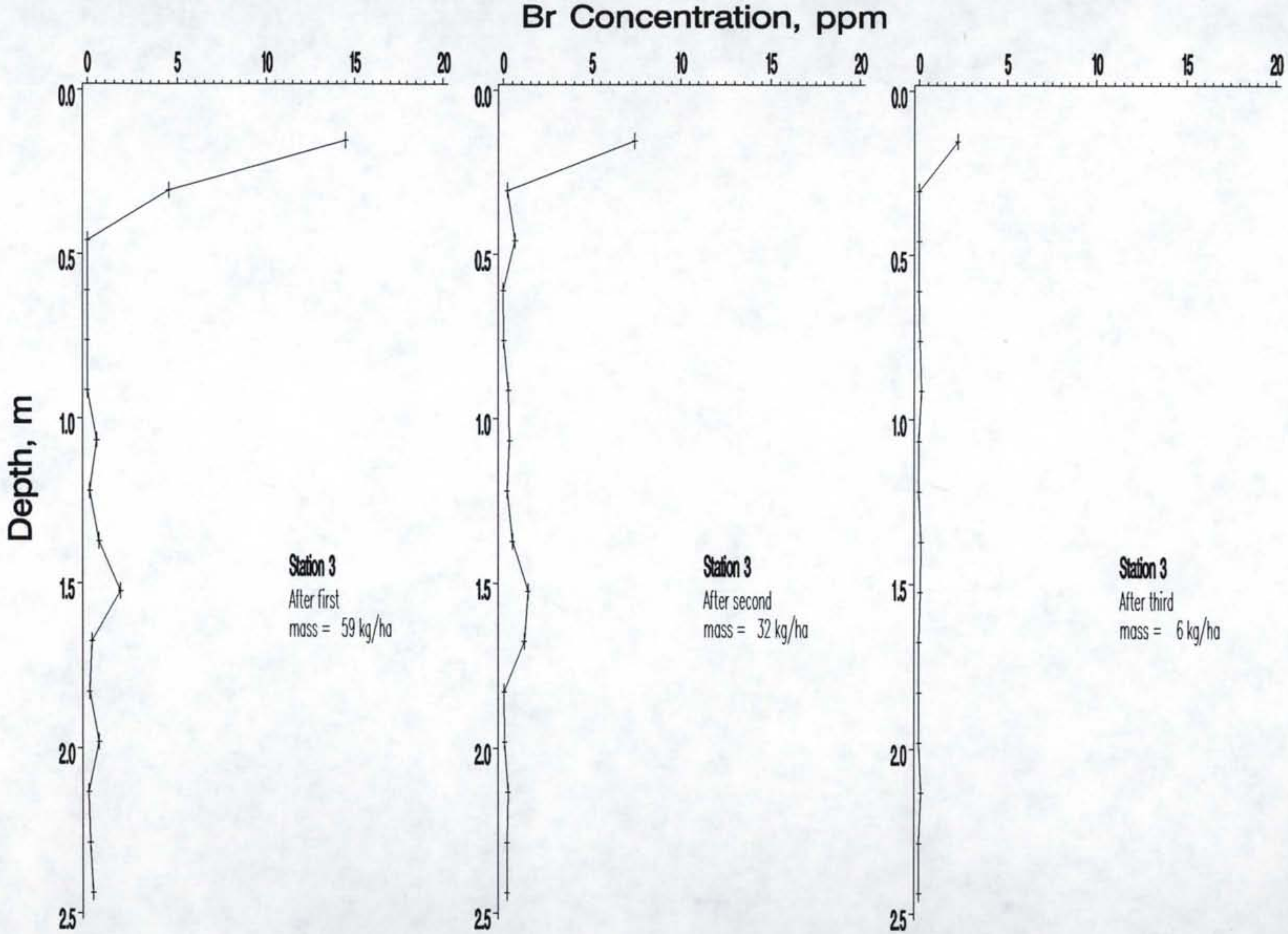
Br Concentration, ppm
0
5
10
15
20
Depth, m
0.0
0.5
1.0
1.5
2.0
2.5
Station 3
After first
mass = 59 kg/ha
Station 3
After second
mass = 32 kg/ha
Station 3
After third
mass = 6 kg/ha

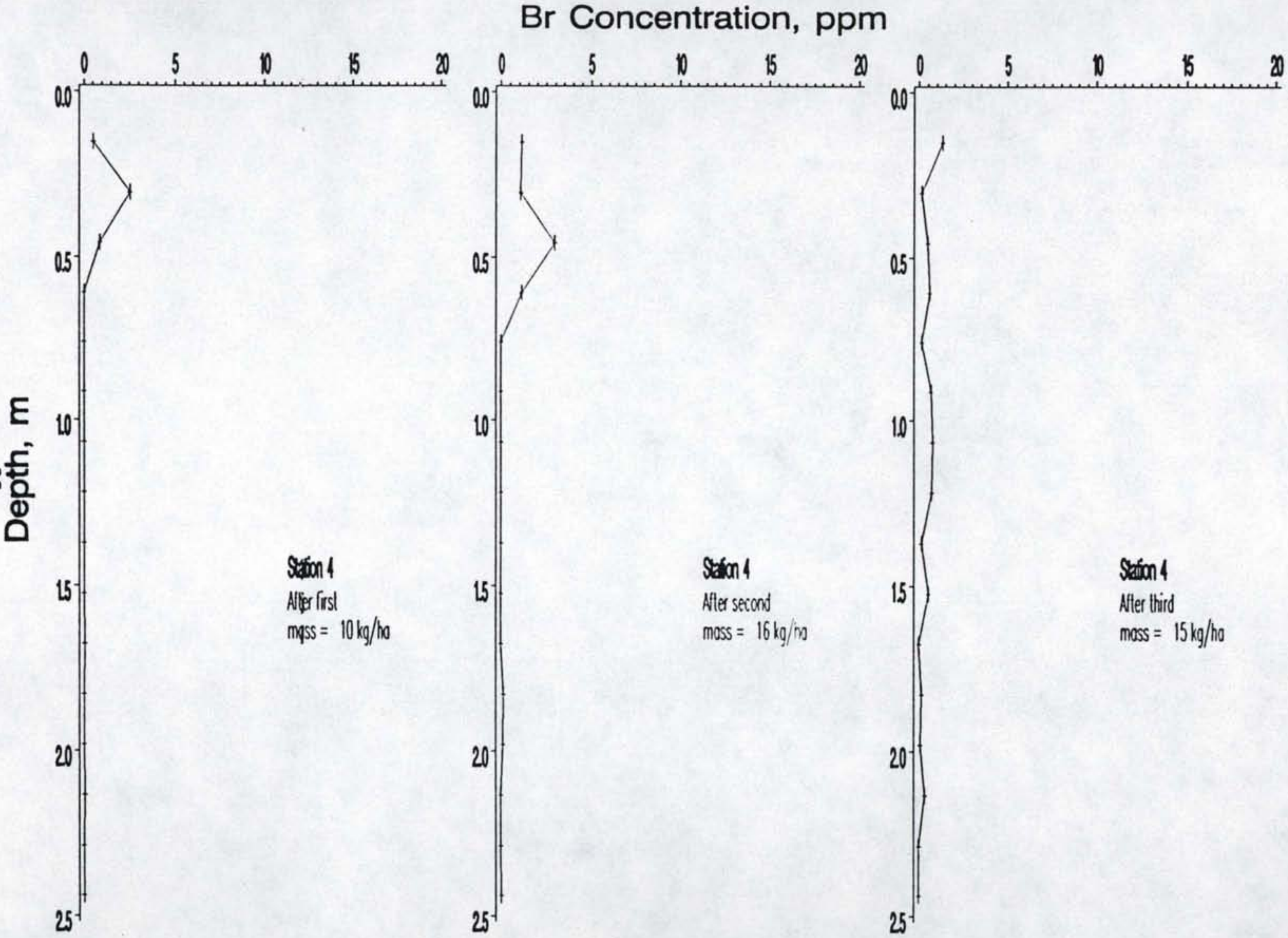
Br Concentration, ppm
Depth, m
0
5
10
15
20
0.0
0.5
1.0
1.5
2.0
2.5
Station 4
After first
mass = 10 kg/ha
Station 4
After second
mass = 16 kg/ha
Station 4
After third
mass = 15 kg/ha

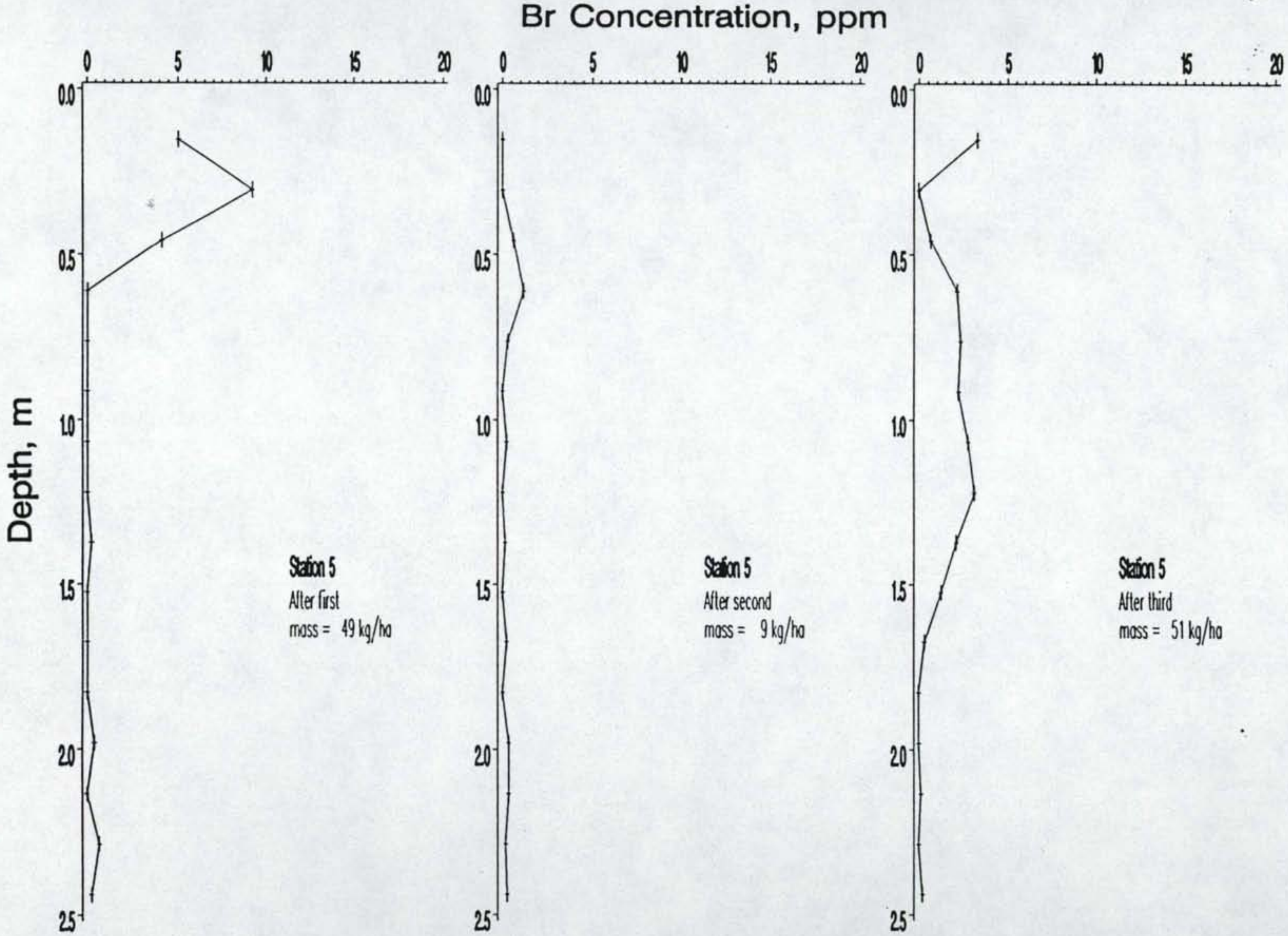
Br Concentration, ppm
Depth, m
0
5
10
15
20
0.0
0.5
1.0
1.5
2.0
2.5
Station 5
After first
mass = 49 kg/ha
Station 5
After second
mass = 9 kg/ha
Station 5
After third
mass = 51 kg/ha

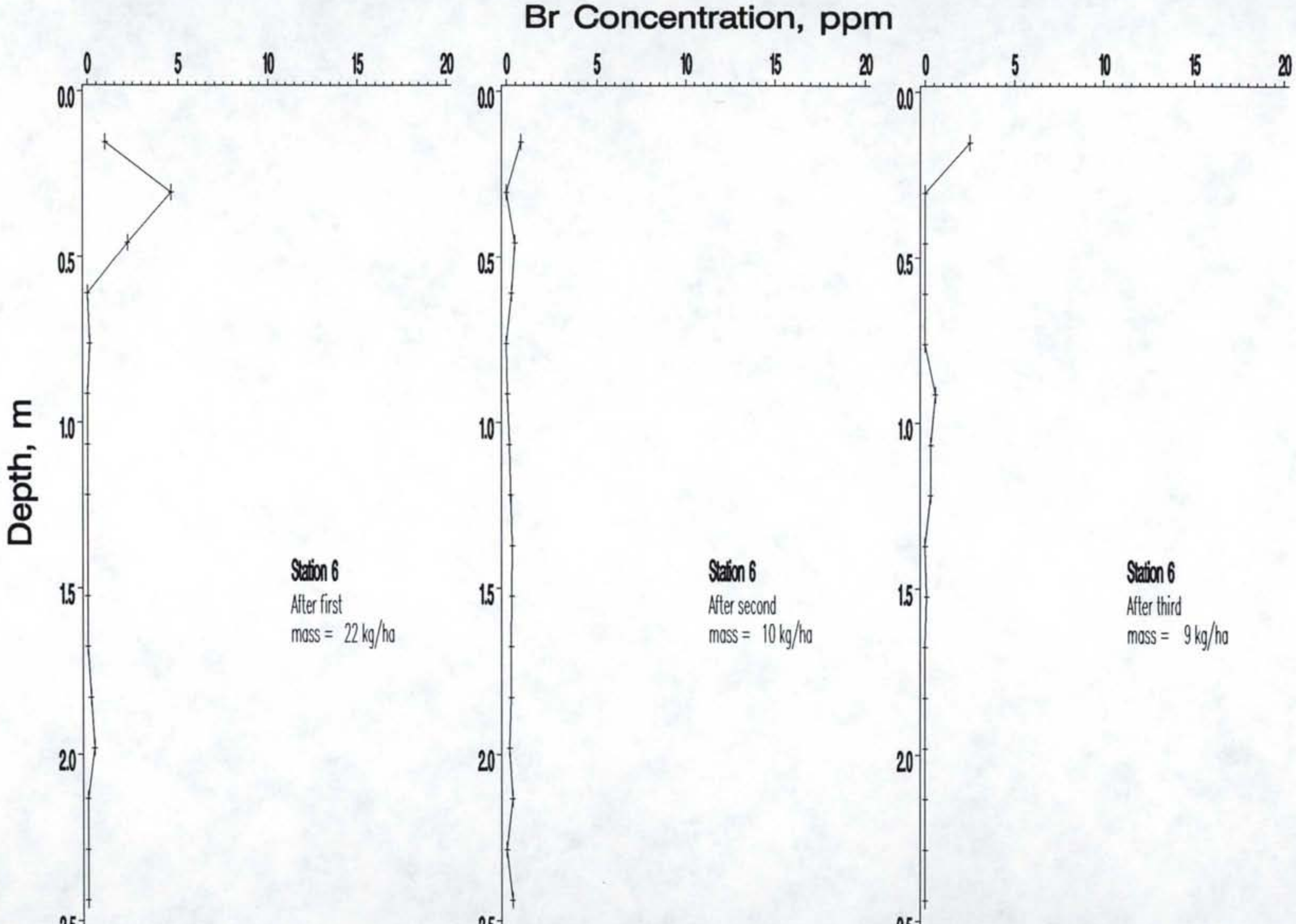
Br Concentration, ppm
Depth, m
0
5
10
15
20
0.0
0.5
1.0
1.5
2.0
2.5
Station 6
After first
mass = 22 kg/ha
Station 6
After second
mass = 10 kg/ha
Station 6
After third
mass = 9 kg/ha

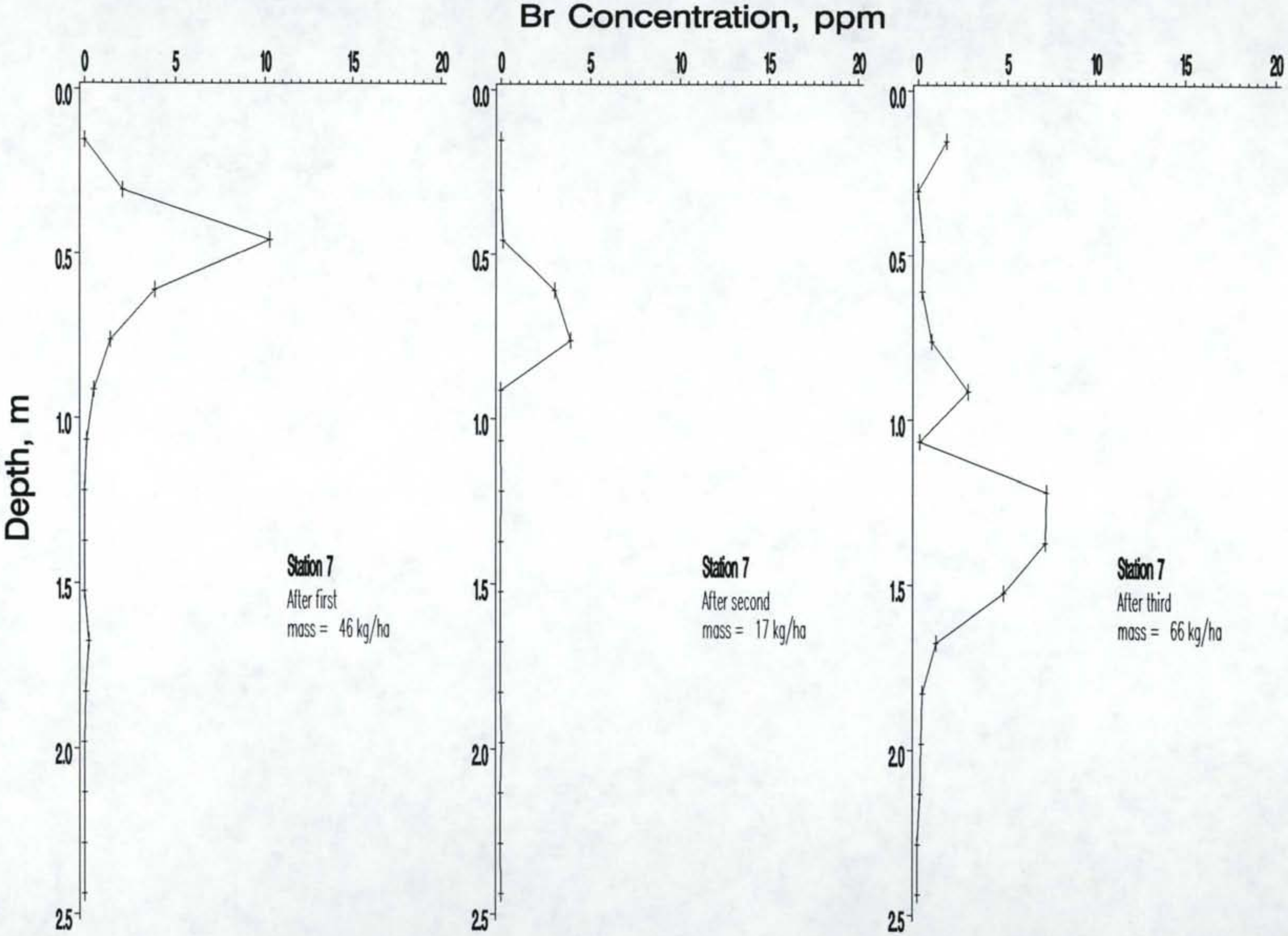
Br Concentration, ppm
0
5
10
15
20
Depth, m
0.0
0.5
1.0
1.5
2.0
2.5
Station 7
After first
mass = 46 kg/ha
Station 7
After second
mass = 17 kg/ha
Station 7
After third
mass = 66 kg/ha

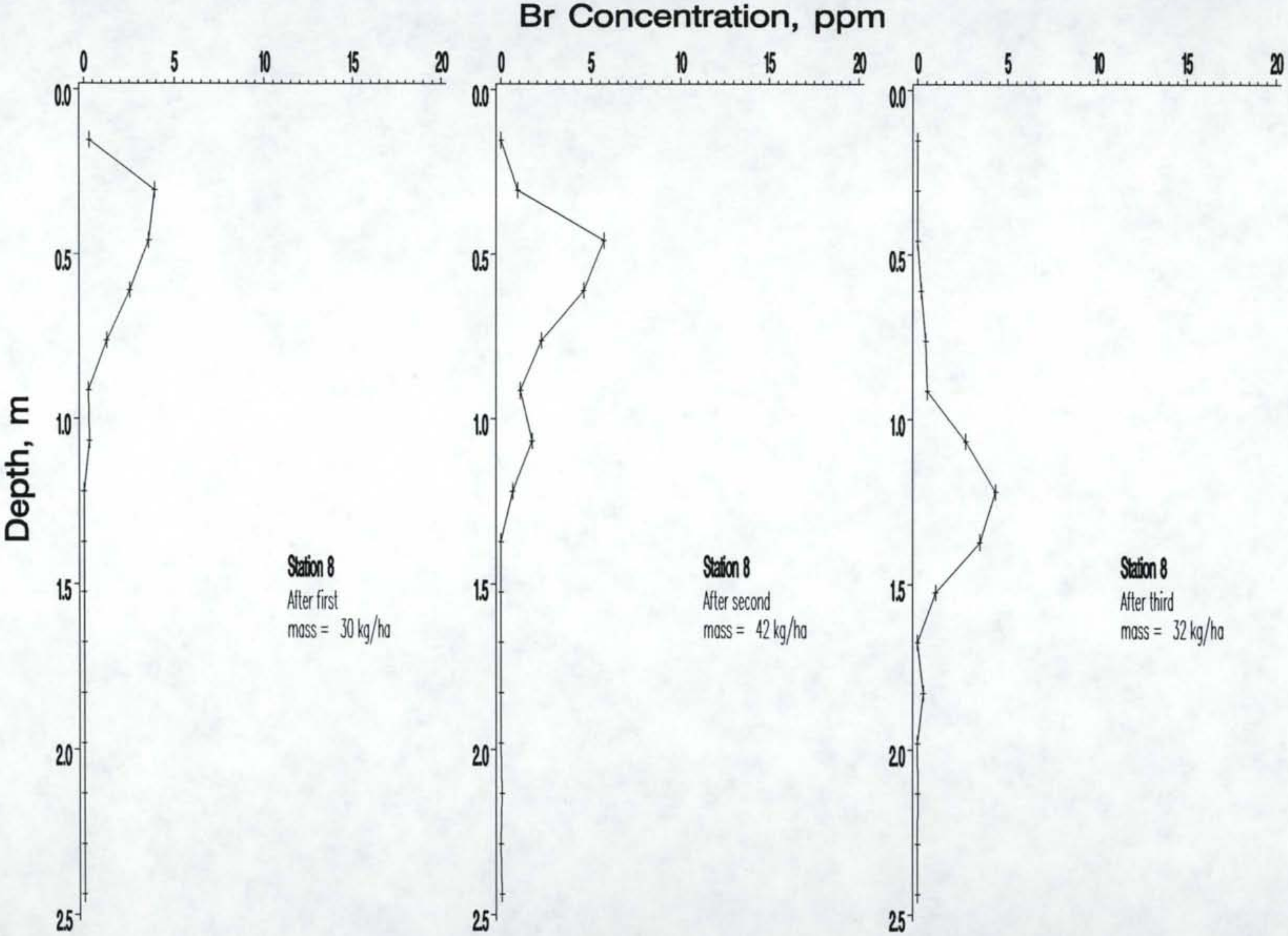
Br Concentration, ppm
Depth, m
0
5
10
15
20
0.0
0.5
1.0
1.5
2.0
2.5
Station 8
After first
mass = 30 kg/ha
Station 8
After second
mass = 42 kg/ha
Station 8
After third
mass = 32 kg/ha

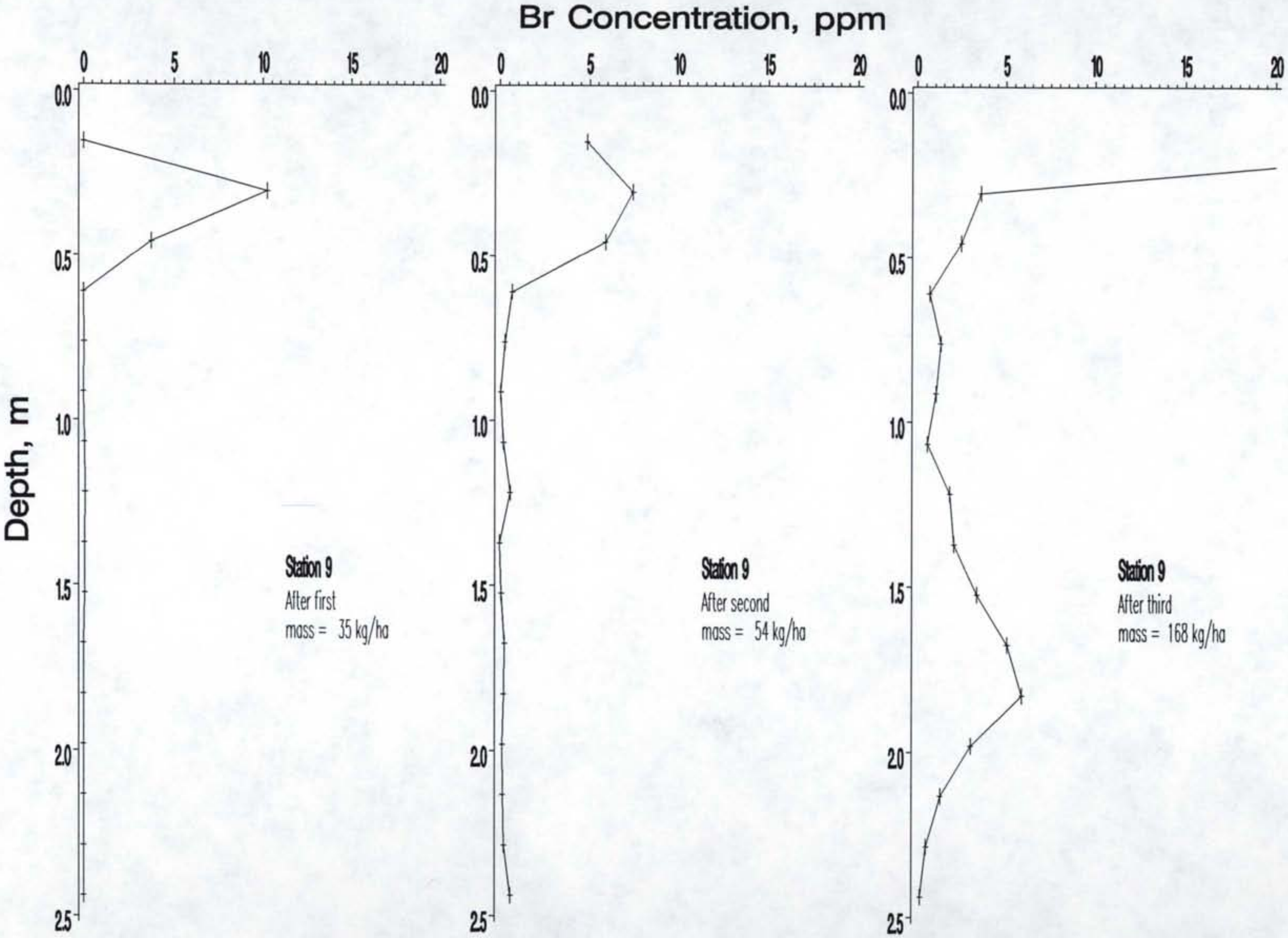
Br Concentration, ppm
Depth, m
0
5
10
15
20
0.0
0.5
1.0
1.5
2.0
2.5
Station 9
After first
mass = 35 kg/ha
Station 9
After second
mass = 54 kg/ha
Station 9
After third
mass = 168 kg/ha

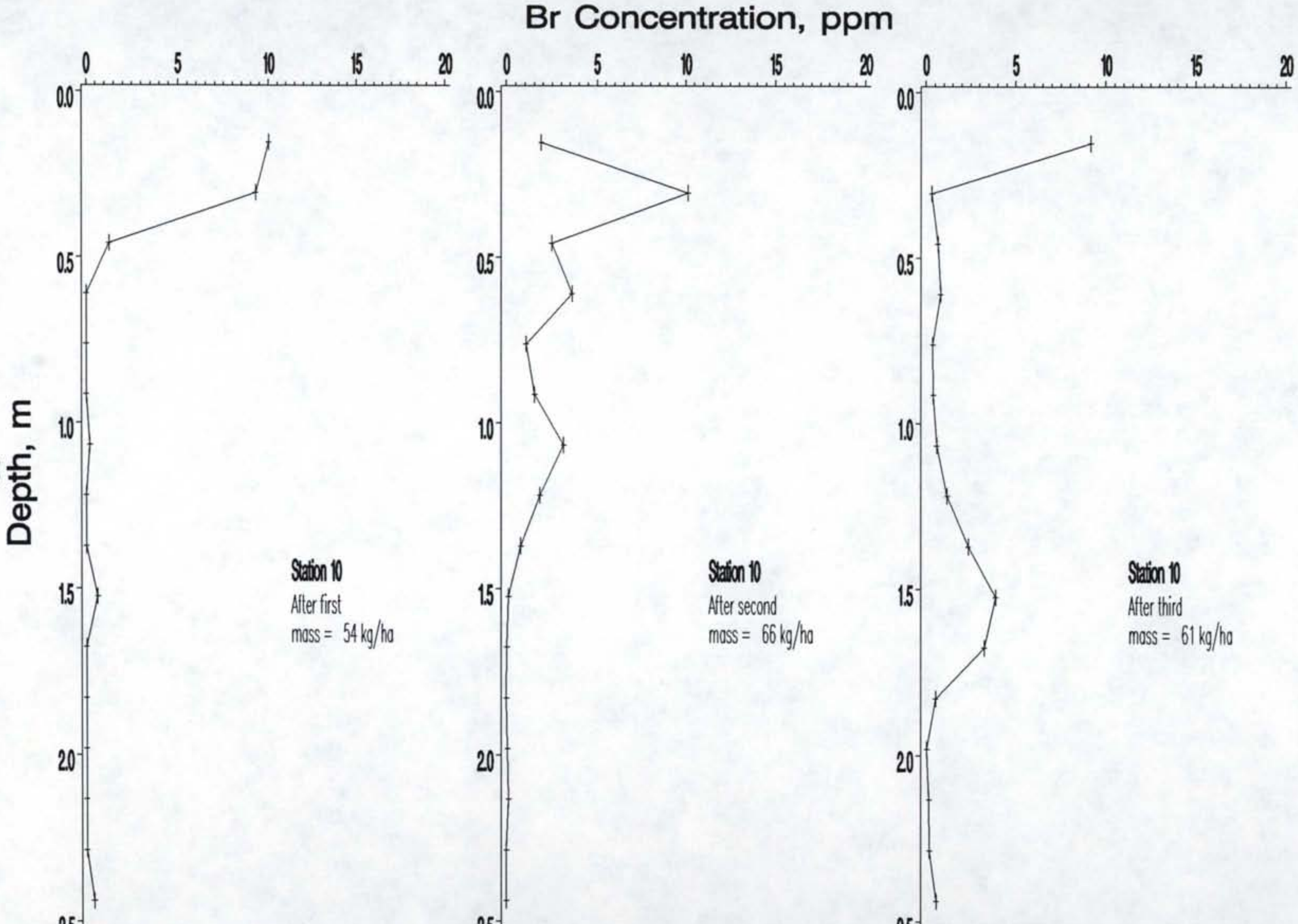
Br Concentration, ppm
0 5 10 15 20
Depth, m
0.0 0.5 1.0 1.5 2.0 2.5
Station 10
After first
mass = 54 kg/ha
Station 10
After second
mass = 66 kg/ha
Station 10
After third
mass = 61 kg/ha

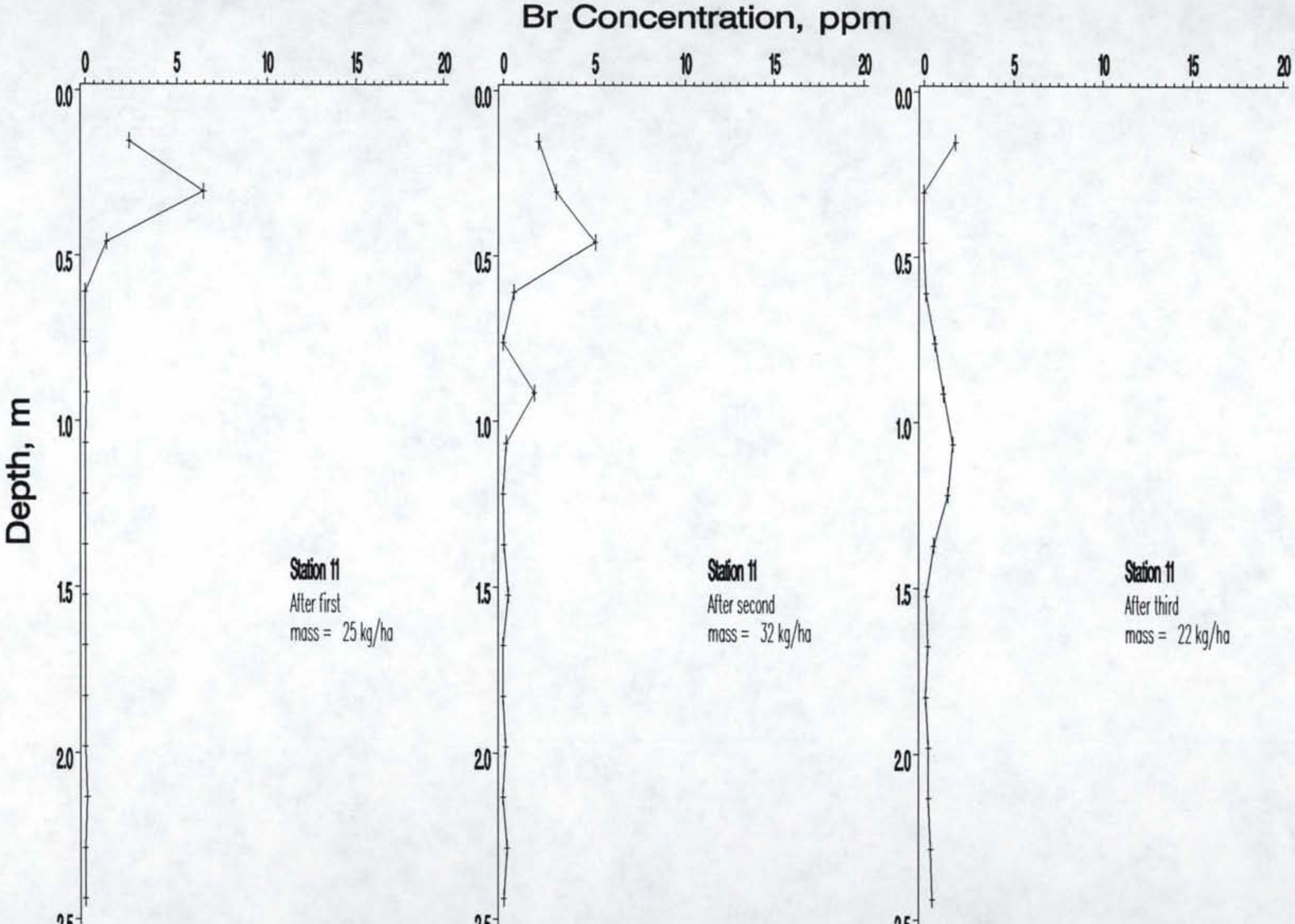
Br Concentration, ppm
Depth, m
0
5
10
15
20
0.0
0.5
1.0
1.5
2.0
2.5
Station 11
After first
mass = 25 kg/ha
Station 11
After second
mass = 32 kg/ha
Station 11
After third
mass = 22 kg/ha

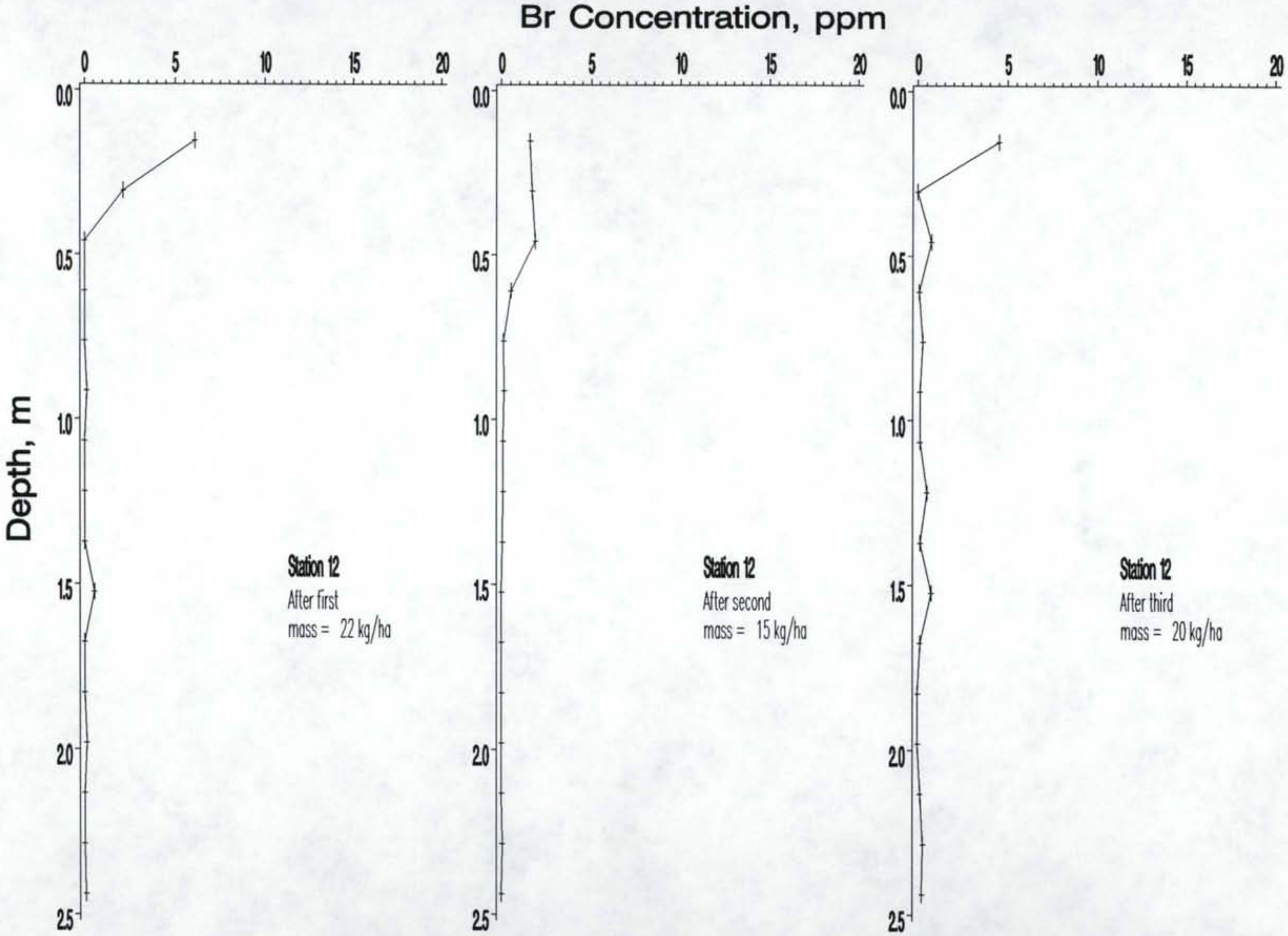
Br Concentration, ppm
0
5
10
15
20
Depth, m
0.0
0.5
1.0
1.5
2.0
2.5
Station 12
After first
mass = 22 kg/ha
Station 12
After second
mass = 15 kg/ha
Station 12
After third
mass = 20 kg/ha

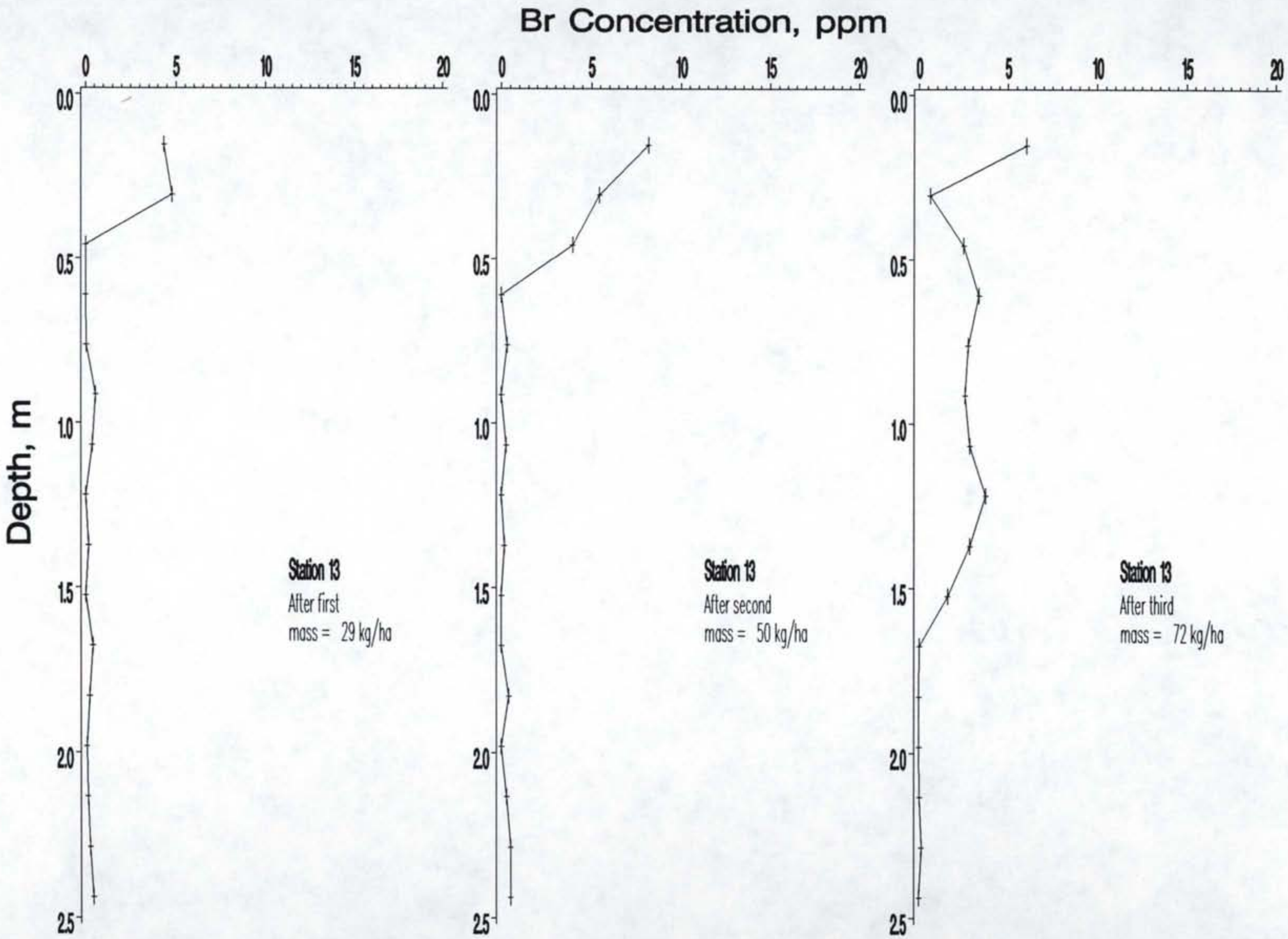

Br Concentration, ppm
Depth, m
0
5
10
15
20
0.0
0.5
1.0
1.5
2.0
2.5
Station 13
After first
mass = 29 kg/ha
Station 13
After second
mass = 50 kg/ha
Station 13
After third
mass = 72 kg/ha

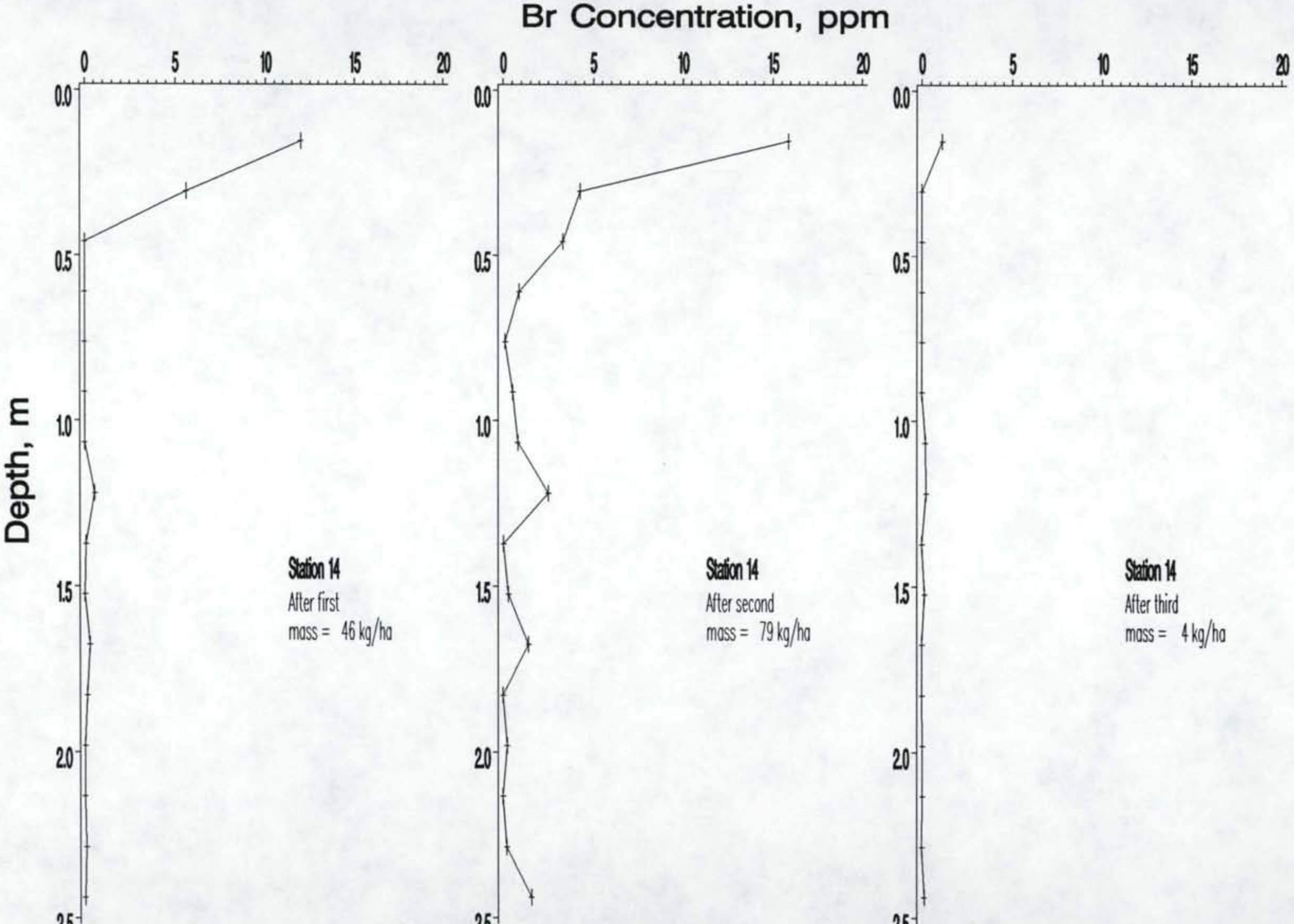

Br Concentration, ppm
0
5
10
15
20
Depth, m
0.0
0.5
1.0
1.5
2.0
2.5
Station 14
After first
mass = 46 kg/ha
Station 14
After second
mass = 79 kg/ha
Station 14
After third
mass = 4 kg/ha

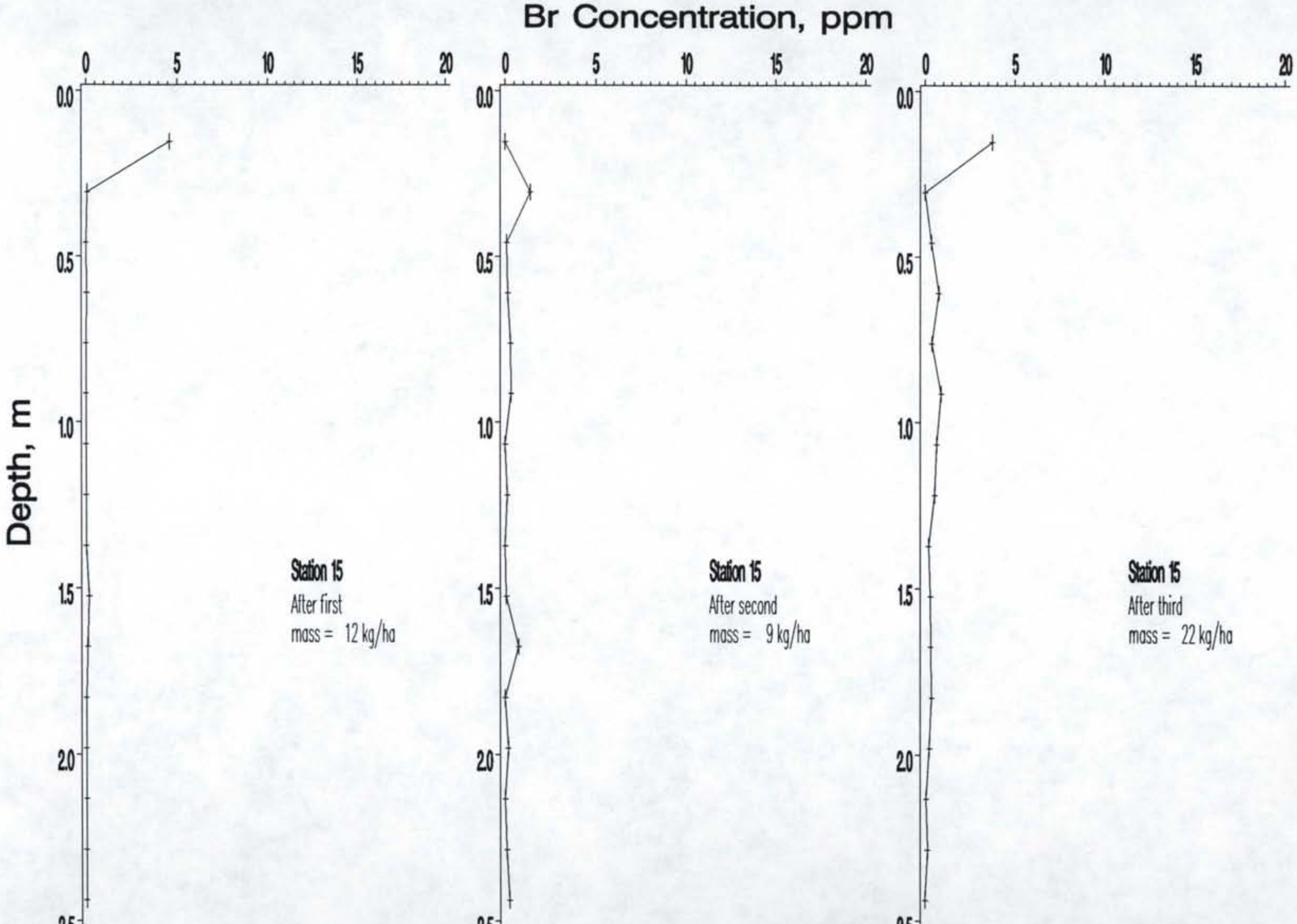
Br Concentration, ppm
0 5 10 15 20
0.0 0.5 1.0 1.5 2.0 2.5
Depth, m
Station 15
After first
mass = 12 kg/ha
Station 15
After second
mass = 9 kg/ha
Station 15
After third
mass = 22 kg/ha

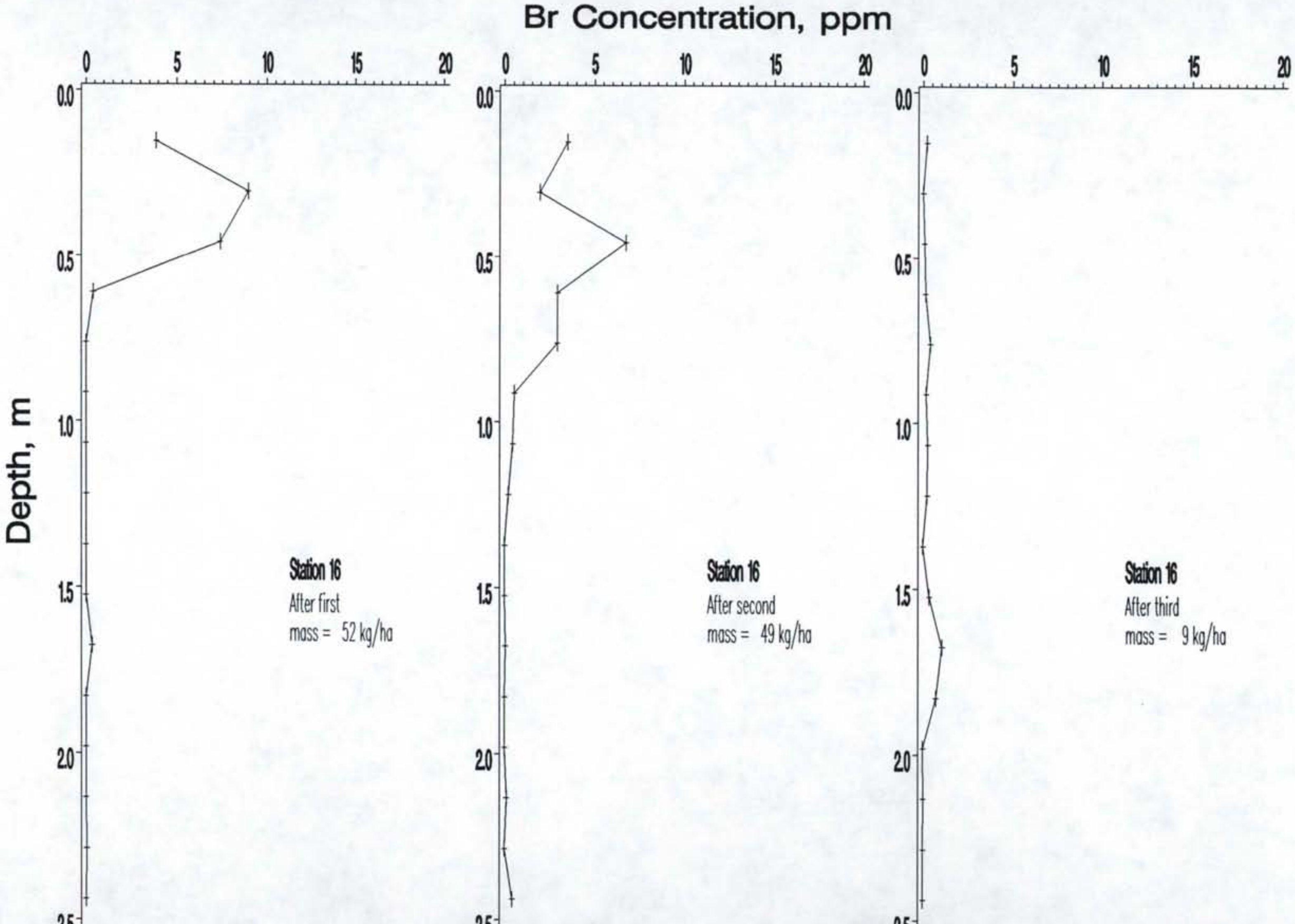
Br Concentration, ppm
0
5
10
15
20
Depth, m
0.0
0.5
1.0
1.5
2.0
2.5
Station 16
After first
mass = 52 kg/ha
Station 16
After second
mass = 49 kg/ha
Station 16
After third
mass = 9 kg/ha

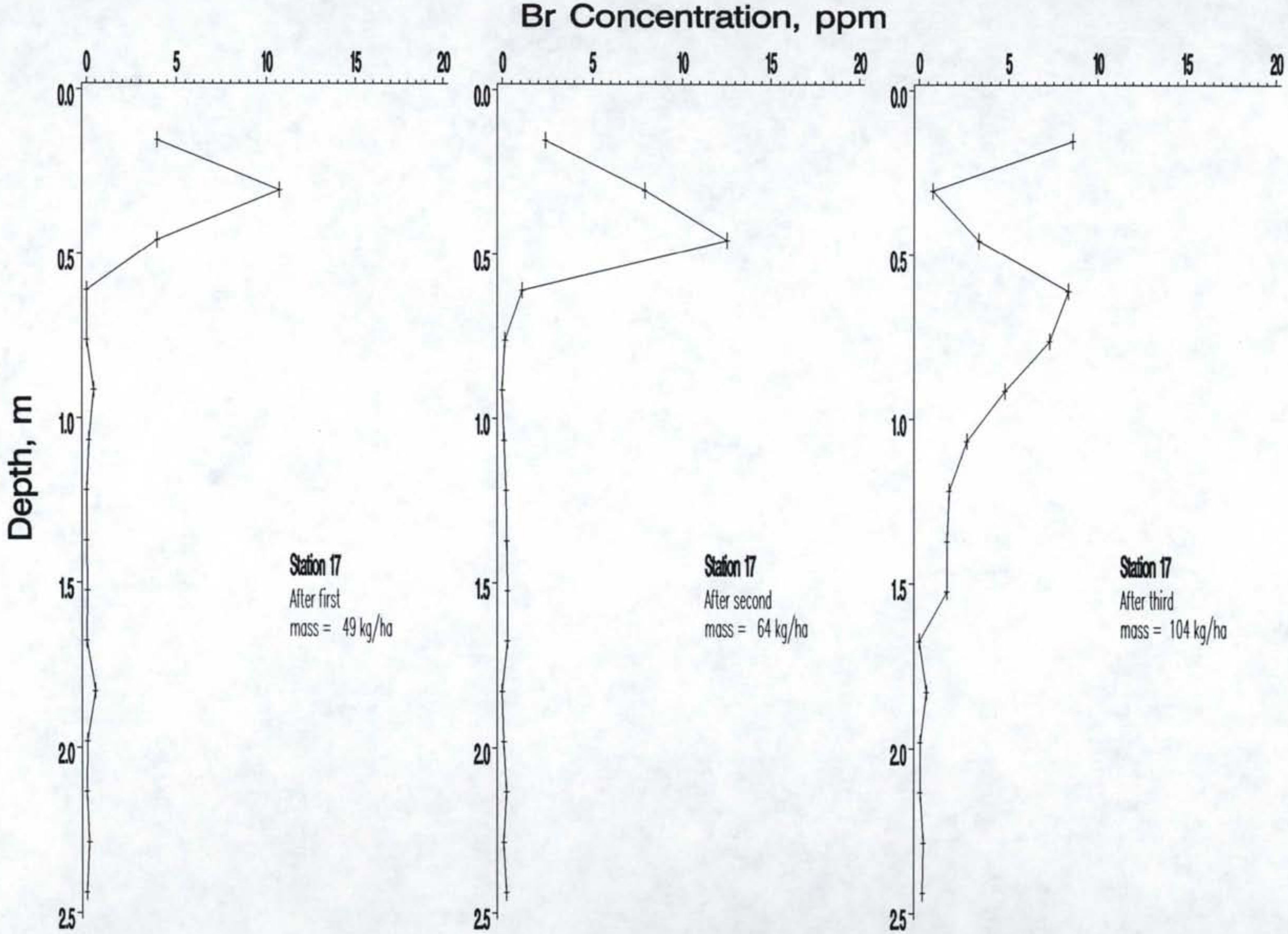
Br Concentration, ppm
Depth, m
0 5 10 15 20
0.0 0.5 1.0 1.5 2.0 2.5
Station 17
After first
mass = 49 kg/ha
Station 17
After second
mass = 64 kg/ha
Station 17
After third
mass = 104 kg/ha

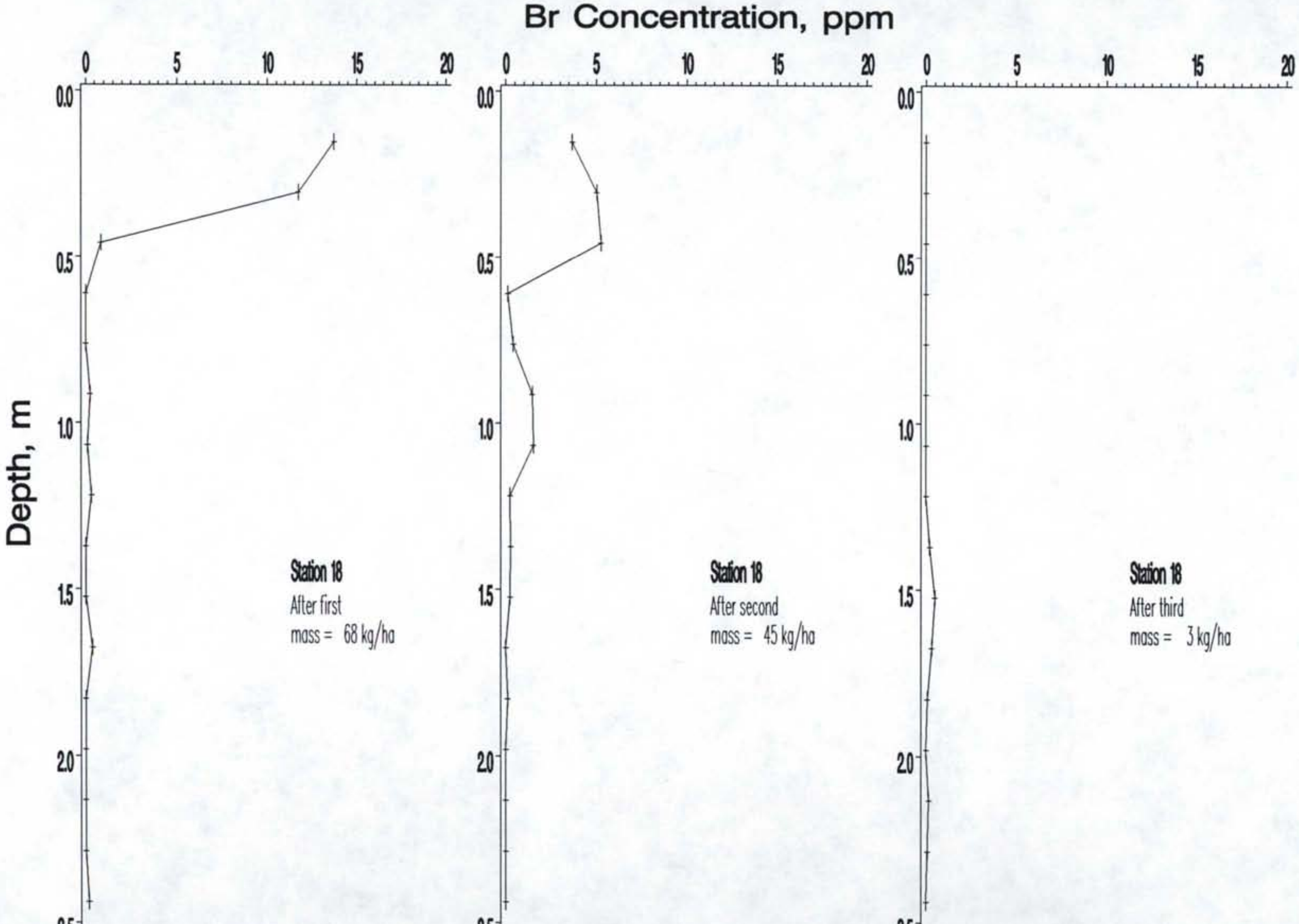
Br Concentration, ppm
Depth, m
0
5
10
15
20
0.0
0.5
1.0
1.5
2.0
2.5
Station 18
After first
mass = 68 kg/ha
Station 18
After second
mass = 45 kg/ha
Station 18
After third
mass = 3 kg/ha

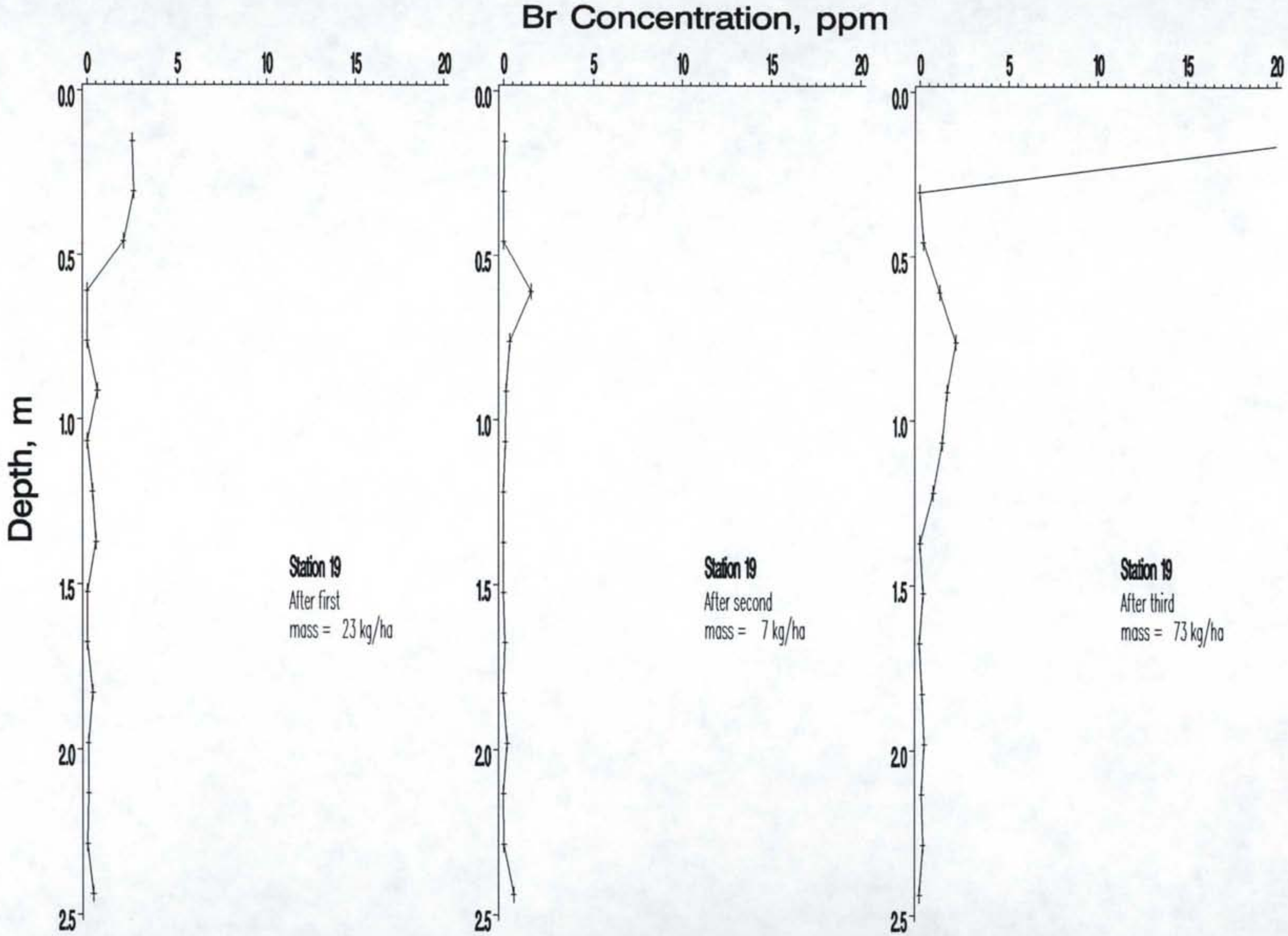
Br Concentration, ppm
0 5 10 15 20
Depth, m
0.0 0.5 1.0 1.5 2.0 2.5
Station 19
After first
mass = 23 kg/ha
Station 19
After second
mass = 7 kg/ha
Station 19
After third
mass = 73 kg/ha

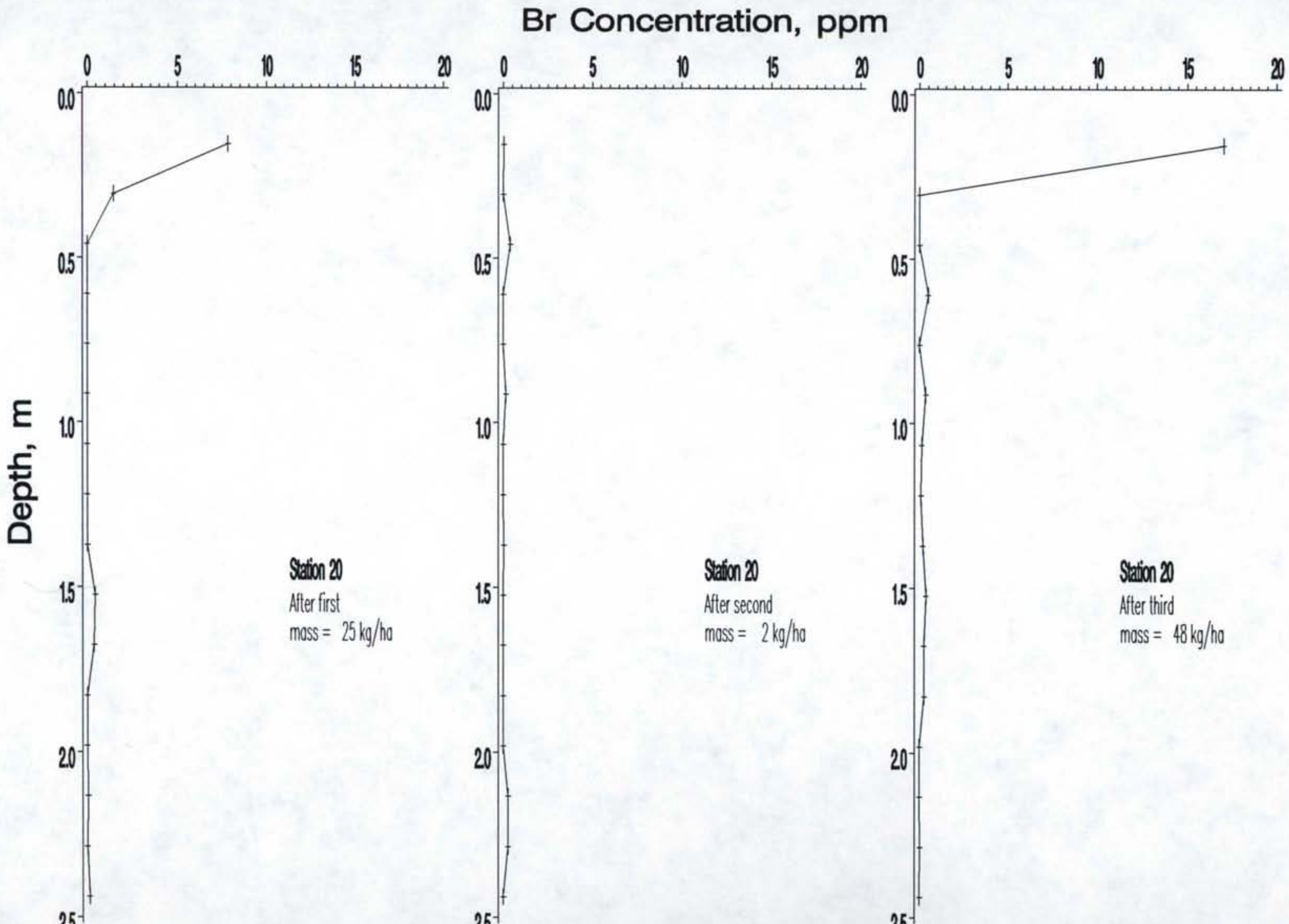

Br Concentration, ppm
Depth, m
0 5 10 15 20
0.0 0.5 1.0 1.5 2.0 2.5
Station 20
After first
mass = 25 kg/ha
Station 20
After second
mass = 2 kg/ha
Station 20
After third
mass = 48 kg/ha

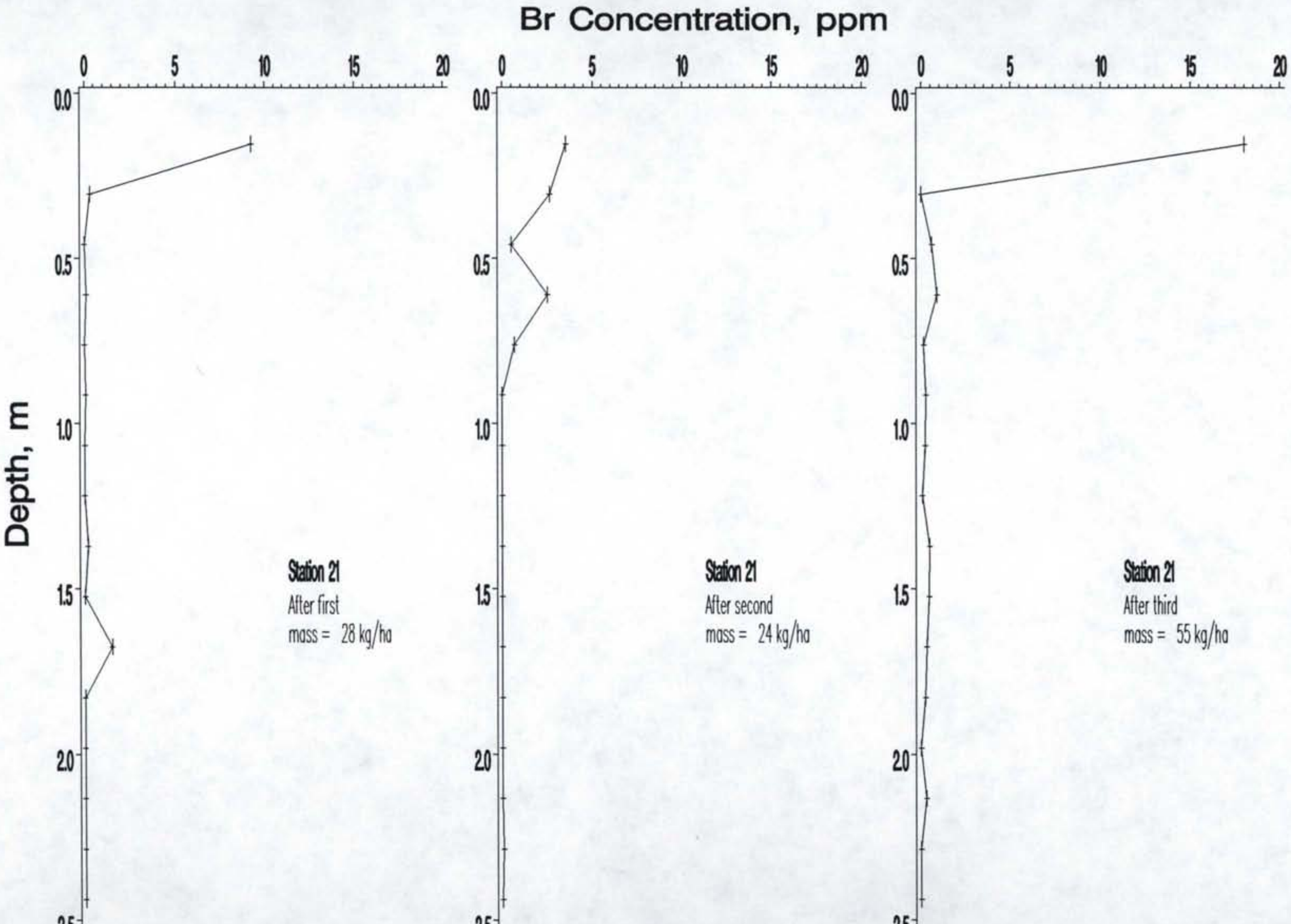
Br Concentration, ppm
Depth, m
Station 21
After first
mass = 28 kg/ha
Station 21
After second
mass = 24 kg/ha
Station 21
After third
mass = 55 kg/ha